TABLE OF CONTENTS

ACKNOWLEDGEMENTS

I would like to express my special appreciation and thanks to my adorable supervisor "***Prof. Massimo Negrini***" for enlightening me the best glance of research. You have been a tremendous mentor for me and your advice on both research as well as on my career have been priceless. I would also like to express my sincere gratitude to my Coordinator ***"Prof. Antonio Cuneo "*** for allowing me to grow as a research scientist. I would also like to thank, ***Prof. Silvia Sabbioni*** for all kindly assistance and brilliant comments and suggestions, thanks to you. My sincere thanks also goes to my fellow lab mates at the University of Ferrara**: *Dr. Elisa Callegari, Cristian Bassi,*** *, Dr.Laura Lupini, Dr.Manuela Ferracin, LucillaD'Abundo, Dr.Barbara Zagatti, Dr.Elena Miotto, Fabio Corrà, Dr.Bahaeldin K. Elamin* for the stimulating discussions, the technical and scientific knowledge that offer to me and for all the fun we have had in the lab. A special thanks to my family. Words cannot express how grateful I am to my mother *"Shahin Heidari"* and father *"Dr. Ahmad Moshiri"* for all of the sacrifices that you've made on my behalf. Your prayer for me was what sustained me thus far. Also I would like to thanks my brother *"Dr. Farhad Moshiri"*, my sisters *"Dr. Fereshteh* and *Farnoosh Moshiri*" ,my mother-in law *"Manije MalekAhmadi"* , father-in-law *"Eisa Sattari"* and all family members for their kindly help. I would also like to thank all my friends with special thanks to Dr. Faranak Gharavi, *Dr.Reza Rezazadeh, Dr.Pantea Shafiee, Dr.Behnam Makoee* who supported me and incented me to strive towards my goal.

At the end I would like express deepness appreciation to my beloved husband ***"Dr. Arash Sattari"*** who spent sleepless nights with and was always my support in the moments when there was no one to answer my queries. Also my best appreciation goes to my Son " Small but Grand, Glorious and Honorable Man" ***RADMAN***" for offering the moments that were belong him to me and consistently following me every time and everywhere.

DEDICATION

I would like to dedicate my dissertation

To

My Father & My Mother

For giving all my need and all of sacrifices

My Beloved Husband

Who have never failed to give me support each step of the way

My Lovely Son

Who give me the unbelievable moral support

&

All HCC patients

LIST OF FIGURES

List of Tables

ABBREVIATION

3'UTR	3'untranslated region
°C	Celsius degree
<	Less-than sign
µg	Microgram
µl	Microliter
µM	Micromolar
AAV	Adeno Associated Virus
Ad	Adeno Virus
Ago2	Argonaute2
AMO	Antisense miRNA oligonucleotide
Anti-miR	Antisence microRNA
APAF1	Apoptotic Peptidase Activating Factor 1
AR	Androgen receptor
ATCC	American Type Culture Collection
BCL2	B-cell CLL/lymphoma 2
BH3	Bcl-2 homology 3
BMF	B-cell lymphoma 2-modifying factor
bp	Base pairs
Cap	Capsidation
CDAA	Choline-deficient and amino-acid-defined
CDK	Cyclin-dependent kinase
CDKN1B/p27/kip1	Cyclin-dependent kinase inhibitors 27
CDKN1C/p57/kip2	Cyclin-dependent kinase inhibitors 57
cDNAs	Complementary DNAs
CLL	Chronic lymphocytic leukemia
cm	Centimeter
CMV	Cytomegalovirus
CRAds	Conditionally replicating adenoviruses
Ct	Threshold cycle
CTCF	CCCTC-binding factor
DDIT4	DNA damage-inducible transcript 4
DGCR8	DiGeorge Critical Region 8
DMSO	Dimethyl sulfoxide
DNA	Deoxyribonucleic acid
DNase	Deoxyribonuclease
dNTP	Deoxynucleotide Triphosphate
dsRNA	Double Strand RNA
E. coli	Escherichia coli
E1A	Adenoviral Eleary1A gene
E1B	Adenoviral Eleary1B gene

E2	Adenoviral Eleary2 gene
E3	Adenoviral Eleary3 gene
E4	Adenoviral Eleary4 gene
EBV	Epstein-Barr virus
EDTA	Ethylene diamine tetra acetic acid
EGFP	Enhanced Green Fluorescence protein
ER	Estrogen receptor
ERK	Extracellular signal-regulated kinase
EtOH	Ethanol
FASLG	Fas Ligand
FBS	Fetal bovine serum
FDA	Food and Drug Administration
fg	Fentogram
g	Gram
GFP	Green fluorescence protein
h	Hour(s)
H_2O	Water
HBV	Hepatitis B virus
HCC	Hepatocellular carcinoma
HCV	Hepatitis C virus
HEK293	Human embryonic kidney 293 cells
Hep3B	Human liver cancer cells
HepG2 cells	Human liver cancer cells
IC_{50}	Inhibition concentration to kill 50% of cells population
IMEM	Dulbecco's Modified Iscove's Medium
IRES	Internal ribosomal entry site
ITRs	Inverted Terminal Repeat
IU	Infectious units
kb	Kilobase
Kg	Kilogram
KSRP	KH-type splicing regulatory protein
LAR	Luciferase Assay Reagent
Luc	Luciferase
M	Molar
mg	Miligram
min	Minute(s)
miR	MicroRNA
mir-221	MicroRNA-221
miRISC	MiRNA induced silencing complex
miRNA	MicroRNA
MOI	Multiplicity of Infection
mM	Milimolar
MMP	Matrix metalloproteinase
mRNA	Messenger RNA

mTOR	Mammalian Target of Rapamycin
NC	Negative control
ng	Nanogram
nM	Nanomolar
NR	Nuclear receptors
NSCLC	Non Small Cell Lung Cancer
nt	Nucleotide
NTC	Non-transfected
ORF	Open reading frame
OTSCC	Toncue squamous cell carcinoma
P53	Phosphoprotein 53
pAAV	Adeno Associated Virus Plasmid
pAd	Adeno virus Plasmid
PAGE	Polyacrylamide Gel Electrophoresis
PCR	Polymerase Chain Reaction
pg	Picogram
pHelper	Helper plasmid
PNK	Polynucleotide Kinase
Pre- miRNAs	Precursor miRNA
Pri- miRNAs	Primary miRNAs
PS	Phosphatidylserine
PTEN	Phosphoinositide 3-kinase pathway phosphatase and tensin homolog
PUMA	p53 upregulated modulator of apoptosis
PVDF	Polyvinylidene difluoride
qPCR	Quantitative PCR
rAAV	Recombinant Adeno Associated Virus
rAd	Recombinant Adeno Virus
RAS	Rat Sarcoma Virus oncogene
RB	Retinoblastoma
Rep	Replication
RIPA	Radio Immuno Precipitation Assay
RNA	Ribonucleic acid
RNA pol II	RNA Polymerase II
RNA pol III	RNA Polymerase III
rpm	Rounds per minute
RTPCR	Real Time PCR
s	Second(s)
SD	Standard deviation
SDS	Sodium Dodecyl Sulfate
SOD2	Manganese superoxide dismutase2
SNU398	Human liver cancer cells
SV40	Simian vacuolating virus 40
TAE buffer	Tris-Acetate EDTA buffer
TGF	Transforming Growth Factor
TIMP3	Tissue inhibitor of metalloproteinase 3
TP53INP1	Tumor suppressor protein 53-induced nuclear protein 1
TRBP/TARBP	Transactivation-responsive RNA-binding protein
U	Unite

vp	Viral particle
WNT	Wingless-Type
wtAd5	Wild type adenovirus serotype 5
X	Times

KEY WORDS

Hepatocellular carcinoma(HCC)

microRNA(miRNA, miR)

Adenovirus

Adeno Associated Virus

microRNA- Based Therapy

microRNA Sponge

Antisence miRNA oligos(AMOs)

Mimics miRNA

Sorafenib

CHAPTER 1.

INTRODUCTION

1.1. Hepatocellular Carcinoma

Primary liver cancer mainly refers to hepatocellular carcinoma (HCC), intrahepatic cholangiocarcinoma (ICC), and hepatic angiosarcoma(1). Hepatocellular carcinoma (HCC) accounts for 85% to 90% of primary liver cancers which ranks as the fifth most common malignancy worldwide and the third most common cause of cancer-related mortality(2).

New Cases: An estimated 30,640 new cases of liver cancer (including intrahepatic bile duct cancers) are expected to occur in the US during 2013. More than 80% of these cases are hepatocellular carcinoma (HCC), originating from hepatocytes, the predominant liver cell type. Liver cancer incidence rates are three times higher in men than in women. From 2005 to 2009, rates increased by 3.7% per year in men and by 3.0% per year in women(3).

Deaths: An estimated 21,670 liver cancer deaths (6,780 women, 14,890 men) are expected in 2013. From 2005 to 2009, death rates for liver cancer increased by 2.3% per year in men and 1.3% per year in women(3).

Risk factors: In the US and other western countries, alcohol-related cirrhosis, and possibly nonalcoholic fatty liver disease associated with obesity, account for the majority of liver cancer cases. Chronic infections with hepatitis B virus (HBV) and hepatitis C virus (HCV) are associated with less than half of liver cancer cases in the US, although they are the major risk factors for the disease worldwide. In the US, rates of HCC are higher in immigrants from areas where HBV is endemic, such as China, Southeast Asia, and sub-Saharan Africa. Other risk factors for liver cancer, particularly in economically developing countries, include parasitic infections (schistosomiasis and liver flukes) and consumption of food contaminated with aflatoxin, a toxin produced by mold during the storage of agricultural products in a warm, humid environment(3).

Pathogenesis: The exact pathophysiology of HCC is poorly understood .However alterations in molecular pathways involved in the process of HCC are depicted as follows:(a) activation of the Wnt/Frizzled/β-catenin pathway through mutations in β-catenin as well as up-regulation of upstream elements, such as Frizzled receptors, (b) alteration of the MAPK signaling pathway through HBV or HCV infection, (c) activation of the JAK/STAT pathway through inactivation of JAK-binding proteins, (d) inactivation of the tumor suppressor gene p53 through gene mutation and posttranscriptional interaction with viral proteins as well as oxidative stress, (e) alteration of the tumor suppressor retinoblastoma (pRb Pathway) and p16INK4 genes through mutations or promoter

methylation and (f) alteration of the transforming growth factor-β pathway. So far, many HCC-related oncogenes, including AFP, RAS, c-FOS, c-JUN, RHO, TGF-a, HGF, CerbB2, HER-2, HER-2/neu, NEU, NGL, MDM2, MMP and IGF-β have been found. The abnormal expression of these genes with regard to a lasting cell proliferation results in carcinogenesis ultimately(4). Despite of deregulation of critical genes involve in cellular processes such as cell cycle control, apoptosis and cell migration, recent studies showed that molecules that regulate these events, including microRNAs (miRNAs) also play key role in development and progression of HCC(1, 5).

Early detection: Screening for liver cancer has not been proven to improve survival. Nonetheless, many doctors in the US screen high-risk persons (e.g., HCV-infected persons with cirrhosis) with ultrasound or blood tests(3).

Survival: The overall 5-year relative survival rate for patients with liver cancer is 15%. Forty percent of patients are diagnosed at an early stage, for which 5-year survival is 28%. Survival decreases to 10% and 3% for patients who are diagnosed at regional and distant stages of disease, respectively(3).

1.1.1. Treatment of HCC

Early stage liver cancer can sometimes be successfully treated with surgery in patients with sufficient healthy liver tissue; liver transplantation may also be an option(3). Surgical treatment of early stage liver cancer is often limited by the high frequency of tumor recurrence and metastasis after curative resection. Statistics show that the survival rate of patients who have had a resection is 30% to 40% at 5 years, postoperatively(4). Patients whose tumors cannot be surgically removed may choose ablation (tumor destruction) or embolization, a procedure that cuts off blood flow to the tumor(3). Chemotherapy and radiotherapy are the two other conventional therapies applied in the treatment of cancer, which also get an unfavorable score because of the resistance of HCC. Moreover, occurrence of HCC often coupled with liver dysfunction, leads to restrict the use of conventional chemotherapeutics as there is more or less non-selective toxicity with significant systemic side effects(6). Fewer treatment options exist for patients diagnosed at an advanced stage of the disease. Sorafenib (Nexavar) is a targeted drug approved for the treatment of HCC in patients who are not candidates for surgery(3). Sorafenib is a multi-kinase inhibitor that targets proteins of multiple signaling pathways simultaneously—VEGFR2, VEGFR3, PDGFR, Flt-3, c-kit and the Raf/MEK/ERK pathway—to inhibit tumor growth and to induce apoptosis of

tumor cells(5). In a phase III trial, patients with advanced HCC treated with the molecular targeted agent sorafenib, reported an increase in survival of approximately 3 months(7, 8).Viral vectors, for example, recombinant adeno-associated virus (rAAV), mediated microRNAs targeted therapy which is targeting liver by hydrostatic pressure injection, is considered to be the appealing approach for liver disease as it is quite effective, associated with higher infectious rate and prolonged expression(4).

1.2. microRNAs: Biogenesis, Processing and Function

microRNAs (miRNAs) are a highly conserved group of endogenous small non-coding RNA (ncRNAs) molecules, which can be expressed in a tissue specific manner (9-11). miRNAs negatively regulate gene expression through binding of 6–8 nucleotide sequences (miRNA seed) to complementary sequences of target messenger RNA (mRNA), in the form of ribonucleoprotein complexes that mediate mRNA destabilization(12). In this way, they resulting in transcript degradation or translation inhibition(9-11). In the past 3 years, the number of microRNA loci annotated in miRBase has grown by approximately two-thirds, from 15 172 loci in 142 species (release 16, October 2010) to 24 521 loci in 206 species(release 20, June 2013)(13). Each miRNA can influence hundred of gene transcript and more than one miRNA can regulate any specific mRNA, which creates complexity in their capacity to modulate fundamental biological processes(14).

From a historic standpoint, it is curious to note that miRNAs have long been discovered (in 1993, by Victor Ambros et al.) before the 1998 Nature paper by Andrew Fire and Craig Mello, which introduced the term RNAi and was later rewarded with the Nobel prize (15, 16). lin-4 was the first miRNA, discovered from C. elegans in 1993(16). Seven years later, the second miRNA let-7 was also discovered from C. elegans(17). This publication was certainly distinct and unique, as it suggested, for the first time, that small dsRNAs could play key roles in gene expression. In 2001, this kind of endogenous tiny non-protein coding single-stranded RNAs were first designated as “microRNAs” (18). Subsequently, more and more miRNAs were identified in many species ranging from plants to human(19).

miRNAs are predicted to affect the expression of nearly 60% of protein-coding mammalian genes and thereby to control diverse cellular processes(20, 21). Fundamental changes at the cellular and organism level including development(22), aging(23), the stress response(24), cell proliferation(25) and apoptosis(26, 27), were shown to be regulated by

miRNAs. Furthermore, miRNAs have been implicated in various diseases, such as diabetes(28), cancer(29), hepatitis C(30), neuro-developmental(31) and mental (32) disorders. Rapidly growing knowledge of miRNAs as potent regulators in health and disease, makes miRNAs attractive as targets for therapeutic intervention(33, 34) as well as for diagnostic markers(35, 36).

1.2.1. The Biogenesis of miRNAs and Target Recognition

MicroRNAs are 20-23 nucleotides in length(10). In mammalian cells, miRNAs are typically transcribed by RNA polymerase II (exceptions: a few are manuscript of RNA polymerase III) as long pri-miRNA molecules from intergenic regions of the genome, but may also be derived from intronic and exonic regions of coding and non-coding genes(12). The mechanism of transcriptional regulation of miRNAs is not fully determined, because identification of the miRNA promoters is still a challenging task(37). In the nucleus, canonical pri-miRNAs are capped with 7-methylguanosine and polyadenylated and cleaved by the RNAse III enzyme Drosha and its cofactor Pasha (or DGCR8) to produce a 60–100 nt precursor miRNA (pre-miRNA) hairpin molecule(38).

RAN-GTP and exportin-5 complex, subsequently transport the pre-miRNAs into the cytoplasm. In cytoplasm, Dicer, also an RNAse III endonuclease, interacts with TRBP (Tar RNA Binding Protein) to mediate further processing of pre-miRNA to form a mature 20–23 nt miRNA–miRNA* duplex(39). The duplex is unwound by a helicase and the mature miRNA is incorporated into effectors' complex known as miRISC (miRNA induced silencing complex)(37, 40, 41), while the miRNA* (read as miRNA "star") is degraded. The core components of miRISC are Argonaute proteins (AGO/EIF2C)(5) and GW182/TNRC6 protein families(42, 43). Within the RISC complex, miRNAs bind through imperfect base pairing to the 3'untranslated region (3'UTR) of target mRNAs(44). The binding specificity and efficiency is believed to be determined by 6–7 nucleotide sequence near 5′ region of miRNA. This sequence is called the "seed sequence" and is the initial binding site of the miRNA to the 3'UTR of the target mRNA(21). The subsequent procedures, depend on the degree of complementarily between the miRNAs and their targets. Imperfect complementarily of the miRNAs and the target mRNA, will cause translational repression of gene targets, while perfect matching, recruite the CAF1–CCR4 mRNA deadenylation complex to initiate mRNA degradation (40)**(Figure 1.1).**

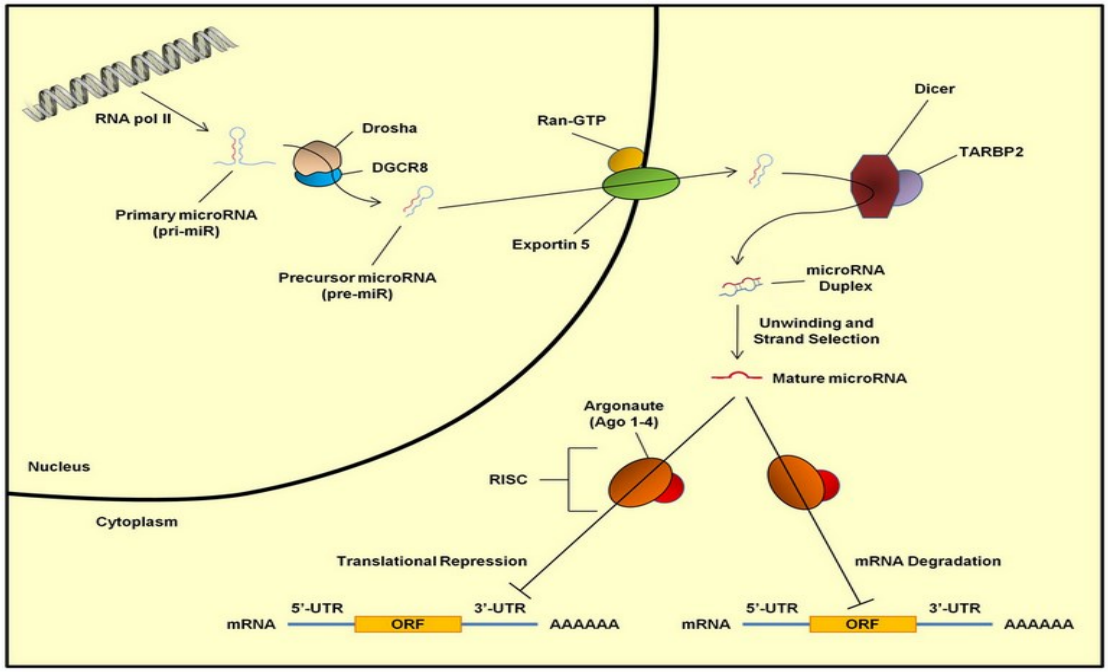

Figure 1.1. MicroRNA biogenesis. MicroRNA (miRs) are encoded by sequences located within intergenic regions or embedded in intronic sequences throughout the genome and transcribed by RNA polymerase II (RNA pol II) to generate long primary miR transcripts(pri-miR). The hairpin structure of pri-miRs are cleaved by the Drosha or DiGeorge syndrome critical region 8 (DGCR8) complex to yield precursor miRs (pre-miR). The pre-miR translocates from the nucleous into the cytoplasm via exportin5/Ran-GTP, and is consequently processed by the Dicer/TARBP2 (transactivation-responsive RNA-binding protein, also known as TRBP2) complex generating a miR:miR duplex. After unwinding and strand selection by unclear mechanisms, the mature miR is formed and loaded onto RISC (RNA-induced silencing complex) associated to Argonaute proteins (Ago1-4). The miR-RISC/Ago assembly complex can then target mRNAs through binding of the 3'-UTR (untranslated region) sequence or the mRNA open reading frame (ORF) which results in translation repression or mRNA degradation mediated possibly by Ago proteins(45).

1.2.2. Functional and Genomic Organization of miRNAs

Many miRNAs share the same seed sequence that is used in mRNA targeting. Four hundred twenty-six of the 1,112 mature and miRNA*s can be organized into sequence families(46). Two hundred ninety-nine of the 557 miRNA precursors can be organized into transcriptional units (cistrons, also known as genomic clusters). These cistronic miRNAs are typically located within 5 kb of each other in intergenic regions or within the same intron/exon and are co-transcribed and yield similar read counts for each member of a given miRNA precursor cluster(47).

1.2.3. Regulation of microRNA Expression

Several mechanisms, including gene amplification, deletion, epigenetic alterations, and single-nucleotide substitution, have been implicated in altered miRNA expression(48). Yang et,al in 2011 reviewed regulation of microRNA expression and function by nuclear receptor signaling. Nuclear receptors (NRs) are ligand-activated transcription factors that regulate the expression of target genes by binding to cis-acting DNA sequences. Since miRNAs are encoded by genes that are mainly transcribed by RNA polymerase II, their transcription can be regulated by a variety of transcription factors including NRs. For example, ERα binds directly to the promoter region of miR-221/222 and recruits NCoR and SMRT to suppress miR-221/222 expression. Androgen receptor(AR) can also bind to the promoter region of miR-221 to repress miR-221 expression in LNCaP cells. AR is a ligand-dependent transcription factor that regulates the expression of androgen target genes(49).

Post-transcriptional regulation has also been shown to essentially influence miRNA turnover rate or inhibitory activity. The 3′ end of mature miRNA can further be subject to a series of additional modifications such as uridylation that blocks Dicer processing and induces miRNA degradation and adenylation that affects miRNA stabilization. On the other hand in plants, 2′-O-methylation protects miRNA from uridylation, decay, and miRNA editing that makes an adenosine to inosine conversion resulting in altered mRNA target specificity. miRNAs expression can be dynamically regulated under certain conditions. For example, under inflammatory conditions, KH-type splicing regulatory protein (KSRP) can promote miR-155 maturation through binding to the terminal loop of pre-miRNA. In addition, expression of Dicer can be suppressed upon activation of various stress pathways, suggesting an implication of stress in alteration of miRNA expression(50). It has been demonstrated that the infection of Epstein-Barr virus (EBV) could influence human cellular miRNA expression. Godshalk et al. found that 99.5% of tested miRNAs displayed an average down-regulation of 19.92-fold upon initial EBV infection of primary cultured human B-cells, suggesting an activation of global suppression of miRNA-generating machinery(51).

Taken together, the growing body of literature has indicated that the miRNA biogenesis and its expression regulation are highly complicated, requiring participation of multiple

layers of transcriptional and post-transcriptional modifications and subject to tight and dynamic control under distinct physiological and pathological conditions(50).

1.3. microRNA and Cancer

Dysregulated miRNA expression is a common feature of solid and hematopoietic malignancies(52). The first demonstration of the link between miRNAs and cancer was reported in 2002 by Calin et al(52). They found that miR-15 and miR-16 are involved in the pathogenesis of chronic lymphocytic leukemia(CLL). Their evidence that suggests a role of tumor suppressor for miRNAs supported by the observation of down-regulation of miR-15a and miR-16–1 in two CLL patients(52-54). A study by Cimmino et al. in 2005, showed that miR-15a and miR-16–1 act as tumor suppressors by down-regulating B-cell CLL/lymphoma 2 (BCL2), a gene that is frequently up-regulated in CLL(55). Therefore, down-regulation of miR-15a and miR-16–1, which is mainly due to a genetic deletion, might promote B-cell proliferation in CLL (56).

Following, Several groups have studied the miRNA expression in cancer patients and found that miRNAs are differentially expressed in normal versus tumor tissues in different cancer types including leukemia(53), lymphoma(57), glioblastoma(58, 59), neuroblastoma(60), papillary thyroid carcinoma(61, 62), lung(63), breast(64, 65), liver (30), pancreas(66), gastric(35), colorectal(27, 67), ovarian(68), prostate(64, 69, 70), kidney and bladder cancer(71). Such researches revealed the aberration expression of miRNAs during carcinogenesis. The first report of miRNA deregulation in solid tumors was the observation of a consistent down-regulation of miR-143 and miR-145 in colorectal cancer(72). In the case of Lung cancer a reduction of >80% of let-7 expression was found by northern blotting in 44% (7 out of 16) of patients compared with healthy controls. Consequently many researches showed that profiles of miRNA expression are highly informative for tumor classification, prognosis, and response to therapy. Lu et al. at 2005 showed that miRNA expression profiles can be used in cancer diagnosis and human cancer classification(73).

In 2005, three reports provided the first mechanistic insight into how miRNAs might contribute to carcinogenesis. Two independent reports illustrated an interaction between miR-17-92 cluster and Myc(74, 75), and the third one uncovered the regulation of Ras by let-7(76). Lee et al showed that miRNA precursor processing reduce in cancer cells compared to normal human cell lines and tissues(77). Also miRNA processing

machineries, Drosha and Dicer, have a decreased expression in cancer cells. In ovarian cancer cases, the reduction of Dicer and Drosha correlates with a poor prognosis, suboptimal surgical cytoreduction and an advanced tumor stages(78).

1.3.1. miRNAs as Oncogenes or Tumor Suppressor Genes

There are strong evidences that miRNAs can function as tumor suppressors (anti-oncomiRs) or tumor promoters (oncomiRs)(56). miRNAs are often down-regulated in cancerous tissues and target oncogenic proteins. They are classified as tumor suppressor miRNAs(79). Let-7 is widely viewed as a tumor suppressor miRNA. Consistent with this activity, the expression of let-7 family members is down-regulated in many cancer types when compared to normal tissue and during tumor progression(80). Moreover many human let-7 genes, map to regions altered or deleted in human tumors, indicating that these genes may function as tumor suppressors(25). Takamizawa et. al. observed that postoperative survival time in lung cancer patients directly correlated with let-7 expression levels: patients with lower let-7 expression survived for less time than those with higher let-7 expression(81). Development of spontaneous tumors induced by deletion of a single miRNA, miR-122, in the liver indicates that this miRNA indeed functions as a tumor suppressor. MiR-122, the most abundant miRNA in liver, was first suggested as a tumor suppressor in liver due to its diminished expression in primary HCCs of human and rodent origin, and its ectopic expression studies in HCC cell lines and xenograft models(31, 32). Loss of miR-122 results in the up-regulation of its target genes, including Adam10/17, Igf1R, Srf, and Ccng1, and inhibits tumorigenic properties of HCC cells(32). Similarly down-regulation of miR-199a-3p that abundantly expressed in the liver, induces ERK signaling pathway partly through targeting PAK4(82). Moreover Dramatic tumor suppression by the adeno-associated viral delivery of miR-26a in a Myc driven mouse model of HCC suggests that miR-26a may inhibit tumor growth by directly targeting genes involved in the control of cell cycle, such as Ccnd2 and Ccne2(34).

However, microarray analysis has identified that there is an increase in some miRNAs in tumor tissues compared to normal tissues. miRNAs with increased expression in the tumor ,often target tumor suppressors, are considered as "oncomiRs"(79, 83). The OncomiRs promote tumor development by negatively inhibiting tumor suppressor genes and/or genes that control cell differentiation or apoptosis. OncomiRs are significantly over-expressed in various tumors because of gene amplification, epigenetic mechanisms or transcriptional

dysregulation(84). miR-17-92 cluster is a typical example, which is located at chromosome 13q31, a region amplified in lung and other malignancies(84). Myc-induced up-regulation of miR-17-92 cluster has been shown to enhance tumorigenesis and angiogenesis(85). Recent studies also revealed that miR-17-92 was up-regulated in sonic hedgehog-driven medulloblastomas and induced by N-myc in sonic hedgehog-treated cerebellar neural precursors(86). Among others oncogenic miRNAs, miR-21 which is widely up-regulated in different types of cancers has been shown to promote tumor growth by targeting phosphatase and tensin homolog (PTEN). PTEN is an important tumor suppressor that is involved in control of cell migration and invasion by inhibiting its downstream targets including FAK, MMP2 and MMP9(36). Also in breast cancer cells, silencing of miR-21 inhibited cell growth *in vitro* and *in vivo* by causing down-regulation of Bcl-2 and induction of apoptosis(87).

miRNA expression profiling have reported increased expression of miR-155 in various cancers. It's expression was significantly correlated with poor survival in pancreatic cancer patients(88). In another study, transfection of antimiR-155 oligonucleotides into pancreatic cancer induced the expression of tumor suppressor protein 53-induced nuclear protein 1 (TP53INP1) and enhanced apoptosis(89).

Furthermore, in a choline-deficient and amino-acid-defined (CDAA) diet-induced HCC model, many oncogenic miRNAs, including miR-155, miR-221/222, miR-21 and miR-181b/d, were up-regulated at an early stage of hepatocarcinogenesis(40-43). Interestingly, these miRs were reported to target tissue inhibitor of metalloprotease 3 (TIMP3)(40, 42, 43), which is involved in tumor invasion and metastasis as PTEN(37). miR-372 and miR-373 are two additional examples of oncogenic miRNAs that are shown to promote cell proliferation and tumor development by neutralizing p53-mediated CDK inhibition, possibly through direct targeting of the tumor suppressor gene LATS2. Further research is likely to add many more miRNAs to the growing list of oncomiRs(90).

1.3.1.1. miRNA-221: Its Role in Tumor Progression

miR-221 is a highly homologous miRNAs ,located in an intergenic region at chromosome Xp11. Sequence location Starts at 45605585 and ends at 45605694bp from pter (according to hg19-Feb_2009). miR-221 encoded along with miR-222 in cluster, containing identical seed sequences and both map to the X chromosome separated by 727 bases. In general, the microRNA genes are transcribed by RNA polymerase II, whereas RNA polymerase III is

also responsible for transcription of some other microRNAs. It is not known which RNA polymerase transcribes miR-221/miR-222. miR-221 and miR-222 were shown to be expressed as a single pri-microRNA transcript in c-kit positive HUVEC cells. In the following Pre-microRNA221 (Accession: MI0000298) with 110bp length has been formed and finally processed to 23 base pair mature miR-221 (Accession: MIMAT0000278)(91).

- **Regulation of miR-221**

Regulation of miR-221 has been investigated in rare research. In neuroblastoma miR-221 was shown to induced by MYCN. Given that MYCN is a major regulator of neuroblastoma tumor biology, Schulte et al in 2008 investigated if specific miRNAs are regulated by the MYCN transcription factor in neuroblastoma cells. Using a miRNA microarray containing 384 different miRNAs and a set of 160 miRNA real-time PCR assays to validate the microarray results, they showed the role of MYCN in regulation of 7 miRNA including miR-221. Additionally, they reported miRNA induction to be a new mechanism of gene expression down-regulation by MYCN(60). Santhekadur et al in 2012 unraveled a linear pathway in which Staphylococcal nuclease domain-containing 1 (SND1)-induced activation of NF-_B resulted in induction of miR-221 and subsequent induction of angiogenic factors Angiogenin and CXCL16. CXCL16 can be induced by TNFβ treatment via NF-_B activation, and both CXCL16 and angiogenin activate NF-_B, thus establishing a positive feedback regulation. Both CXCL16 and angiogenin activate Akt/mTOR signaling, which in turn is involved in CXCL16 and angiogenin expression and secretion. On the other hand, miR-221 targets phosphatase and tensin homolog (PTEN) and DDIT4, inhibitors of the Akt/mTOR pathway. Thus, an expansive protumorigenic signaling network lies downstream of SND1(92).

- **miR-221 in Tumorogenesis**

Many studies to date have been reported on the role of miR-221/222 in cancer development either as oncomiR or as tumor suppressors-miRs (anti-oncomiRs) which summarized in Table 1.1 and 1.2. The two studies that evidenced a tumor suppressive role for miR-221/222 in OTSCC and erythrocytes, indicating that microRNA function is exclusively dependent on the cellular contest and tumor type(93). In Luminal Breast Cancer , most high-grade tumors express low levels of miR-221/222(94). The roles of

miR-221/222 in cellular signaling pathways as an oncomiR or onco-suppressor-miR depicted in Figure 1.2 and 1.3. These findings provide evidence that a single miRNA, through its ability to modulate different genes that involved in the same network, may act as a strong inhibitor of the entire cellular pathway, suggesting a possible greater therapeutic potential for miRNAs than for a single gene(93).

Table 00.1.miR-221/222as oncogene

miRNA Target	**Deregulation in Cancer**
P27/Kip1	Giloblastoma, thyroid papillary carcinomas, hepatocellular carcinoma, breast, prostate and pancreatic cancer(95-100)
P57	Hepatocellular carcinoma(99, 100)
Puma	Glioblastoma(101)
ER-α FOXO3	Breast(102)
PTEN TIMP3	NSCLC, Hepatocarcinoma, giloma, gastric canser(100)
DDIT4	Hepatocellular carcinoma(103)
Bim	Prostate cancer(104)

Table 1.2.miR-221/222 as tumor suppressor genes

miRNA Target	**Deregulation in Cancer**
SODI MMP1	tongue squamous cell carcinoma (OTSCC)(105)
c-Kit	erythrocytes(106)
α6β4 integrin	luminal breast cancer(94)

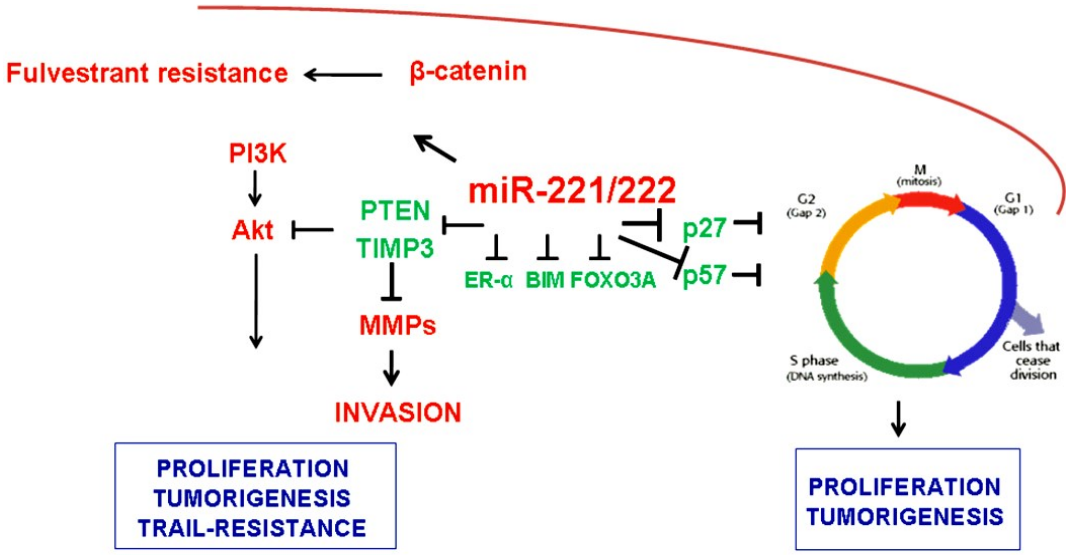

Figure 1.2.MiR-221/222 as oncomiRs MiR-221/222 act as oncomiRs by targeting important tumor suppressor genes such as PTEN, TIMP3, p27Kip1, p57, Bim. MiR-221/222 over-expression induces cell proliferation through the activation of cell cycle and the Akt pathway and blocks TRAIL-induced apoptosis. Moreover, miR-221/222 determine fulvestrant resistance through the activation of the β-catenin pathway**(93)**

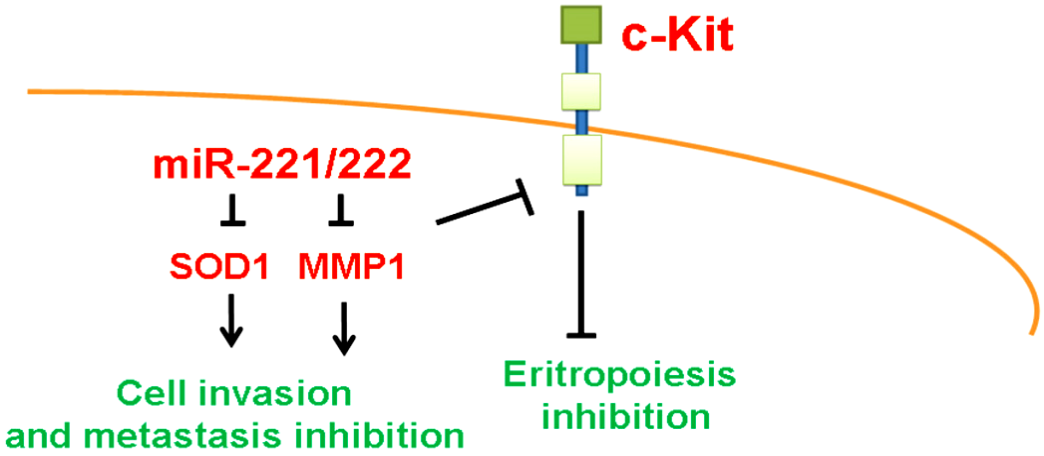

Figura 1.3. MiR-221/222 as tumor suppressor miRs. MiR-221/222 act as tumor suppressor miRs in the erythropoietic lineage cells, and oral tongue squamous cells by targeting c-Kit, matrix metalloproteinase 1 (MMP1) and manganese superoxide dismutase (SOD2) **(93).**

Almost all of the proposed target genes of miR-221 are associated with hallmark of cellular processes that characterized in cancer cells. miR-221 impairs apoptosis and induces cell proliferation in different types of cancer cells(93). These functional changes occur because miR-221 is capable of targeting and down-regulating known tumor suppressors; including p27Kip1, p57Kip2(70, 107), phosphatase, tensin homolog(PTEN)(107, 108), a tissue inhibitor of metalloproteinase-3(100), and the DNA damage-inducible transcript 4 (DDIT4)(103), a modulator of the mTOR pathway and p53 up-regulated modulator of apoptosis (PUMA)(107), a Bcl-2 homology 3 (BH3)-only Bcl-2 family member and a critical mediator of p53-dependent and p53-independent apoptosis.

Functional studies by Medina et al showed that miR-221 and miR-222 prevent quiescence when elevated during growth factor deprivation and induce precocious S-phase entry, thereby triggering cell death(109). Thus, the physiologic up-regulation of miR-221 and miR-222 is tightly linked to a cell cycle checkpoint that ensures cell survival by coordinating competency for initiation of S phase with growth factor signaling pathways that stimulate cell proliferation.

Gene expression profiling of miR-221-transfected-SNU-398 cells was analyzed by Negrini's research group in 2013. This analysis revealed that enforced expression of miR-221 in SNU-398 cells caused the down-regulation of 602 mRNAs carrying sequences homologous to miR-221 seed sequence within their 3_UTRs. Pathways analysis performed on these genes revealed their prominent involvement in cell proliferation and apoptosis. Activation of E2F ,MYC ,NF-kB ,and β-catenin pathways was experimentally proven. Some of the new miR-221 target genes, including RB1, WEE1(cell cycle inhibitors),APAF1(pro-apoptotic),ANXA1,CTCF (transcriptional repressor) , were individually validated as miR-221 targets in SNU-398, HepG2, and HEK293 cell lines(110). Regard to their inhibition of RB1 expression , levels of miR-221/222 appear to be major factors in cell-cycle control(111).

Yang et al (2014) showed a negative correlation between miR-221 or miR-222 and SIRT1(Sirtuin Histone Deacetylase SIRT1), but no direct target relationship was identified. Inhibition of miR-221 or miR-222 leads to reduced cell proliferation and migration and increased apoptosis in prostate cancer cells. These effects showed potentially mediated by up-regulation of SIRT1(112).

1.3.1.2. miR-199a: Its Role in Tumor Progression

miR-199 has been shown to be a vertebrate specific miR family that emerge at the origin of the vertebrate lineage. In 2003, two mature forms derived from the same precursor, miR-199-s (from the 5' half) and miR-199-a (from the 3' half), were cloned from human osteoblast sarcoma cells and mouse skin, respectively(113). Expression of the microRNA was validated in zebrafish, and its ends mapped by cloning. The two microRNA sequences were named miR-199a and miR-199a* (from the 3' arm), respectively. Later it was shown that both mature forms are expressed in humans, and it was renamed miR-199a-5p and miR-199a-3p, respectively(114). There are two loci that encode the precursor of miR-199a-5p and -3p in the human genome; one is on Chromosome 1(miR-199a-2, miRBase Accession MI0000281) and the other on Chromosome 19 (miR-199a-1, miRBase Accession MI0000242)(114, 115).

miR-199a-1 located on Chromosome 19 (Chr19) is embedded in the anti-sense strand of intron 15 of Dynamin 2 (DNM2), whereas miR-199a-2 located on Chromosome 1 (Chr1) is embedded in the anti-sense strand of intron 14 of Dynamin 3 (DNM3). Within Dynamin3 gene (Dnm3), miR-199a is associated with miR-214 and both miRs are transcribed together as a common primary transcript, demonstrated in mouse, human and zebrafish(116). The biological significance of the co-expression of miR-199a and miR-214 was revealed recently(115). it suggested that TP53 was activated by miR-214 and participated in the positive regulation of miR-199a/miR-214 via repressing DNMT1(Figure 1.4.). DNMT1 is primarily responsible for the maintenance, while DNMT3A and DNMT3B (de novo methyltransferases) are responsible for the establishment of genome DNA methylation patterns(115).

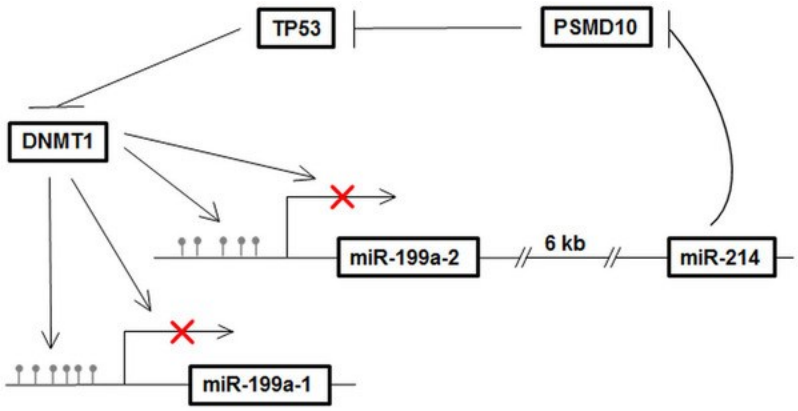

Figure 1.4. diagram describes the miR-199a/miR-214 self-regulatory network via TP53 and DNMT1 in TGCT(133).

There is no evidence of functional correlation between the expression of the dynamin genes and the miR-199a precursors: this may be due to the fact that the expression of the miRNA precursors is controlled by their own promoters.

- **Regulation of miR-199a**

Currently, two mechanisms that control the expression of miR-199a have been discovered. One is the regulation by transcription factors TWIST1 and EGR1 on Chr1; the other is the methylation status of miR-199a promoters on both Chr1 and Chr19. Studies in several cell lines showed that both promoter regions on Chr1 and Chr19 were hypermethylated (higher than 90%) in cancer cells but hypo- or not methylated in normal fibroblasts. Correspondingly the expression of miR-199a was higher in normal fibroblasts than cancer cells(117). Genome-wide DNA methylation profiling revealed that the promoter region of miR-199a-2 on Chr1 was hypermethylated in testicular germ cell tumors compared to the hypomethylation status in normal testicular fibroblasts. Apparently hypermethylation in testicular cancer cells caused severely reduced expression of miR-199a(118). Similar observations were made in non-small cell lung cancer, colorectal cancer and breast cancer cell lines (119).

Besides TWIST1, EGR1, and DNA methylation, other factors have been reported to control expression of miR-199a. Reduced expression of miR-199a-3p in hepatocellular carcinoma was shown to be mediated by histone modification and was independent of DNA methylation(120). *In vitro* cell model studies of liver injury and fibrosis showed that farnesoid X receptor (FXR) could negatively regulate miR-199a-3p at the post-transcriptional level(121). In mice cardiac myocytes, miR-199a-5p was upregulated during cardiac hypertrophy via β-adrenergic receptor (β-AR) stimulation, but downregulated by AKT activation during hypoxia (122). Another transcription factor, signal transducer and activation of transcription 3 (STAT3) was demonstrated to negatively regulate miR-199a-2 by suppressing its promoter activity in mice cardiocytes (123).

- **miR-199a in Tumorigenesis**

miR-199a has been shown to be implicated in a wide variety of cellular and developmental mechanisms such as various cancer development and progression, cardiomyocytes protection or skeletal formation(114).

During tumorigenesis, depending on the nature of the cancer, miR-199a, especially its -3p mature form, may act as either a potential tumor suppressor (anti-oncomiR) or an oncogene (OncomiR) (Table 1.3.).

- **miR-199a as Anti-oncomiRs**

MiR-199a was frequently down-regulated in human hepatocellular carcinoma (HCC)(124). HIF-1α was identified as a direct target. MiR-199a through targeting of HIF-1α could inhibit cell proliferation , as it shown in virto and in vivo studies(125). Another study in HCC showed that miR-199a-3p could target tumor-promoting PAK4 to suppress HCC growth through inhibiting the PAK4/RAF/MEK/ERK pathway both in vitro and in vivo(120). CD44+(126), pro-invasion molecule DDR1(127) and mTOR(128) has been shown as other targets of miR-199a in HCC.

Aside from the down regulation in HCC, In serous ovarian cancer patient tissues, miR-199a was down-regulated and significantly correlated with a poor prognosis. In osteosarcoma, miR-199a-3p showed reduced expression(129). Which affecting proliferation, migration and cell cycle progression. Molecules that were affected and which might be targets of miR-199a-3p include MET, mTOR and STAT3(130). Peng et al (2013) suggested that miRNA-199a-3p is associated with human gastric cancer through its ability to decrease cancer cell proliferation and target the mTOR signaling pathway(131). Similarly, Wu et al in 2013 reported that microRNA-199a-3p regulates endometrial cancer cell proliferation by targeting mammalian target of rapamycin (mTOR)(132). Using microarray and immunoblotting analyses it has been shown that miR-199a* targets the Met proto-oncogene(117).

Table 1.3.miR-199a regulation and function in human cancer

Cancer	miR-199a Expression	miR-199a Involved Biological Processes	Validated Targets #
Renal cell cancer	Down-regulated in RCC cells and tissues		GSK-3β (protein only)
Gastric cancer	miR-199a-3p up-regulated in patients with recurrence, miR-199a up-regulated in gastric cancer/metastatic tissues/Japanese gastric cancer tissues	Promotes proliferation and metastasis, progression-related	MAP3K11 (protein only)
Biliary tract cancer	miR-199a-3p up-regulated during malignancy		
HCC	miR-199a down-regulated	Anti-proliferation, anti-growth of HCC, PAK4/Raf/MEK/ERK pathway, anti-invasion modulator of cell cycle	HIF-1α (protein), PAK4 (protein), CD44 (mRNA), DDR1(mRNA), mTOR (mRNA)
Osteosarcoma	miR-199a down-regulated in cells and tissues	Anti-proliferation, anti-migration and affect cell cycle	MET? mTOR? STAT3?
Esophageal adenocarcinoma	miR-199a-3p and -5p up-regulated in worse survival patients		
Testicular germ cell tumors	miR-199a-3p and -5p down-regulated in cells and tissues	anti-invasion, anti-migration,anti-proliferation	PODXL (mRNA)
Breast Cancer	miR-199a down-regulated in tissues		
Ovarian cancer	miR-199a-2 up-regulated in ovarian cancer stem cells; miR-199a down-regulated in serous ovarian cancer	IKKβ/NFκB pathway,	IKKβ (protein)
Melanoma	miR-199a up-regulated in older adults (>60)	TLR-MyD88-NFκB	
Bladder cancer	down-regulated in cells and tissues Tumor	miR-199a-3p suppressive	KRT7 (mRNA)

- **miR-199a as OncomiRs**

Comparing two sets of acute myeloid leukemia (AML) patients, miR-199a was expressed much higher in patients with worse overall and event-free survival. High expression of miR-199a was also identified in AML patients with isolated trisomy 8. Chen et al showed that the property of ovarian cancer cells to enhance the inflammatory microenvironment as a result of the expression of an active IKKβ pathway. They identified that miR-199a-2 due to stimulation by TWIST1 down regulated IKKβ, shut down the IKKβ/NFκB pathway(133). Lijun et al identified a dramatically up-regulated microRNA, miR-199a-5p, in ADPKD(Autosomal Dominant Polycystic Kidney Disease) tissues and cell lines. Their data show that inhibition of miR-199a-5p suppressed cyst cells proliferation and induced cell apoptosis. We found that miR-199a-5p might exert this effect through targeting CDKN1C/p57(134).

Summary of key factors relating to miR-199a and its functions on different targets illustrated in Figure 1.5.

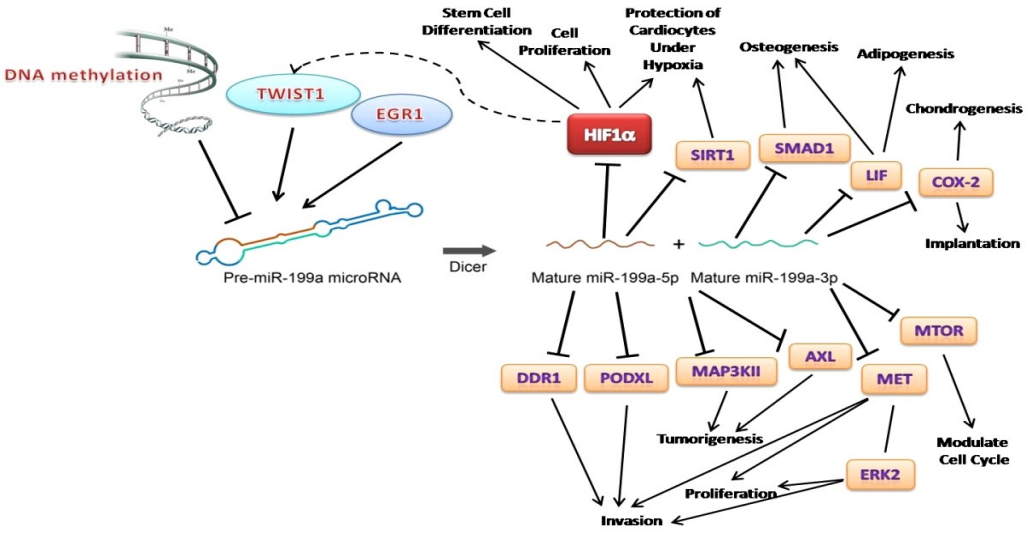

Figure 1.5. key factors relating to miR-199a function(114).

1.4. microRNAs in Liver Health and Diseases

1.4.1. The Role of miRNAs in Liver Development

MicroRNAs fine-tune all physiological and many pathological processes that are fundamental to normal liver functions as well as liver diseases. In the liver miRNAs regulate various cellular processes like inflammation, fibrosis, lipid and glucose metabolism(14). lin-4 and let-7, two miRNAs identified in C. elegans, are critical components to regulate different stages of development in C. elegans(135). However, its role in liver development has not been addressed because two studies that have reported phenotype of liver-specific Dicer 1 knockout mice used Alb-Cre mice where the gene is deleted after the development of the liver bud(136). Crossing Dicer 1 floxed mice to Afp-Cre or Foxa3-Cre may be helpful to address the role of miRNAs in liver development. Shu-hao Hsu et al have established essential role of miR-122 the most abundant, highly conserved, liver-specific miRNA in maintaining the differentiation state of the liver, since its loss induced proliferation of oval and bile duct cells in young adult mice and hepatocellular carcinoma HCC with age(137). In addition to miR-122, several other miRNAs appear to be involved in liver differentiation like miR-30a which its knockdown, results in defects in the intrahepatic bile duct in zebrafish and miR-23b which governs differentiation of hepatocytes and cholangiocytes by silencing Smad 3, 4 and 5. Many studies have revealed differential expression of miRNAs between embryonic and adult livers and correlated these findings with the critical factors involved in liver development. However, the expression of miRNA which is often observed in the total liver RNA, may not reflect the actual biological role of differentially expressed miRNA in specific cell types. Therefore, it is necessary to analyze the miRNA expression at different stages of liver development by monitoring their expression in specific cell types. Also, in absence of knockout animal models, it is difficult to pinpoint the developmental role of these miRs(37).

1.4.2. Involvement of Specific miRNAs in HCC

It has been well established that dysregulation in miRNAs is associated with liver diseases such as hepatocellular carcinoma(14). Pineue et al profiled miRNA expression in tissue samples (104 HCC, 90 adjacent cirrhotic livers, 21 normal livers) as well as in 35 HCC cell lines. They revealed set of 12 miRNAs (including miR-21, miR-221/222, miR-34a, miR-519a, miR-93, miR-96, and let-7c) was linked to disease progression from normal liver through cirrhosis to full-blown HCC and had the highest diagnostic value(103).

Some other studies have been revealed that specific miRNAs modulate various cellular processes in the liver and their aberrant expression correlates with the severity and poor prognosis of HCC. In one study, the expression of miR-199a, miR-92, miR-106a, miR-222, miR-17-5p, miR-18 and miR-20 correlated with the degree of tumor differentiation, suggesting the involvement of these miRNAs in HCC progression(138).

miRNA-122, an abundant liver-specific miRNA that modulates hepatic lipid metabolism(139), is often down-regulated in human HCC(140). Loss of expression of miR-21 correlates with loss of mitochondrial metabolic function that negatively affect on critical liver function, thereby contributing to the morbidity and mortality of liver cancer patients(141).

Examination of miRNAs in HCC with cirrhotic background revealed that members of the let-7 family and miR-145 were down-regulated(142). In these tissues and in HCC cell lines, miR-122 was also down-regulated, and its target gene product, cyclin G1, was highly expressed, promoting the growth of cancer cells(142). Other studies have shown that miRNAs associated with cell cycle inhibition (miR-34a, miR-101, miR-199-a-5p and miR-223) were down-regulated in HCC(143) , and those involved in cell proliferation and inhibition of apoptosis (miR-17-92 polycistron, miR-21, miR-96, miR-221 and miR-224) were up-regulated(99, 144-146). Furthermore, miRNA-221 is associated with tumor multifocality(147).

As demonstrated in other examples (Table 1.4 and Figure 1.6), aberrant miRNA expression leads to the dysregulation of critical cellular mechanisms and activation of tumorigenic pathways involved in tumor differentiation, diagnosis, staging, progression, prognosis and response to therapy(139-143, 148-152).

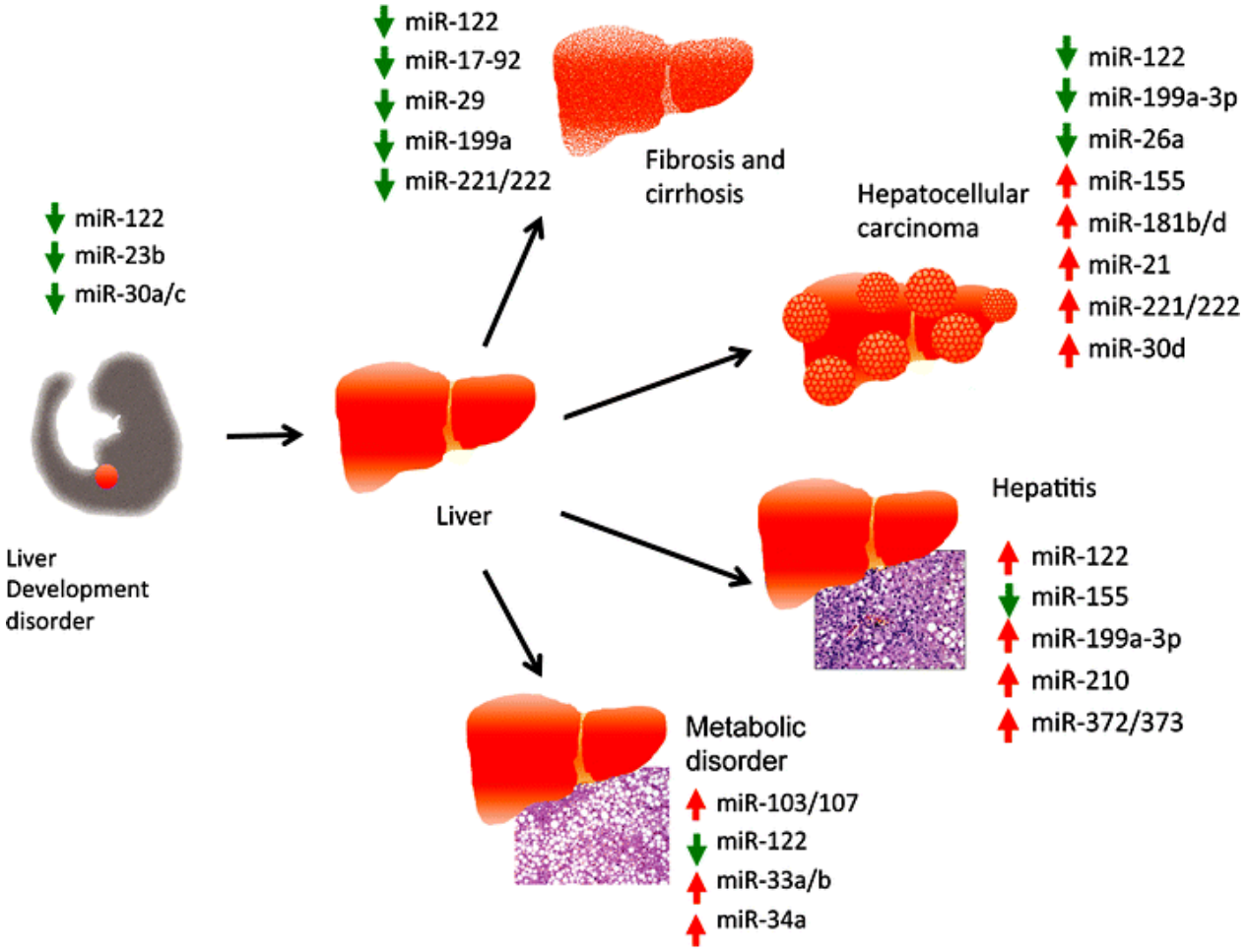

Figure 1.6: Summary of deregulated miRNAs identified in different liver disease. The arrow indicates the abnormal expression pattern of each miRNA in the designated disease. Red, up-regulated; Green, down-regulated(37).

Table 1.4. Differentially expressed miRNAs in liver tissues and hepatocellular carcinoma (HCC)

Sample type	Methods	miRNA*	Cellular target/Mechanism	References
Tumor tissue	Microarray,qPCR	miR-199a, miR-92, miR-106a, miR-222, miR-17-5p, miR-18, miR-20	Tumor progression	(138)
Tumor tissues, rat model of hepatoma	Microarray, Northern blot	*miR-122*, *let-7a*, miR-21, miR-23, miR-130, miR-190, miR-17-92 family	Tumorigenesis	(148)
Tumor tissue	Microarray	*miR-122*	Loss of mitochondrial metabolism	(141)
HCC cell lines	qPCR	*miR-122*	NDRG3	(149)
Tumor tissues, HCC cell lines	Microarray, qPCR Northern blot	*miR-122* *let-7 family, miR-145*	Cyclin G1	(142)
HCC cell lines	Western blot, Soft agar assay	*miR-122*	ADAM17, migration, invasion, anchorage-dependence, angiogenesis, metastasis	(150)
Tumor tissues, HCC cell lines	qPCR, Western blot	*miR-34a*	c-Met, apoptosis, cell cycle arrest, senescence	(151)
Tumor tissues, HCC cell lines	Microarray, Northern blot, Western blot	*miR-101*	Mcl-1, apoptosis, tumor suppression	(153)
Tumor tissues	Microarray, qPCR	*miR-199-a-5p, miR-223*	Cell cycle inhibition	(143)
Human and Woodchuck HCC cell lines	qPCR, Northern blot	miR-17-92, miR-21	Cell proliferation, apoptosis	(144)
Tumor tissues	qPCR, Northern blot	miR-221	CDKN1C/p57, CDKN1B/p27	(99)
Tumor tissues	Microarray, qPCR, Northern blot	miR-21	PTEN	(145)
Tumor tissues	Microarray	miR-224	Apoptosis inhibitor-5	(146)

1.4.3. microRNA-221 and HCC

Highly expression of miR-221 has been described as part of a cancer signature in human hepatocellular carcinoma (HCC) and its targeting by tailored treatments has been proposed. (124). The evidence supporting the role of miR-221 in HCC has been mainly focused on the discovery of miR-221 targets as well as on its possible therapeutic exploitations. Negrini in 2008 showed over-expression of miR-221 cause down-regulation of CDKN1B/p27 and CDKN1C/p57, known inhibitors of the cell cycle, indicating a reverse relation between their expressions in HCC. Down-regulation of both CDKN1B/p27 and CDKN1C/p57 occurred in response to miR-221 transfection into HCC derived cells and a significant up-regulation of both CDKN1B/p27 and CDKN1C/p57 occurs in response to antimiR-221 transfection. Also they proved that through controlling these two CDKIs, up-regulation of miR-221 can promote growth of HCC cells by increasing the number of cells in S-phase. Moreover the relevance of these studies in primary tumors matched HCC and cirrhosis samples were assayed for miR-221 as well as for CDKN1B/p27 and CDKN1C/p57 expression. They showed that MiR-221 was up-regulated in 71% of HCCs cases, whereas CDKN1B/p27 and CDKN1C/p57 proteins were down-regulated in 77% of cases. Significantly, the observed down-regulation of CDKIs were not present at the RNA level, indicating that the protein down-regulation was post-transcriptionally regulated. No association was found between miR-221 levels and the causes of underlying liver disease, in particular with viral infections, gender, histopathological grading and a-fetoprotein levels. So they proved *In vivo* regulation of CDKN1B/p27 and CDKN1C/p57 by miR-221 and suggested that miR-221 has an oncogenic function in hepatocarcinogenesis by targeting CDKN1B/p27 and CDKN1C/p57, hence promoting proliferation by controlling cell-cycle inhibitors(99). Negrini et al in 2009 showed that miR-221 also targets Bmf, a pro-apoptotic BH3-only protein and inhibits apoptosis of HCC cells. The analysis of HCC tissues revealed an inverse correlation between miR-221 and Bmf expression and a direct correlation between Bmf and activated caspase-3, as a marker of apoptosis. They also showed that high miR-221 levels were associated with tumor multifocality and reduced time to recurrence after surgery(147). miR-221 targets other tumor suppressors including phosphatase and tensin homolog, a tissue inhibitor of metalloproteinase-3(100), and the DNA damage-inducible transcript 4 (DDIT4), a modulator of the mTOR pathway(103) in HCC. Almost all of the proposed target genes are associated with hallmark cellular processes that characterize liver cancer cells: apoptotic resistance, increased cell growth

and proliferation and enhanced invasiveness(100). Santhekadur et al in 2012, unraveled a linear pathway in which SND1-induced activation of NF-κB resulted in induction of miR-221 and subsequent induction of angiogenic factors Angiogenin and CXCL16. Because SND1 regulates NF-κB and miR-221, two important determinants of HCC controlling the aggressive phenotype, they suggested SND1 inhibition might be an effective strategy to counteract this fatal malady(92). Recently, Fornari et.al was identified, MDM2, a known p53 (TP53) modulator, as a direct target of miR-221 and a feed-forward loop was described that sustains miR-221 aberrant expression. Interestingly, miR-221 can activate the p53/MDM2 axis by inhibiting MDM2 and, in turn, p53 activation contributes to miR-221 enhanced expression. Moreover, by modulating p53 axis, miR-221 impacts cell cycle progression and apoptotic response to Doxorubicin in HCC-derived cell lines. Finally, CpG island methylation status was assessed as a causative event associated with miR-221 up-regulation in HCC cells and primary tumor specimens. In HCC-derived cell lines, pharmacologically-induced DNA hypomethylation potentiated a significant increase in miR-221 expression. These data were confirmed in clinical specimens of HCC in which elevated miR-221 expression was associated with the simultaneous presence of wild-type p53 and DNA hypomethylation. In all, they revealed a novel miR-221 sustained regulatory loop that determines a p53-context-specific response to Doxorubicin treatment in HCC(154).

Yuan et al in 2013 hypothesized that modulation of miR-221 targets in primary hepatocytes enhances proliferation, providing novel clues for enhanced liver regeneration. They demonstrated that miR-221 enhances proliferation of *in vitro* cultivated primary hepatocytes. Furthermore they showed that adeno-associated virus-mediated over-expression of miR-221 in the mouse liver also accelerates hepatocyte proliferation *in vivo*. They identified Aryl hydrocarbon nuclear translocator (Arnt) messenger RNA (mRNA) as a novel target of miR-221, which contributes to the pro-proliferative activity of miR-221 and concluded that Pharmacological intervention targeting miR-221 may thus be therapeutically beneficial in liver failure by preventing apoptosis and by inducing liver regeneration(155). In 2011 Sharma et al. showed that ectopic expression of miR-221 protects primary hepatocytes and hepatoma cells from apoptosis. Importantly, in vivo over-expression of miR-221 by adeno-associated virus serotype 8 (AAV8) delays FAS-induced fulminant liver failure in mice. Additionally they demonstrate that miR-221 regulates hepatic expression of p53 up-regulated modulator of apoptosis (Puma), a well-known

proapoptotic member of the Bcl2 protein family. They suggested that miR-221 may serve as a potential therapeutic target for the treatment of hepatitis and liver failure(156).

Expression patterns of miRNAs and their role in the pathogenesis of hepatocellular carcinoma (HCC) was assessed by Pineau et. al. using 104 HCC, 90 adjacent cirrhotic livers, 21 normal livers as well as in 35 HCC cell lines. miR-221/222, the most up-regulated miRNAs in tumor samples, are shown to target the CDK inhibitor p27 and to enhance cell growth *in vitro*. In addition, they showed, using a mouse model of liver cancer, that miR-221 over-expression stimulates growth of tumorigenic murine hepatic progenitor cells. Taken together, these data revealed an important contribution for miR-221 in hepatocarcinogenesis and suggested a promising approach to liver cancer treatment(103). Park et al in 2011 conducted a preclinical investigation of the therapeutic efficacy of oligonucleotides directed against the oncogenic microRNA miR-221, which has been implicated in HCC. Chol-anti-miR-221 significantly reduced miR-221 levels in liver within a week of intravenous administration and in situ hybridization studies confirmed accumulation of the oligonucleotide in tumor cells *in vivo*. In the same period, chol-anti-miR-221 reduced tumor cell proliferation and increased markers of apoptosis and cell-cycle arrest, elevating the tumor doubling time and increasing mouse survival. They offered a preclinical proof of efficacy for chol-anti-miR-221 in a valid orthotopic mouse model of HCC, suggesting that this targeted agent could benefit treatment for patients with advanced HCC(79). The relationship between miR-221 over-expression and clinicopathological parameters in HCC formalin-fixed paraffin-embedded (FFPE) tissues was showed by Rong et.al. in 2013. They showed the relative expression of miR-221 in clinical TNM stages III and IV was significantly higher than that in the stages I and II. The miR-221 level was also up-regulated in the metastatic group compared to the non metastatic group. Furthermore, miR-221 over-expression was related to the status of tumor capsular infiltration in HCC clinical samples. Functionally, cell growth was inhibited, cell cycle was arrested in G1/S-phase and apoptosis was increased by miR-221 inhibitor *in vitro*. Likewise, miR-221 mimic accelerated the cell growth. They concluded that expression of miR-221 in FFPE tissues could provide predictive significance for prognosis of HCC patients. Moreover, miR-221 inhibitor could be useful to suppress proliferation and induce apoptosis in HCC cells. Thus miR-221 might be a critical targeted therapy strategy for HCC(157). High expression of miRNA-221 also can be used to predict local recurrence of HCC, and fold changes in miRNA-221 less than 1 can be used as a predictive

marker of metastasis after curative surgical resection in patients with HCC(158). Youn et al in 2011 proposed the potential of microRNA-221 dysregulation for predicting local recurrence and distant metastasis after curative surgery(158).

To investigate whether the serum miR-221 expression correlates with clinicopathologic features and the prognosis of hepatocellular carcinoma (HCC)patients, Serum miRNA expression was investigated in 46 HCC patients and 20 healthy normal controls by using real-time PCR technique, and then correlations between miR-221 expression and the clinicopathological features and prognosis of HCC patients were evaluated by Li et al in 2011. Results showed that high level of miR-221 expression was correlated with tumor size ($P < 0.001$), cirrhosis ($P = 0.003$) and tumor stage ($P = 0.016$). In addition, Kaplan–Meier survival analysis showed that the overall survival rate of the high miR-221 expression group (27.6%) was significantly lower than that of the low miR-221 expression group (62.3%, $P < 0.05$). Therefore serum miR-221, can provide a potential predictor for prognosis of HCC patients(159).

1.4.4. microRNA-199 and HCC

Among down-regulated miRNAs, the miR-199–miR-214 cluster is of particular interest because it is down-regulated in the majority of hepatocellular carcinomas (HCCs) (138, 142, 145, 160). Both Kim and Migliore identified the c-Met proto-oncogene as a target of the miR-199a-3p(117, 161). Particularly, they demonstrated that miR-199a-3p inhibits not only proliferation, but also motility and invasive capabilities of tumor cells by downregulating both c-Met and its downstream effector ERK2 (117). Its tumor suppressor function has been more strengthened because the mammalian target of rapamycin (mTOR) was also shown to be a target of miR-199a-3p. The inhibitory role of this microRNA in mTOR pathway is able to modulate cell proliferation and the invasion capability(128). The other strand of the same precursor miR-199a, miR-199a-5p, was demonstrated by Shen Q et al, to target Discoidin Domain Receptor (DDR1) gene. DDR1 is a tyrosine kinase receptor that is over-expressed in several human cancers(162, 163). More than 50% of HCC tissues and cells showed significant down-regulation of miR-199a-5p, with increased expression of the pro-invasion molecule DDR1. A down-regulation of miR-199a-5p expression, reported in HCC patients, could promote tumor progression enhanced by DDR1 up-regulation(127) . Interestingly, miR-199a was also involved in inflammatory

reactions associated with alcoholic diseases, most of which are mediated by molecules of the hypoxia-associated pathway(164). In this context, the expression of HIF-1α mRNA (hypoxia-inducible factor-1 α) and its coregulated gene, ET-1, were shown to be targets of miR-199(165), suggesting a new potential approach in the control of ethanol induced inflammation. Studies on steatohepatitis indicated that mice fed with different diets to induce alcoholic or non-alcoholic fatty livers showed different miR-199a-3p profiles, with down-regulation in the former and up-regulation in the latter (166).

In liver samples from patients with hepatitis C virus (HCV) infection, and mouse fibrosis livers induced by CCL4, both miR-199a-3p and -5p were up-regulated in a fibrosis progression-dependent manner(167). Detailed research showed that activated FXR protected liver cells from injury through the induction of LKB1. However, in fibrotic livers, lowered expression of FXR resulted in elevated miR-199a-3p, which in turn suppressed the expression of its direct target LKB1(121). miR-199 was shown to have an anti-viral effect. MiR-199-a was also identified as having a target sequence in the internal ribosomal entry site (IRES) of HCV viral genome, highly conserved in all HCV genotypes(168). Murakami et al. have shown that the inhibition of miR-199 activity by a specific AMO causes an increase of HCV replication, suggesting that this miRNA could negatively regulate the viral replication and proliferation(169). The viral replication effects of miR-199a-3p were also demonstrated for hepatitis B virus (HBV). Besides interaction with viral elements, its antiviral effects were shown to be caused by the down-regulation of several pathways including ERK/MAPK signaling, prostaglandin synthesis, oxidative stress signaling and PI3K/AKT signaling. miR-199a-3p may also play a role in regulation of HBV replication by targeting the HBV S protein coding region, the pre-S coding region and the ORF of HBV polymerase (170).

In summary, miR-199a is involved in various processes that become derailed in liver cancer in consequence of its stable down-modulation in cancer cells. In addition and notably, it also is involved in modulating the effects of HCC risk factors, such as the replication of hepatitis viruses or the effect of alcohol consumption.

1.5. Strategies for the Development of Therapeutics miRNAs

Since primary hepatic malignancies are typically characterized by frequent recurrence and poor response to therapy, there is a need for the discovery of novel bimolecular target in order to achieve efficient response to therapy(1).

In consideration of the advent of onco- and tumor suppressor-miRs, much interest has been focused on taking microRNAs from the bench to the bedside. The advantages of miR-based therapies are their smaller size and their ability to regulate a large number of cellular targets.

The application of miRNAs in cancer therapeutics normally involves one of the two strategies: (1) miRNA replacement by re-introducing miRNAs with tumor suppressor functions to restore their function 2) Inhibition of tumor-inducing miRNAs (also termed as oncomiRs) using antimiRNA oligonucleotides (AMOs), small molecule inhibitors, miRNA masking and miRNA sponges(171). Reasonable approaches for therapy would include achieving “gain” or “loss” of miRNA functions in the cancer cells depicted in Figure 1.7. In all, studies that assessed these approaches suggested that silencing or restoration of miRNA function can serve as a promising therapeutic strategy for cancer treatment. Furthermore, As miRNAs are associated with chemo- and radio-sensitization of cancer cells (172), a combination approach can also be developed for improved therapeutic outcome(84).

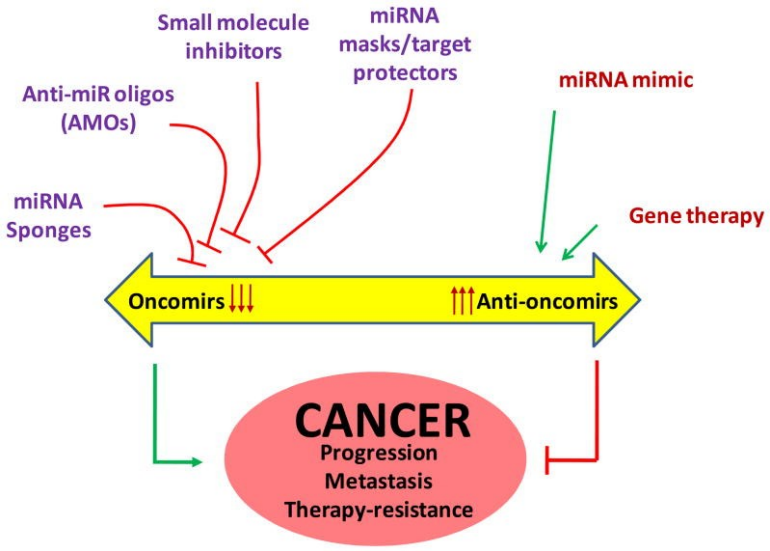

Figure 1.7. miRNA-based therapeutic strategies against cancer. (84)

- **miRNA mimic**

miRNA mimics are used to restore a loss of function. This approach, also known as 'miRNA replacement therapy', aims to re-introduce miRNAs into diseased cells that are normally expressed in healthy cells(171). In many cases, the re-introduction of these miRNAs leads to a re-activation of pathways that are required for normal cellular welfare and block those that drive the disease. Proof-of-concept for miRNA replacement therapy has been demonstrated by mimics of tumor suppressor miRNAs that stimulate antioncogenic pathways, apoptosis and ultimately lead to an eradication of tumor cells(34). Considering that most targeted cancer therapeutics developed to date tackle a gain-of-function, much of the excitement around miRNA replacement therapy stems from the fact that it provides a new opportunity to exploit tumor suppressors. miRNA mimics can be delivered systemically using technologies that are also used for therapeutic siRNAs. Therefore, the application of miRNA mimics will face less of a delivery hurdle compared with protein-encoding plasmid DNA previously used in gene therapy. Besides, miRNA mimics are expected to be highly specific and well tolerated in normal tissues. This supposition is based on the fact that miRNA mimics carry the same sequence as the naturally occurring equivalent and are expected to target the same set of genes. Since most normal cells already express the miRNA in question, administration of miRNA mimics to normal tissue is unlikely to induce adverse events as the cellular pathways affected by the mimic are already activated or inactivated by the endogenous miRNA(171).

- **Anti-microRNA oligonucleotides (AMOs)**

Anti-microRNA oligonucleotides (AMOs) have been generated to directly compete with endogenous microRNAs(173). AMOs can block the interactions between miRNA and its target mRNAs through competitive inhibition of base-pairing(174). AMOs against miR-21 were shown to inhibit the growth of MCF-7 cells *in vivo* (87). Other study has shown that intravenous administration of AMOs against miR-16, miR-122, miR-192 and miR-194 in animals offer efficient and sustained silencing of corresponding miRNAs(175). In the mouse model, inhibition of miR-221 with Chol-anti-miR-221 (a cholesterol-modified isoform of anti-221) resulted in reduction of tumor cell proliferation and increased levels of markers of apoptosis and cell- cycle arrest and, as a consequence, increased survival(79). Lab of Negrini has recently showed the effects of a modified AMO against miR-221 in reducing the number and size of HCC tumors in a miR-221 transgenic mouse

model(176). From these studies it is apparent that antimiR-221 could be exploited as a potential therapeutic target in HCC-related malignancies. However, the ability of AMOs to specifically inactivate endogenous targets has been shown to be quite inefficient. Thus, several modifications of AMOs have been generated to improve their effectiveness and stability such as the addition of 2'-Omethyl and 2'-O-methoxyethyl groups to the 5' end of the molecule(177). Studies have shown that targeting of miR-21, a microRNA that is over-expressed in many cancer types, by such methods effectively reduced tumor size in a xenograft mouse model based on MCF-7 cells(178).

AMOs conjugated to cholesterol (antagomirs) have been also been generated and have been described to efficiently inhibit microRNA activity *in vivo*(179). In addition, locked nucleic-acid antisense oligonucleotides (LNAs) have been designed to increase stability and have been shown to be highly aqueous and exhibit low toxicity *in vivo*(179). Antisense oligonucleotides targeted to miRNA was also effective primates(180, 181).

- **Small molecules inhibitors**

The down-regulation of miRNAs can also be achieved by targeting their biogenesis. In a recent study, several small organic molecules were screened for their potential to block miR-21 function and azobenzene was identified as an efficient inhibitor of miR-21 expression(182).

- **miRNA masking**

miRNA masking are relatively new strategies employed to down-regulate miRNAs. miR-masks are like AMOs, however, they do not directly interact with its target miRNA but instead bind to the pairing site of miRNAs in the 3' UTR of the target mRNA by fully complementary mechanism. In a rat model, miR-masks complementary to HCN2 and HCN4 genes masked the actions of their respective targeting miRNAs, miR-1 and miR-133(183). In another study, protection of squint or lefty mRNAs from miR-430 was also reported(184).

- **MicroRNA "Sponges"**

A novel technique for reducing the interaction between microRNAs and their targets is the use of microRNA sponges. MicroRNA sponges are single-stranded transcripts with repeated miRNA antisense sequences that can sequester miRNAs from endogenous targets(185). Repetitive antisense miRNA binding site in the microRNA sponges structure, assume to saturate the cellular pool of microRNA(173, 185, 186). Lewis et al. at 2003 have shown that when the sponge is expressed at high levels, it specifically inhibits the activity of a family of miRNAs sharing a common seed(187).

Sponges offer advantages over chemically modified antisense oligonucleotide inhibitors for many research applications. First, these antisense inhibitors appear to be specific for one miRNA as they depend upon extensive sequence complementarily beyond the seed region. Thus, to neutralize a family of miRNAs may require the delivery of a mixture of perfectly complementary oligonucleotides. In addition, many cells both *in vitro* and *in vivo* are resistant to the uptake of oligonucleotides. By contrast, for difficult-to-transfect cell lines or cells *in vivo*, the sponge transgene can be delivered by a viral vector. Inclusion of an open reading frame for a selectable marker or reporter gene in the vector allows for selection or screening(177). This approach has been successfully used recently to knockdown miR-223 using a lentiviral vectors(159).

1.5.1. Viral Delivery of miRNAs in Liver Disease

The primary challenge for gene therapy is to develop a method that can deliver a therapeutic miRNA to target cells where proper gene expression can be achieved. An ideal delivery method should: (1) allow efficient entry of miRNA and its carrier into the target cell; (2) protect the RNA against degradation by nucleases in intercellular matrices; and (3) be nontoxic. To function effectively in vivo, however, miRNA modulators must cross the membranes of tumor cells first and then bind their targets stably in the cytoplasm. In general, viruses are able to mediate gene transfer with high efficiencies, as they can infect every cell in a tumor tissue and may induce long-term expression of miRNAs in the infected cell. They can also be manipulated to alter their tropism so that they can infect the given cell type by binding to the cell surface receptor of choice. Therefore, viral vectors are the preferred choice for therapeutic studies of human diseases. However, acute immune responses, immunogenicity and insertion mutagenesis uncovered in gene therapy clinical trials have raised serious safety concerns on therapeutic application of commonly used viral vectors(188).

When compared with viral methods, non viral delivery approaches are less efficient. These methods have encountered serious obstacles in recent years, because naked RNAs are highly unstable in bio-fluids and are degraded rapidly by cellular nucleases. To overcome these challenges, efforts are being made to stabilize the miRNA by chemical modification, conjugation and encapsulation; and to improve its delivery to the target tissues and tumor cells in vivo(5).

Recombinant adenoviral (Ad) and AAV vectors were commonly used in such studies, because they do not integrate into the host genome, but replicate as episomes in the nucleus and stably express miRNAs. It was shown recently that AAV vectors transduce hepatocytes efficiently in vivo when injected through the intra-portal or intra-hepatic artery of healthy and cirrhotic rat livers, suggesting that they are convenient for transgene expression in the liver(189). AAV vectors, on the other hand, are single stranded adenoviruses devoid of critical genes involved in viral infection, making them relatively safe to administer in gene therapy trials. However, because of the difficulties in the construction of AAV vectors, self-complementary AAVs (scAAVs) that contain inverted repeats of its genome were developed. scAAVs can fold into dsDNA without the need for additional DNA synthesis or base-pairing between multiple vector sequences(5). Successful therapeutic delivery of miR-26a-expressing AAV vector has recently been reported in a murine liver cancer model(34). They showed that administration of miR-26a using adeno-associated virus (AAV) in an animal model of hepatocellular carcinoma (HCC) also inhibited tumor progression without toxicity .Hsu et al. (137)demonstrated the AAV-mediated delivery of miR-122 precursor genes to Myc-induced HCC model successfully inhibited tumor growth.

Oncolytic adenovirus(Ad)-mediated gene therapy present a new modality to treat cancer. These vectors attack tumors via replicating in and killing cancer cells as well as neighboring tumor cells. Numerous Ad vectors have been generated and tested in preclinical studies(190, 191), some of them reaching human clinical trials(192, 193). Ad5, the serotype most frequently used as the parental virus for vector construction, causes mild, self resolving illness in infants that results in long-term immunity to the virus . *In vivo*, Ad5 and Ad5-derived vectors replicate in various organs of the hamster, most prominently in the liver(194). A Recombinant Conditionally Replicative Adenoviruses (CRAds), whose replication was controlled by miR-199 has been recently developed in our lab by callegari, et al. The rAd-199T virus was designed to replicate in HCC cells which exhibit a strong down-regulation of miR-199. *in vitro* and *in vivo* properties of Ad-199T, demonstrated that this CRAd could replicate very poorly in cells expressing miR-199, while its replication could proceed regularly in cells lacking the expression of this miRNA.

CHAPTER 2.

SPECIFIC AIMS OF THE STUDY

CHAPTER 2 | SPECIFIC AIMS OF THE STUDY

Interest in microRNAs is now more than ever and the literature is getting enriched rapidly with reports on novel miRNAs, their validated gene targets and the development of miRNA-based therapeutics. While these studies are promising, further in-depth studies on candidate miRNAs will allow us to ascertain their potential as therapeutic targets for HCC treatment.

Aims of the present project are (I) Sequestering of miR-221 expression as an oncogene as well as restoration of miR-199a as a tumor suppressor gene in hepatocellular carcinoma through developing an effective viral delivery system for *in vitro* and *in vivo* studies and (II) Identifying new approaches to sensitize the HCC cells to conventional chemotherapy agents by means of microRNAs. These Goals achieve through three steps as follows:

I(a): Inhibition of miR-221 using a novel sequestering technology. We test the potential of “miRNA Sponge” technology for sequestration of endogenous up-regulated miR-221 in HCC cell lines. We study its inhibitory effect on known targets of miR-221 such as p27/kip1. This part of project provides proof of concept for a microRNA "sponge", as a novel microRNA sequestration technique which aid to identify the function of oncomiRs through evaluating the effects of the reduction of specific microRNAs in cellular pathways. This method often require viral vector delivery system, so the constructs can be expressed at high levels. For achieving prolonged inhibition of functional microRNA, we assess delivering of decoy target by engineering two different recombinant viral vectors as adeno(rAd) and adeno-associated (rAAV) virus that can be promisingly used as a therapeutic agent in gene therapy studies. Our optimized sponges provide a precious tool for studying the function of miRNA *in vitro* as well as *in vivo* and in particular for upcoming a need for developing novel and unconventional therapeutic approaches.

I(b): **Restoration of miR-199a through AAV delivery system.** We took advantage of AAV as an viral delivery tools to restore low level expression of miR-199a in HCC cell lines. Pre-miR-199a coding sequence are packaged in recombinant adeno-associated virus to achieve prolonged expression. Interestingly, miR-199a are among the miRNAs that down-regulated in HCC but most highly expressed in normal liver. In addition and notably, it is involved in modulating the effects of HCC risk factors, such as the replication of hepatitis viruses or the effect of alcohol consumption. It means that the functional mechanism of miR-199a is

complicated and delicately regulated. Thereby ,the recombinant AAV created in this study can be used as a promising tool to study the role and underlying molecular mechanisms of miR-199a in HCC by successful *in vitro* and *in vivo* studies. These findings may also have significant translational relevance for development of new targeted therapies.

II: The Assessment of the potency of miR-221 and miR-199a as therapeutic targets alone and in combination with conventional chemotherapeutic agent for HCC therapy. Emergence of miRNAs as a new class of gene regulators and their proven role in cancer progression has opened new avenues for therapeutic discovery. Negrini et al(176) recently showed that delivery of antimiR-221 oligonucleotides leads to a significant reduction of the number and size of tumor nodules in mouse model with inappropriate over-expression of miR-221. So we conceived to test miR-221 loss of function in combination with conventional chemotherapy to potentiates growth inhibitory function of sorafenib in HCC cells. Also we design to test efficiency of miR-199a expression restoration alone and in combination with sorafenib. miR-199a-3p was shown to be a modulator of cell cycle. It can sensitize the cells towards drug treatment through its target mTOR. Experiment using mimics miR-199a oligonucleotide proposed in HCC cell lines and mouse model as well.

By this means, we can be open a promising therapeutic regimen against liver cancer based on microRNA regulation therapy.

CHAPTER 3.

MATERIALS AND METHODS

3.1. Plasmids

A. pGL3-Control Vector (Promega, USA. Catalog No.# E1741):

Vector features:

1 ~ 41: Multiple cloning region

48 ~ 250: Promoter

280 ~ 1932: Luciferase gene (*luc*+)

281 ~ 303: GLprimer2 binding site

1964 ~ 2185: SV40 late poly(A) signal

2205~2441: Enhancer

2499 ~ 2518: RVprimer4 binding site

2756: ColE1-derived plasmid replication origin

3518 ~ 4378: β-lactamase gene (Ampr)

4510 ~ 4965: f1 origin

5096 ~ 5249: upstream poly(A) signal

5198 ~ 5217: RVprimer3 binding site

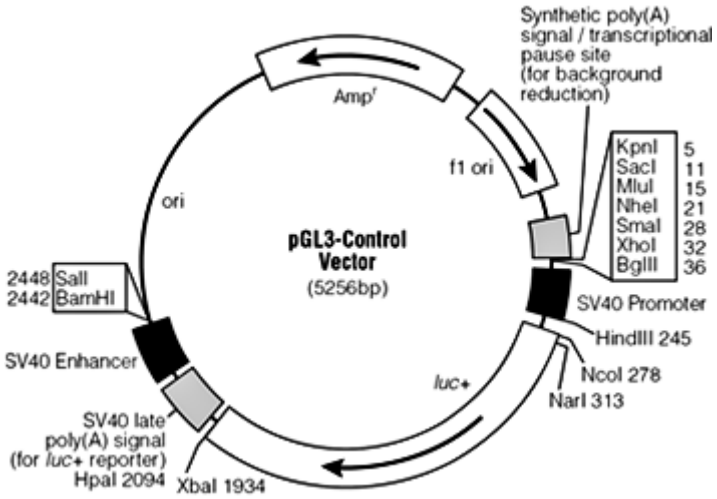

B. pAAV(DJ)-IRES-GFP Expression vector (Cell Biolabs, USA, Catalog No.# VPK-418-DJ)

Vector Features:

1 ~ 141: Left ITR

150 ~ 812: CMV Promoter

820 ~ 1312: human β-globin intron

1319 ~ 1373: MCS

1418 ~ 1996: IRES

1997 ~ 2716: GFP

2728 ~ 3206: PolyA

3246 ~ 3386: Right ITR

4303 ~ 5163: Ampicillin Resistance

• MCS Enzyme Sites: 5'- ClaI, BamHI, EcoRV, XhoI, EcoRI, XhoI -3'

• MCS Sequence:

CATCGATTGAATTGGATCCGATATCTAGACAGAAGCTTGACCTCGAGCACGAATTCCTGCAGGCCTCGAGG

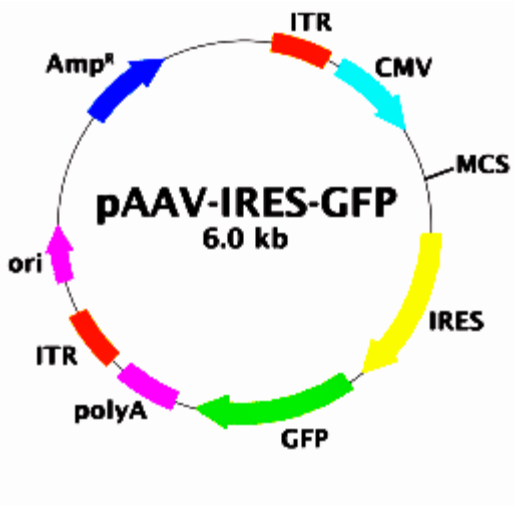

C. pAAV-DJ Vector (Cell Biolabs, USA. Catalog No. # VPK-418-DJ)

Vector Features:

6 ~ 1871: AAV-2 Rep

1888 ~ 4101: AAV-DJ Cap

5606 ~ 6466: Ampicllin Resistance

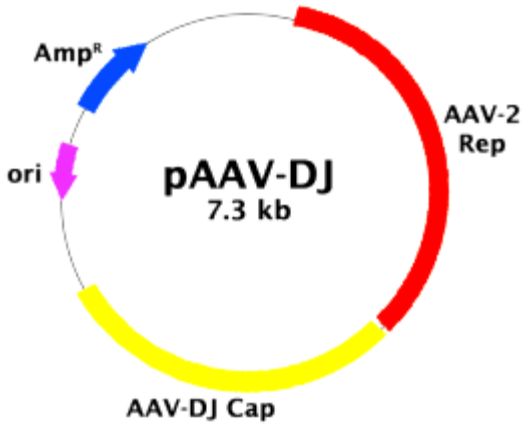

D. pHelper Vector (Cell Biolabs, USA. Catalog No. # VPK-418-DJ)

Vector Features:

1 ~ 5336: Adeno E2A

5337 ~ 8537: Adeno E4

8535~ 9280: Adeno VA

10182 ~ 11042: Ampicillin Resistance

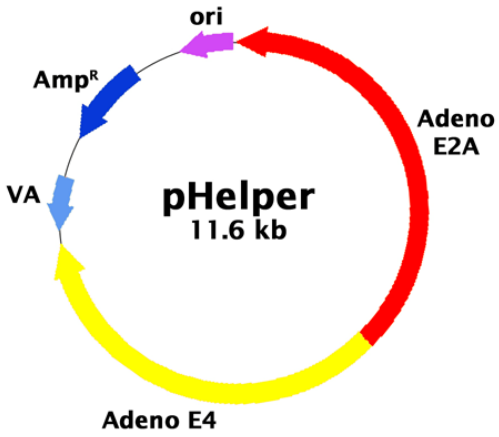

E. pAAV-GFP Vector (Cell Biolabs , Catalog No. # VPK-418-DJ)

Vector Features:

1 ~ 141: Left ITR

150 ~ 812: CMV Promoter
820 ~ 1312: human β-globin intron
1335 ~ 2075: GFP
2134 ~ 2612: PolyA
2652 ~ 2792: Right ITR
3709 ~ 4566: Ampicllin Resistance

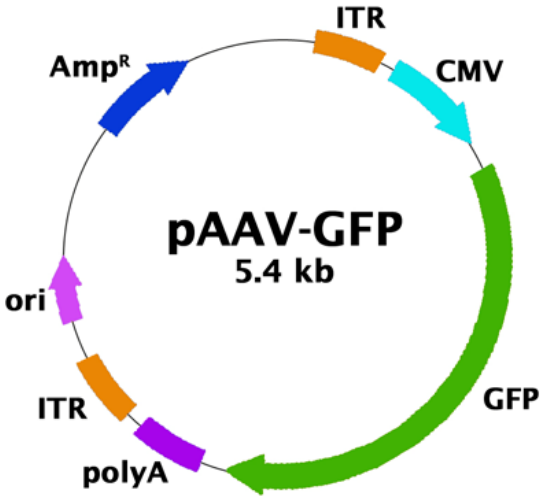

F. pIRESneo2 miR-199a

Gifted from Lab of Prof. Negrini

Vector Features:

This vector express miR-199a under control of CMV promoter. Also it consist of Ampicillin and Neomicin resistance genes. In this study, pIRESneo2 miR-199a was used as a source of miR-199a sequence.

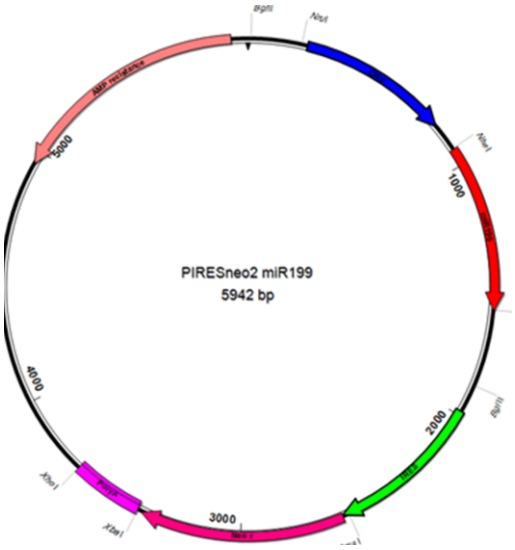

3.2. Primers

The Primers and probes that used in this study are listed in Table 3.1.

Table 0.1.List of primers and probes

Name	Sequence	Application
pAAV-antimiR221-1339F	5'TATCTAGTCTAGACCCGAAACCCA3'	Cloning steps of pAAV-miR-221sponge-IRES-GFP
pAAV-antimiR221_1941R	5'TACGCTTGAGGAGAGCCATT3'	
miR-199NheI FWD	5'GCTAGCGACCCCCAAAGAGTCAGACA3'	Cloning steps of pAAV-miR-199-IRES-GFP
miR-199NheI REV	5'GCTAGCCCACCCTCTTAGATGCCTCA3'	
luc_296_F	5'GTTCGGTTGGCAGAAGCTAT3'	Cloning steps of pAAV-IRES-luc constructs
luc_764_R	5'ATAGGATCTCTGGCATGCGA3'	
Hβ-actinDNA2810Fwd	5′-AGCTGTCACATCCAGGGTCC-3′	Quantitative real time PCR for normalizing
Hβ-actinDNA2960Rev	5′-TCATACTCCTGCTTGCTGATCC-3′	
wtAd5Fwd	5′-CGCATACGAGCAGACGGT GAAC-3′	Quantitative real time PCR
wtAd5Rev	5′-GCACTATAAGGAACAGCTGCGCC-3′	
EGFP_ 1318_Fwd	5'ACGTAAACGGCCACAAGTTC3'	Real time PCR
EGFP_1584_ Rev	5'AAGTCGTGCTGCTTCATGTG3'	
hsa-miR-221 **(Target Sequence)**	5'AGCUACAUUGUCUGCUGGGUUUC3'	TaqMan® MicroRNA Assays. miRBase Accessio Number MIMAT0000278, Primer Cat≠RT000524 Probe Cat ≠TM000524
hsa-miR-199a-3p **(Target Sequence)**	5'ACAGUAGUCUGCACAUUGGUUA3'	TaqMan® MicroRNA Assays. miRBase Accessio Number MIMAT0000232 Primer Cat≠RT2304 Probe Cat ≠TM002304
RNU6B **(Target Sequence)**	5'CGCAAGGAUGACACGCAAAUUCGUGAA GCGUUCCAUAUUUUU3'	TaqMan® MicroRNA Assays Primer Cat≠RT001093 Prob Cat≠TM001093

3.3. DNA and Protein Marker/Ladder

- **DNA Ladder(Gene Ruler):**

I. 123bp DNA Ladder(Invitrogen corporation, USA, Catalog No.# 15613-011) with size range between 123 to 3075bp.

II. 1 kb DNA Ladder(New England Biolabs, USA, Catalog No.# N3232S)with effective size range between 500bp to 10,002bp.

III. Lambda *Hind*III dsDNA Markers (Ambion, Inc. Applied Biosystems, USA, Catalog No.≠AM7720). 0.5 mg/mL.

- **Protein Marker**

SeeBlue® Plus2 Pre-Stained (Novex®)Life technology,USA. Catalog No.≠LC5925

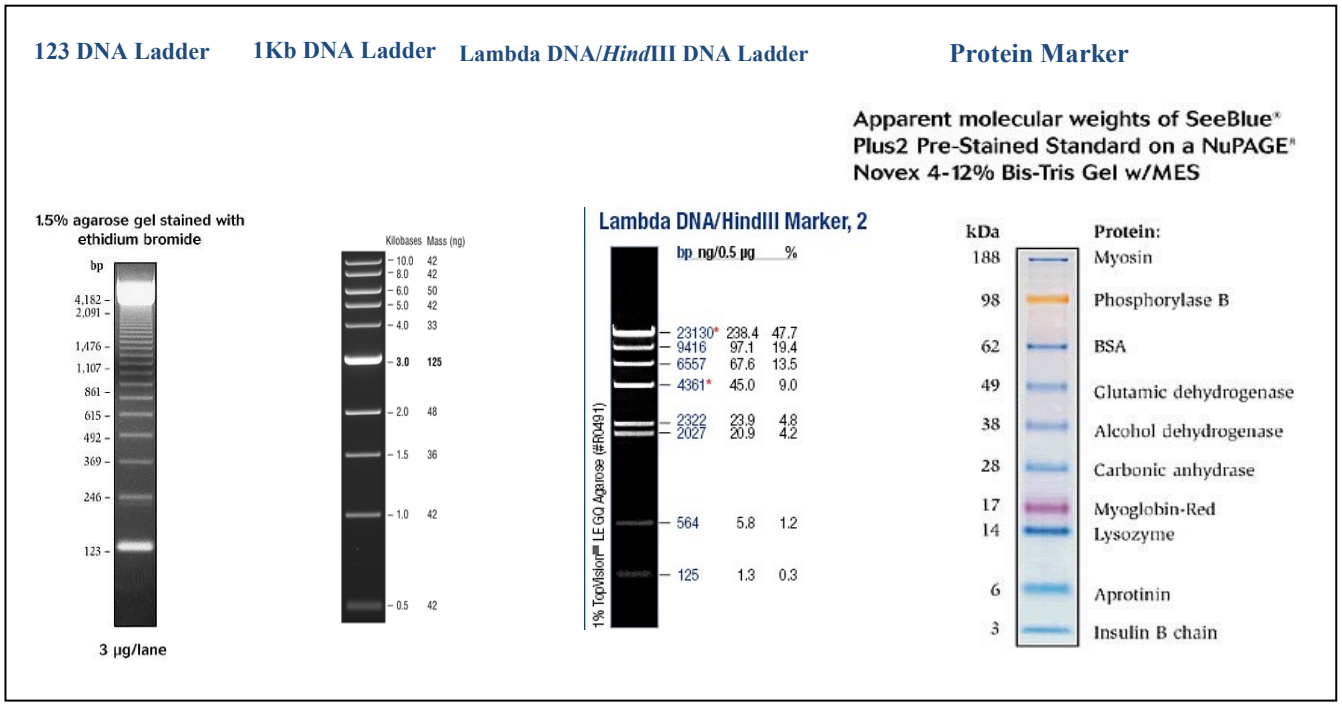

3.4. Vector Construction

3.4.1. Competent cell perparation

we used *E.coli* DH10β (Invitrogen, Carlsbad, CA, USA) in the form of competent cell in the cloning and sub-cloning steps. This strain is both endonuclease deficient (endA1) and recombination deficient (recA). recA1 mutation, improves clone stability by inhibiting the homologous recombination system; endA1 mutation, which inactivates the encoded periplasmic DNA-specific endonuclease, thereby enhancing DNA stability during transformation and greatly improves the quality of plasmid miniprep. the Genotype of host strain has indicated in Table below.

Host strain	Genotype
DH10B™	F– *mcr*A Δ(*mrr-hsd*RMS-*mcr*BC) Φ80*lac*ZΔM15 Δ*lac*X74 *rec*A1*end*A1 *ara*D139 Δ(*ara leu*) 7697 *gal*U *gal*K *rps*L *nup*G λ–

competent cells were prepared according to chemically protocol of B.calabretta,s lab, from Carmen Martin Seisdedos , a modification of C. T. Chung and R. H. Miller(195). The efficiency of competent cells was calculated after transformation of 100µl bacteria with 1 ng of pBluescript SKII at $3*10^7$ CFU/ug.

3.4.2. Glycerol Stocks Preparation

Every plasmid construct, whether it was created or purchased, preserved as a glycerol stock.

A. Reagent and solutions:

- Appropriate LB media, liquid & solid.
- 80% Glycerol (80ml autoclaved glycerol was mixed with 20ml autoclaved ddH_2O).

B. Procedure:

I. To create a glycerol stock:

1. Picked a single colony of the clone off of a plate and grew an overnight in the appropriate selectable liquid medium (e.g., LB with desired antibiotic).
2. Made a label (clone ID # and date) for the construct. Placed this label onto a sterile screw cap of cryo-vial and put them on ice
3. Added 0.5ml of the o/n culture to 0.5ml of 80% sterile glycerol in the sterile screw cap microcentrifuge tube (**on ice**) and vortexed.
4. Froze the glycerol stock at –80 ^{o}C.
5. Entered any and all pertinent information (host strain, vector, cloning site(s), selection criteria, date prepared, origin/source and/or reference, and any other important information) regarding this accession into the lab stock collection book. Also include a map or sequence if possible.

II. To streak out from a glycerol stock:

1. Determined the location of the construct
2. Took the tube and place it onto dry-iced box
3. Scraped off a portion from the top of the frozen glycerol stock using a plastic inoculating loop and stroke it onto your plate.

3.4.3. Restriction Enzyme Digestion

A. Material and reagents:

• DNA sample in water or TE buffer
• 10x digestion buffer
• Restriction enzyme

B. Procedure:

1. Pipetted the following material into a microfuge tube:

Material	Final concentration
Vector	0.1 to 4µg
RE Buffer (10X)	1X
RE enzyme	1-5u/µg DNA
ddH2O	Up to 30µl

2. Incubated for 2 hours at 37◦C.
3. 2 to 5 µl of the digested sample along with the un-cut DNA and a DNA marker were run on agarose gel and checked for the exact size of resulted fragments.

Tips:

• For checking DNA, 0.1 µg DNA used

• For cloning, 4 µg DNA used.

3.4.4. Ligation

Ligation was done with 50ng of cut and purified vector in combination with 3-fold molar excess of insert in the presence of 1µl T4 ligase (Fermentase,USA) and 1µL of 10X T4 Ligase buffer. Total volume was adjusted at 10µl with ddH2O. Ligation control was included with substituting the amount of insert with water. It allows evaluating the relegation efficiency. The ligation reactions were incubated at 15^{o}C in a thermocycler for overnight.

3.4.5. Transformation

A. Reagents and Solutions:

1. **5x KCM** KCl 0.5M
   $CaCl_2$ 0.15M
   $MgCl_2$ 0.25M

For Preparation of 10 ml 5x KCM,5 ml KCl (1 M)+ 1.5 ml CaCl2(1M)+ 2.5ml $MgCl_2$ (1M)+ 1ml miliQ H_2O were mixed , autoclaved and kept in4°C.

2. **SOC medium**

   2.0g Bacto-Tryptone, 0.5g Bacto-Yeast extract
   1ml 1M NaCl, 0.25ml 1M KCl
   1ml 2M Mg stock (1M MgCl2-6H2O, 1M MgSO4-7H2O), filter sterilize
   1ml 2M Glucose, filter sterilize
   Up to 100 ml ddH2O

Bacto-Tryptone, Bacto-Yeast extract, NaCl and KCl were added to 97ml ddH2O, stirred to dissolve, Then it was autoclaved and cooled to room temp. 2M Mg stock and 2M Glucose, each to a final concentration 20mM were added. The complete medium was filtered through a 0.2um filter. The pH was adjusted to 7.0.

B. Procedure:

1. The competent cells were allowed to thaw on ice for 30 minutes.
2. A tube containing :

arrangement	material	volume	Final concentration
Second	KCM(5X)	20µl	1X
Third	Ligation product or control vector	5µl	
First	Nuclease free water	75µl	--
Final volume:		100µl	--

was prepared

3. The cells were mixed by flicking the tube gently, then 100ul of bacteria added into tube(step 2)
4. Placed on ice for 20-30min.
5. Incubated at room temperature for 10 min.
6. 250ul of SOC medium(preheated at 37°C) was added and incubated for 45 min at 37 °C with shaking at ~225 rpm.
7. 100ul / and residue of the transformation mix were plated onto 100 µg/mL ampicillin plates(preheated at 37°C) and kept in the 37°C incubator and grown overnight.

3.4.6. Manipulation of DNA

In cloning and sub-cloning steps of plasmid DNA, GenElute™ Plasmid Miniprep Kit (cat≠PLN350) (Sigma life science, St Louis, MO) was used according the manufacturer's instruction . Also QIAGEN Plasmid Mini kit (cat≠12125) (Qiagen, Hilden, Germany) was used for amplifying the AAV Helper-Free System plasmids and preparation of high quality and quantity pAAV vectors for production of recombinant AAV according the manual of the company. For extraction of total genomic DNA from cultured cells QIAamp® DNA Mini and Blood Mini kit (cat≠51304) (Qiagen, Hilden, Germany) was used according to the manual of product supplier. Recovery and purification of DNA fragments from the agarose gel was performed with use of Wizard® SV Gel and PCR Clean-Up System (cat≠A9282) (Promega, Madison, WI, USA) according to its instruction.

3.4.7. Quantification of DNA and RNA

The amount of DNA and RNA was measured by a Nanodrop® spectrophotometer (ND-1000)(Thermo scientific), and the RNA quality of the samples was assessed by electrophoresis on agarose gel.

3.5. Cell Culture

3.5.1. Cell Lines and Culture

The hepatocellular carcinoma cell lines HepG2(P53 mutant) (ATCC HB-8065) and Hep3B(Null p53)(ATCC HB-8064)was obtained from the American Type Culture Collection (ATCC, Manassas, VA,USA). The human embryonic kidney cells, HEK293 and HEK293FT transformed with the SV40 large T antigen and Hela cells were obtained from Invitrogen (Carlsbad, CA, USA). Cell lines were Cultured in Dulbecco's Modified Iscove's Medium (IMDM) supplemented with 10% fetal bovine serum (FBS), 100U/ml 0.1% (v/v) Gentamycin (Sigma, St Louis, MO). Cells were maintained in a humidified incubator at 37°C and 5% CO2 and sub-cultured every 2-3 days .Early passages (passage 4–7) were used in each steps of this study.

3.5.2. Counting the Cell Number

At the indicated times, cells were trypsinized and the total number of cells per ml of media were counted using Scepter 2.0 Handheld Automated Cell Counter (Millipore Corporation, Billerica, MA, USA).

3.5.3. Transfection

Transient transfection of plasmid DNA was performed with Lipofectamine™ 2000 (Invitrogen, Carlsbad, CA) according to the manufacturer's instructions. The Cells were plated at a density of 1.0×10^5 and 1.0×10^4 cells per well in 24 and 96 well plates, respectively one day prior to transfection. Just prior to transfection the media was replaced with transfection media without antibiotic. Transient transfections were done using 0.4µg of plasmid diluted in Opti-MEM I (Invitrogen, Carlsbad, CA) as recommended by the manufacturer. In the case of antisense oligos transfection, 100nM of antimiR-221 was diluted in Opti-MEM I and used according to the manufacturer's manual. For production of rAAV particle, lipofectamine LTX (Invitrogen, Carlsbad, CA) was used according to manual of the manufacturer. All *in vitro* experiments were performed in triplicate.

3.6. Development of miR-221 Sponge/miR-199a Expressing Adeno and Adeno associated Virus.

3.6.1. Construction of miR-221Sponge Oligonucleotids

The Sponge oligonucleotids containing 4X miR-221 binding sites and its reverse complement were synthesized at IDT (Coralville, Iowa, USA). The sequences were as following:

1);5′CTAGAcccGAAACCCAGCATTGGATGTAGCTcccGAAACCCAGCAATTAATG TAGCTcccGAAACCCAGCAGAGAATGTAGCTcccGAAACCCAGCAGTTCATGTAG CTcccT-3′

and

2);5′CTAGAgggAGCTACATGAACTGCTGGGTTTCGggAGCTACATTCTCTGCTGG GTTTCgggAGCTACATTAATTGCTGGGTTTCgggAGCTACATCCAATGCTGGGTTT CgggT-3′

for miR-221 target and complementary oligos, respectively. Then The two oligonucleotides were annealed to make double stranded DNA fragment with *Xba*I overhangs. Annealing procedure is shown below.

Annealing procedure of forward and Reverse oligos for construction of miR-221sponge.

Material	**volume**	**Final concentration**
Forward oligomer(25 µM)	2 µl	1.66 µM
Reverse oligomer(25µM)	2 µl	1.66 µM
NaCl (0.5M)	6 µl	0.1M
ddH2O	20 µl	--
--	Final volume:**30 µl**	--
Incubate 2 min at 80◦C, switch off the Thermoblock and wait temperature is cooled to 35◦C		

Polynucleotide Kinase (PNK) (Roche Applied Science, Indianapolis,USA) was used to add a phosphate to the 5' end of a DNA fragment, for facilitating the cloning step. Phoshorylation was done as following:

Phosphorylation procedure of sponge fragment.

Material	**volume**	**Final concentration**
Sponge	µl	5 ng/ µl
PNK buffer (10X)	1.5 µl	1X
PNK enzyme	1 µl	
ATP (10mM)	1.5 µl	1mM
ddH2O	µl	--
--	Final volume:15 µl	--
Incubate 30 min at 37◦C and 10 min at 70◦C in thermoblock		
• PNK enzyme (Roche) • Store it at -20◦C until ligation		

We cloned annealed miR-221sponge into pGl3-Control vector (Promega, Madison, USA) using *Xba*I site immediately downstream of the firefly luciferase reporter gene.

3.6.2. Luciferase Expression Test

For luciferase expression test which demonstrate the expression of inserted luciferase reporter in pAAV-miR-221sponge-IRES-Luc, pAAV-miR-199-IRES-Luc and pAAV-IRES-Luc, HEK-293 cells were plated in triplicate wells of a 24-well plate at density of 1.0×10^5 and transfected one day later with 0.4µg of the indicated firefly luciferase reporter construct and 0.04µg (1:10 ratio of reporter construct) of pRL-TK vector (Promega Madison WI, USA), which contains the Renilla luciferase gene (Promega). A Renilla luciferase vector (pRL-TK)(promega) was used to normalize experimental variability caused by differences in cell viability or transfection efficacy. Cells were harvested after 24hr and washed with PBS following lysing using Passive Lysis Buffer (Promega,

Madison WI, USA). Firefly and renilla luciferase were measured by employing a Promega Dual-Luciferase® Reporter Assay System according to the supplemental manual. Data are represented as mean values ±SD from a representative experiment conducted with triple technical replicates and was shown as fold changes of average FF/renilla luminescence activity to non-transfected (NTC) control.

3.6.3. Duel Luciferase Reporter Assay

HEK-293 cells were seeded at density of 1.0×10^5 cells/well in 24-well plate. 24 h after seeding the cells were transfected by 200 ng of pAAV-miR-221Sponge–IRES-GFP vector or pAAV-IRES-GFP as a control, co-transfected along with 200 ng of firefly luciferase construct: pGL3-3'UTR p27(99) which encodes for a known target of miR-221; p27 upstream of firefly luciferase gene. The pRL-TK (Promega Corporation) was also transfected as a normalization control at 1:10 ratio respect to firefly luciferase plasmid. The Renilla luciferase vector (pRL-TK)(promega) was used to normalize experimental variability caused by differences in cell viability or transfection efficacy. One seeded well was left non-transfected (NTC) as a negative control. Transfection efficiency was monitored by fluorescence microscopy 24h after transfection due to appearance of expression of green fluorescent protein. Cells were trypsinized and collected 24 h after transfection and luciferase activity was measured using a dual-luciferase reporter assay kit (Promega Corporation, San Diego, CA, USA) and recorded by illuminometer. In brief, The cells were washed with PBS and lysed with Passive Lysis Buffer (PBL) (promega, cooperation) following shaking for 15 minutes. 20µl of lysed cells was added to a illuminometer tube containing 100µl of Luciferase Assay Reagent II (LAR II) (promega, cooperation), and placed into the illuminometer without vortexing. This reagent induces luminescence from the firefly luciferase expressed from pGL3. After recording the luminescence, 100µl of Stop & Glo® Reagent (promega, cooperation) was added to the reaction, vortexed quickly, and the tube was returned to the illuminometer. This reagent quenches the luminescence of firefly luminescence and simultaneously induces the reaction of the Renilla luciferase (as a transfection normalizer). So Firefly luciferase activity was used as the primary reporter to monitor the regulation of P27/kip1(known target of miR-221) and Renilla luciferase acted as a control reporter for normalization. The relative reporter activity was obtained through normalization to the firefly-renilla luc activity. Data were represented as mean values from three replicate and shown as percentage activity by setting the firefly luciferase of control transfected sample to 100%.

3.6.4. Development of Recombinant Adenoviruses

To produce the adenoviral vector, the adenoviral backbone from the replication-competent adenovirus vector Ad-199T (196) was employed. A 2,181bp fragment containing the SV40-Luciferase-miR-221sponge fragment from the engineered pGL3-control vector was sub-cloned into pAd-199T. pAd-Control vector without miR-221sponge sequence was also developed. The viral progeny were packaged with the use of 293FT cells and purified using PEG-it Virus Precipitation Solution (System Biosciences, Mountain View, CA), according to manufacturer's instructions. To determine the titer of rAd-199T-miR-221sponge and rAd-199T control viruses, 7.5×104 HepG2 cells were seeded in a 24 well plate; after 24 hours cells were infected with 1 microliter of either viruses. One day after infection, cells were harvested and total genomic DNA purified by QIAamp DNA Mini Kit (Qiagen, Hilden, Germany) according to manufacturer's instructions. 50ng of genomic DNA was analyzed by quantitative Real Time PCR, using EVA green (Biotium.Inc, Hayward, CA, USA) and primers specific for wild type Ad5 sequences: wtAd5Fwd, 5′-CGC ATA CGA GCA GAC GGT GAA C-3′; wtAd5Rev, 5′-GCA CTA TAA GGA ACA GCT GCG CC-3′. PCR was performed by initial denaturation at 95°C for 15min followed by 40 cycles of 95°C 30 sec, 58°C 30 sec and 72°C 30 sec. A standard curve was generated by using serial dilutions of the plasmid pAd-Control DNA (from 10ng to 100fg) spiked in 50ng of HepG2 non infected genomic DNA. The number of viral infectious units (I.U.) was determined comparing the threshold cycle (Ct) values of each sample with those of standard samples. Fluorescence was measured by using a Bio-Rad light Cycler Chromo 4 thermal cycler.

3.6.4.1. Assessment of Adenoviral Replication

Genomic DNA from infected cells was extracted with the QIAamp DNA Mini Kit (Qiagen, Hilden, Germany) according to manufacturer's instructions. Real Time PCR using EVA green (Biotium.Inc., Hayward, CA, USA) and primers wtAd5Fwd and wtAd5Rev specific for wild type Ad5 were utilized to assess viral replication in DNA content. Fluorescence was measured by using a Biorad-Chromo4 thermal cycler real time PCR instrument. Human β-actin gene was used to normalize data. Primers were as follows:

Hβ-actinDNA2810Fwd, 5′-AGC TGT CAC ATC CAG GGT CC-3′; Hβ-actinDNA2960Rev, 5′-TCA TAC TCC TGC TTG CTG ATC C-3′.

3.6.5. Development of Recombinant Adeno-Associated Virus

The AAV-DJ Helper Free Bicistronic Expression System (GFP) (Catalog Number : VPK-418-DJ) including: pAAV-DJ-IRES-GFP expression Vector (Part No. VPK-418), pAAV-DJ Vector (Part No. 340001) carrying the replication and capsid formation genes and pHelper Vector (Part No. 340202) harboring adenovirus needed genes for production of AAV viral particle as well as pAAV-GFP Control Vector (Part No. AAV-400) were purchased from Cell Biolabs, Inc.(San Diego, CA 92126 USA). The cassette of miR-221sponge from pGL3-Control was cloned upstream of IRES-GFP sequence into pAAV-IRES-GFP Expression Vector using *Xba*I site to produce "pAAV-miR-221Sponge-IRES-GFP" vector. In the interest of using this system *in vivo*, pAAV vector which simultaneously expressed miR-221sponge and Luc reporter gene were prepared by substituting the GFP cassette with Luc firefly gene in pAAV-miR-221Sponge-IRES-GFP. Recombinant pAAV-199-IRES-GFP was created by substitution of miR-199a expressing fragment by miR-221Sponge in pAAV-miR-221Sponge-IRES-GFP. The recombinant AAV expression and helper plasmids were prepared in sufficient quantities with high quality and purity using QIAGEN Plasmid Mini kit (cat≠12125) (Qiagen, Hilden, Germany). One day before transfection, sufficient 293FT cells plated to achieve 70-80% confluence on the day of transfection. Infectious rAAV was generated by triple-transfection of pAAV Expression Vector (pAAV-miR-221Sponge, pAAV-miR-199a or control vectors), pAAV-DJ, and phelper at molar ratio of 1:1:1 into 293FT a commonly used AAV production cells, contains the adenoviral E1A/E1B genes. A Total of 30µg of plasmid DNA was considered per each 175 cm2 cell culture flask. Transfection efficiency was monitored under fluorescence microscope by observation of bright green fluorescence. Following incubation for 3 days, the 293FT cells were harvested for virus purification. In brief, 0.5 M EDTA to a final of 10mM was added to the plate and incubated for 3 min at room temperature. Then the culture plate was gently shacked several times. Because viruses are present in both intact cells and the growth medium, all media including cells were harvested. The cell suspension was centrifuged at 1000 RPM for 5 min. rAAV crude lysates were prepared by resuspending the cell pellet in 2ml sterile PBS followed by four round of freezing-thawing by placing it alternately in a dry ice/ethanol bath and a water

bath of 37ºC. The lysates were centrifuged at 10,000 g for 10 min to remove cell debris of the host cells. rAAV was purified by using ViraBind™ AAV Purification Kits (Cell Biolabs, Inc.San Diego, CA 92126 USA) according to manufacturer's protocol. Purified Viral stocks were aliqouted and stored at –80°C.

3.6.5.1. Adeno-Associated Virus Titration by Real Time PCR

Genomic Titration of AAV

Titration of Genomic particle of virus was carried out in Bio-Rad light Cycler chromo 4 by absolute quantitative real-time PCR approach using EVA green (Biotium Inc, Hayward, CA, USA). The virus crude were supplemented with 10U DNase1 and nuclease reaction buffer (Promega, Madison, WI, USA), and incubated for 30 min at 37 ◦C, followed by an inactivation step (97 ◦C, 15 min). 1µl of virus stock and 10 to1000 serial diluted was analyzed by quantitative Real-Time PCR, using primers specific for GFP sequences(EGFP_ 1318_Fwd and EGFP_1584_ Rev ,see table 3.1 for details). Final concentration of 0.2µM of each EGFP 1318F and EGFP 1584R were used as forward and reverse primes respectively. PCR was performed by initial denaturation at 95°C for 15min followed by 35 cycles of 95◦C for 30 s, 58°C for 30 s and 72◦C for 30 and melting curve analysis. A standard curve was generated by using serial dilutions of the pAAV-IRES-GFP (from 10ng to 100fg). PCR products were analyzed by agarose gel electrophoresis (2%), the expected product length was 187bp through electrophoresis at 80mv in TAE 0.5X Buffer. Genomic particle per ml was calculated as: [a*b/c]*1000 in which **a**: number of molecule **b**: medium of concentration of DNA(pg) for technical triplicate and **c:** molecular weight of (pg).

Infectious Titration of AAV

Titration of infectious of virus was carried out in Bio-Rad light Cycler chromo 4 by absolute quantitative real-time PCR approach using EVA green (Biotium Inc, Hayward, CA, USA). For titration of the infectious particles, 7.5×10^4 Hella cells per well were seeded in 24-well plates and infected with 1µl of purified viral stock. Uninfected Hella cells served as negative control. After 72h, cells were trypsinized, pelleted and washed once with PBS then resuspended in 50µl PBS. Total genomic DNA of cell pellet was extracted by QIAmp DNA Mini Kit (Qiagen, Hilden, Germany) according to

manufacturer's instructions. 200ng of genomic DNA was analyzed by quantitative Real-Time PCR, using primers specific for GFP sequences (see table 3.1). PCR was performed by initial denaturation at 95°C for 15min followed by 35 cycles of 95◦C for 30 s, 58°C for 30 s and 72◦C for 30 and melting curve analysis. A standard curve was generated by using serial dilutions of the pAAV-GFP (from 10ng to 100fg) plus 200ng of Hella non infected genomic DNA. The number of viral infectious units (I.U.) was determined comparing the threshold cycle (Ct) values of each sample with those of standard samples.

3.6.6. Viral Infection for Molecular Assay of rAAV

Hep3B or HepG2 cells were seeded at 1.0×10^5 per well in a 24-well plate. Twenty-four hours post-seeding, rAd-199T-miR-221sponge or corresponding control virus and rAAV-miR-221sponge or rAAV-miR-199a or rAAV-control at appropriate MOI were diluted in 300µl of IMEM(+10%FBS and 1%Gentamicine) and added onto the cells. Transduction efficiency, was monitored using fluorescent microscope. 72hr post transduction, cells were harvested for RNA and protein analysis or subjected for cell viability and apoptosis assay .Trypsinized cells were pelleted in 0.3g for 5 min. Supernatant was removed, cell pellet was homogenized in TRIzol and followed for RNA extraction (see 3.23.1.1.) or frozen at -80◦C. For protein preparation cell pellets was washed with 500µl PBS and centrifuged one more time at 0.3g for 5min. The supernatant was removed and the pellet frozen at -80◦C or subjected freshly for protein analysis.

3.7. Combination therapy of AntimiR-221/miR-199a Oligonucleotides and Sorafenib.

3.7.1. Oligonucleotides and Therapeutic Reagent

A. The anti-miRNA oligonucleotide (AMO)

Anti-microRNA oligonucleotides was purchased from Integrated DNA Technologies (Leuven, Belgium) and scrambled negative control#2 was obtained from Ambion, Life Technologies (Grand Island, NY 14072 USA). Anti-Oligonucleotides contained the natural nucleotides and were chemically modified to contain a phosphorothioate (PS) linkage. The sequence of anti-miRNA oligonucleotide (AMO) against miR-221 was: 5'-mG*mA*mAmAmCmCmCmAmGmCmAmGmAmCmA mAmUmGmU*mA*mG*

mC*mU-3' (where ''m'' represents 2'-Omethyl RNA bases and asterisk [*] indicates the presence of a phosphorothioate internucleoside linkage. While unmodified oligodeoxynucleotides can display some antisense activity, they are subject to rapid degradation by nucleases and are therefore of limited utility. The simplest and most widely used nuclease-resistant chemistry available for antisense applications is the phosphorothioate (PS) modification. In phosphorothioates, a sulfur atom replaces a non-bridging oxygen in the oligo phosphate backbone. PS oligos can show greater non-specific protein binding than unmodified phosphodiester (PO) oligos, which can cause toxicity or other artifacts when present at high concentrations. Non-specific protein binding of PS oligos can be minimized by making the oligonucleotide as short as possible (thereby reducing PS content) or using chimeric designs with 2'-*O*-methyl RNA. The use of 2′-*O*-methyl (2'OMe) RNA in chimeric antisense designs, increases both nuclease stability and affinity (197) of the antisense oligo to the target mRNA [3–5]. These modifications, however, do not activate RNase H cleavage.

B. Pre-miR™ miRNA Precursor Molecule

Pre-miR™ miRNA Precursor Molecules are small, chemically modified double-stranded RNA molecules designed to mimic endogenous mature miRNAs. These ready-to-use miRNA mimics, although are similar to, but not identical to siRNAs. Pre-miR miRNA Precursor Molecules have been modified to ensure that the correct strand, representing the desired mature miRNA, is taken up into the RNA-induced silencing-like complex responsible for miRNA activity. They are not hairpin constructs, So should not be confused with pre-miRNAs

Pre-miR miRNA Precursors were used in this study to assess miRNA function by up-regulation of miRNA activity. They introduced into the cells using standard Lipofection methods for lipofectamine 2000. Thanks to their small size, they are easier to transfect than vectors, and can be delivered using conditions identical to those used for siRNAs. Positive and negative control Pre-miR Precursors be used to optimize transfection of Pre-miR miRNA Precursors. Pre-miR Precursors used in this study was as follows :

miRBase ID	**miRBase Accession #**	**Cat. #**	**Assay ID:**
hsa-miR-199a-3p	MIMAT0000232	AM17100	PM11779

C. Sorafenib(Nexavar®)

Sorafenib[N-(3-trifluoromethyl-4-chlorophenyl)-N0-(4-(2-methylcarbamoylpyridin-4-yl)oxyphenyl)urea] was provided by the Bayer Corporation (West Haven, CT). For *in vitro* studies, sorafenib was dissolved in Cremophor EL/95% ethanol (50:50; Sigma-Aldrich) and diluted in 10% FBS-containing IMDM to the desired concentrations. Drug concentrations were chosen in accordance with serum concentration that can be achieved in clinical settings. Cremophor EL/95% ethanol (50:50) was added to cultures at a concentration equal to that of drug-treated cells, as a solvent control.

3.7.2. IC50 Determination of Sorafenib

For determination of the IC50 of sorafenib in HepG2 and Hep3B cells, 1.0×10^4 cells were seeded in a 96-well plate and treated with increasing doses of sorafenib from 0.01μM to 10μM. After appropriate time point cells were incubated with CellTiter-Glo® Luminescent Cell Viability kits (Promega Corporation , 2800 Woods Hollow Road , Madison, WI 53711-5399 USA)according to manufacturer's instruction. Controls received Cremophor EL/95% ethanol (50:50) at a concentration equal to that of drug-treated cells. The IC50 value of sorafenib, at which 50% of the cells were growth-inhibited compared with control, was calculated based on the changes of luminescence measured by Infinite F200 PRO Multimode microplate reader(TecanGroupLtd,Seestrasse1038708 Männedorf ,Switzerland).

3.7.3. Combined Anticancer Effects of Sorafenib and Oligos (Anti-miR or pre-miR miRNA Precursor)

HCC cells ,Hep3B and HepG2, were seeded in a 24-well plate (1×10^5 cells per well) or a 96-well plate (1×10^4 cells per well) and incubated at 37°C. Just prior to transfection the media was replaced with transfection media without antibiotic (400μl and 50μl in a 24-well and 96-well plate scales respectively). The cells were then transfected with oligo inhibitor or pre-miR miRNA Precursor at a final concentration of 100nmol/L and Sorafenib at established concentration alone or in combination. Scramble miRNA inhibitor, vehicle and untreated negative control also were considered. Transfection were completed by using lipofectamin 2000(invitrogen) as recommended by the manufacturer. Transfection efficiency of Oligonucleotides was measured using a BLOCK-iT™ Fluorescent Oligo control for lipid transfection Catalog No. ≠460926. The

transfected/treated cells were analyzed for apoptosis and cell viability after 24 and/or 48 hours or harvested and cellular or molecular analyses were done on cell pellets. For each experiment triple wells were conducted.

3.7.4. *In vivo* study

All animal experimentation were undertaken in accordance with the National Institute of Health Guide for the Care and Use of Laboratory Animals, with the approval of institutional ethical committee in Italy. The miR-221 transgenic strain (TG221), which is predisposed to the development of liver cancer, were used for evaluating the anti-tumor activity of miR-199a treatments and its combination with chemotherapeutic treatment in vivo. TG221 mouse strain has an increased susceptibility to the carcinogen diethylnitrosammine (DEN) (Sigma-Aldrich, St.Louis, MO, USA) and tumors exhibit a miRNA profile similar to human HCC, including the down-regulation of miR-199a.

The mice were maintained in a vented cabinet at 25°C with 12-hour light-dark cycle and provided food and water ad libitum.

To facilitate tumor development, DEN was injected intra-peritoneally (7.5 mg/kg body weight) at day 10 after birth. At 5 months after birth, mice were randomly distributed into four groups (n=6 per group) and treated as follows:

- Group 1: received three intraperitoneal injections of miRNA-199 mimic every week for three weeks, for a total of nine injections (1 mg in total);
- Group 2: received a dose of Sorafenib (5mg/kg) x os every day for a total of 21 days;
- Group 3: received both miRNA-mimic and Sorafenib treatments as described above;
- Group 4: was untreated and represented as the control group.

The miRNA mimic miR-199a oligonucleotide was obtained from Axolab (Kulmbach, Germany). Sorafenib (Bay 43-9006) was obtained by Selleckchem (Munich, Germany). The mice were sacrificed at 6 months of age and subjected to autopsy. Livers were partly fixed in 10% formalin for histopathological investigations and partly frozen in liquid nitrogen for molecular studies. Liver RNA was isolated by using Trizol reagent (Invitrogen), according to the manufacturers' procedures.

3.8. Quantitative Molecular Assays

3.8.1. miRNA Analysis

- **RNA isolation**

Total RNA was isolated from cultured cells in duplicate at appropriate time point post-transfection and homogenized in 1mL of TRIzol®Reagent(Ambion®) (Invitrogen, Carlsbad, CA, USA). The homogenized samples were incubated for 5 minutes at room temperature to permit complete dissociation of the nucleoprotein complex. 0.2 mL of chloroform per 1mL of TRIzol was added and the tubes were shaked vigorously by hand for 15 seconds. After 2–3 minutes incubation at room temperature, the samples were centrifuged at 12,000 × g for 15 minutes at 4°C. The aqueous phase of the samples were removed and placed into new tubes. 0.5 mL of 100% isopropanol was added to the aqueous phase, per 1mL of TRIzol® Reagent used for homogenization. The samples were incubated at room temperature for 10 minutes followed by centrifuge at 12,000 × g for 10 minutes at 4°C. The RNA pellets were washed with 500µL of 75% ethanol. the samples were vortexed briefly, then centrifuged at 7500 × g for 5 minutes at 4°C. The wash was discarded. the RNA pellets were air dried for 5–10 minutes and resuspended in 30µl of in RNase-free water. Absorbance of RNA at 260 nm and 280 nm was used to determine concentration. Extracted RNA were qualified on the 0.8% agarose gel.

- **miRNeasy Kit Purification**

The miRNeasy Mini Kit allows purification of miRNA with total RNA for use in a variety of applications, including: Quantitative, real-time RT-PCR. miRNeasy Mini Kit used according to manufacturer's manual(Qiagen Catalog NO.≠217004).

- **miRNA TaqMan RT-PCR for Quantification of miRNA**

The mature miRNA was quantified by quantitative PCR (qPCR) using the TaqMan microRNA Assays (Applied Biosystems, Grand Island, NY, USA). To measure the amount of mature miRNA, a two steps TaqMan real-time PCR analysis was performed, using the custom primers and probes supplied in TaqMan® MicroRNA Assays kit (Applied

Biosystems, Grand Island, NY, USA)(see table 3.1). Reverse transcription reaction was done starting from 5ng of total RNA. In a reaction volume of 7.5µl, cDNA was synthesized using reverse transcriptase and the stem–loop primer for miR-221/miR-199a-3p (Applied Biosystems; cat# PN 4427975) or RNU6B (internal control; Applied Biosystems; PN 4373382). The reverse transcriptase reaction was performed by incubating the samples at 16°C for 30 min, 42°C for 30 min, and 85°C for 5 min. Subsequently, qPCR (10mL reaction) was carried out in triplicate using a 1:15 dilution of cDNA , 5µL of the TaqMan 2✕ Universal PCR Master Mix and 0.5µl of TaqMan MicroRNA Assay (20✕). The PCR mixtures were incubated at 95°C for 10 min, and this was followed by 40 cycles of 95°C for 15 s and 60°C for 60 s in Bio-Rad light Cycler chromo 4. The reference gene was U6 snRNA (RNU6B, Applied Biosystems, Grand Island, NY, USA).

Using iCycler iQ5 optical system software (BioRad, Hercules, CA), threshold cycle (beginning of the PCR exponential phase) values were analyzed. The levels of miR-221/ miR-199a-3p expression were normalized after subtracting the Ct value of the U6 snRNA internal control from that of miR-221/ miR199a-3p Ct value for samples. The relative expression levels of miRNAs were calculated using the comparative ΔΔCt method. The fold changes in miRNAs were calculated by the equation $2^{-\Delta\Delta Ct}$. Down/Up regulation of miRNAs were established when the differences in miRs expression were statistically significant between antimiR/ mimics treated and untreated control samples ($P<0.05$).

3.8.2. Protein assay

- **Protein Preparation**

Total protein from mammalian cell lines were prepared using RIPA lysis buffer (150mM NaCl, 0.1% SDS, 0.5% sodium deoxycholate, 1% NP-40) (Sigma, St Louis, MO) with complete protease and phosphatase inhibitor cocktails (Sigma, St Louis, MO,USA). Homogenates were then centrifuged at 13000 rpm for 15 min at 4°C and supernatants collected. Protein concentration was measured using Bradford Reagent and the BSA Protein for tracing a standard curve.

- **Western Blotting**

A. Reagents and Solutions

- **SDS-PAGE Running Buffer**
  Tris-base 3.0 g
  Glycine 14.4 g
  20% SDS 5 ml
  Add ddH2O to 1 L

- **Western Blot Transfer Buffer**
  Tris-base 3.0 g
  Glycine 14.4 g
  Methanol 200 ml
  Add ddH2O to 1 L

- **TBS Buffer(pH 7.4)**

  Tris-base 2.420 g
  NaCl 8.78 g
  Add ddH2O to 1 L
  Adjust the pH to 7.4

- **TBST Buffer**
  0.05 % tween 20

  Add to TBS Buffer

- **Western Blot Blocking Buffer**
  5% milk

  Add to TBS Buffer

  Mix well and filer

- **Ponceau Red Staining Solution**
  Ponceau S 0.5g

  Acetic acid 25 ml

  Add ddH2O to 500 ml

B. Procedure

Thirty micrograms of total protein extracted were loaded onto 4-15% Mini-PROTEAN® TGX™ Precast Gels (Bio-Rad Laboratories,Hercules,CA94547). The separated proteins were transferred to PVDF membranes (BioRad) for 2h at 100mA. After blocking with 5% non-fat milk ,the membrane was incubated with CDKN1B/*p27* primary antibody (BD Transduction Laboratories™, 610242, dilution 1:1500). Beta-actin (Sigma

Aldrich,A4700,dilution 1:1000) was used for normalization purposes at 4◦C overnight for overnight. The membrane was washed three times in TBST buffer, each for 10min. Then followed by incubation with Anti-Mouse IgG (whole molecule)–Peroxidase antibody produced in rabbit (Sigma Aldrich,A9044 dilution 1:10000) to recognize the primary antibodies for 1hr. at room temperature. Signals were developed with Precision Plus Protein Dual Color Standard (BIO-RAD) and Protein bands were visualized using the ChemiDoc^{TM}MP Imaging System and quantified using Image lab 4.0 software (Bio-Rad Laboratories,Hercules,CA94547).

3.9. Quantitative Cell Analysis

3.9.1. CellTiter-Glo® Luminescent Cell Viability Assay

The CellTiter-Glo® Luminescent Cell Viability Assay is a homogeneous method to determine the number of viable cells in culture based on quantitation of the ATP present, which signals the presence of metabolically active cells. Hep3 and HepG2 Cells were plated at 10,000 per well in 96-white-walled microtiter plates and incubated overnight at 37◦C in a humidified incubator containing 5% CO2. On the following day, the cultured cells were expose to drug (sorafenib) for an additional 24 or 48 hours. For each treatment triplicate wells were considered. Also we considered wells without cells as a blank control and untreated and drug solvent treated ones as negative controls. Cell viability was determined by adding 100µl of the CellTiter-Glo luminescent cell viability kit (catalog# G7571) from Promega Corporation (Madison, WI, USA) directly to cells cultured in serum-supplemented medium. The contents were mixed for 2 minutes on an orbital shaker to induce cell lysis .The plate was incubated for 90min at room temperature in a dark room to stabilize luminescent signal. Luminescence was recorded in Infinite F200 PRO multimode microplate reader(Tecan Group Ltd, Seestrasse 1038708 Männedorf ,Switzerland). Calculation of results was done by subtracting the average of luminescence value of the culture medium background from all Luminescence value of experimental wells. Data were confirmed in at least two independent experiments.

3.9.2. CellTiter-Blue® Cell Viability Assay

The CellTiter-Blue® Cell Viability Assay provides a homogeneous, fluorescent method for monitoring cell viability. The assay is based on the ability of living cells to convert a redox dye (resazurin) into a fluorescent end product (resorufin). Resazurin is dark blue in color and has little intrinsic fluorescence until it is reduced to resorufin, which is pink and highly fluorescent ($579_{Ex}/584_{Em}$). Unviable cells rapidly lose metabolic capacity and thus do not generate a fluorescent signal. The visible light absorbance properties of CellTiter-Blue® Reagent undergo a "blue shift" upon reduction of resazurin to resorufin. The absorbance maximum of resazurin is 605nm and that of resorufin is 573nm. Either fluorescence or absorbance may be used to record results; however, we provided fluorescence data because it is more sensitive and involves fewer data calculations. In addition, because CellTiter-Blue® Reagent is relatively non-destructive to cells during short-term exposure, it allows the performance of more than one aasay on the same sample and can be multiplexed with other assay methods such as Caspase-Glo® 3/7 Assay Systems.

10000 Hep3 and HepG2 cells were seeded into 96- well opaque-walled tissue culture plates compatible with our fluorometer. After growing them in the CO2 incubator at 37°C for one day , the media was changed with media lack of antibiotic and cells were treated with 100nM of antimiR-221, 1 , 5, 7 or 10μM sorafenib or both compounds for established time point. Treatment was done using and/or sorafenib in alone or in combination. Triplicate wells were considered for each treatment. Controls that included were :

*Blank Control: Triplicate wells without cells were set up to serve as the negative control to determine background fluorescence that may be present.

*NTC Control: Triplicate wells with untreated cells were set up to serve as a vehicle control.

*CTL Control: Triplicate wells with the same solvent and the vehicle (refers here to transfection reagent) of compound were used to deliver the test compounds to the vehicle control wells.

*Scramble control: Triplicate wells with scramble oligos (negative control#2 , Life technology) to test for possible interference with the miRNA oligos sequences.

Before starting the assay the CellTiter-Blue® Reagent was thawed at a 37°C water bath. The homogeneous assay procedure was performed by addition of 25μl of CellTiter-Blue® Reagent(Catalog#G8081)(Promega Corporation ,Madison, WI , USA), directly to cells

cultured in serum- supplemented medium and the cells were incubated for 1 hours at 37◦C prior to recording fluorescence. During incubation, the plate was protected from light and covered to prevent evaporation. Data are recorded using $560_{Ex}/590_{Em}$ fluorescence filter in the infinite F200 PRO multimode microplate reader (Tecan Group Ltd, Seestrasse 1038708 Männedorf ,Switzerland). The fluorescence values were directly proportional to the number of living cells in the culture. Before calculation of results the average of fluorescence value of the culture medium background was subtracted from all fluorescence value of experimental wells. Finally the cell washed with media to adapt the cells for Caspase-Glo® 3/7 Assay. Viable cells was tittered as fluorescence of treated sample / mock control×100. Data were confirmed in at least two independent experiments.

3.9.3. Caspase-Glo® 3/7 Apoptosis Assay

The Caspase-Glo® 3/7 Assay is a luminescent assay that measures caspase-3 and -7 activities in purified enzyme preparations or cultures of adherent or suspension cells. The assay provides a proluminescent caspase-3/7 substrate, which contains the tetrapeptide sequence DEVD. This substrate is cleaved to release aminoluciferin, a substrate of luciferase used in the production of light. The Caspase-Glo® 3/7 Reagent is optimized for caspase activity, luciferase activity and cell lysis. Addition of the single Caspase-Glo® 3/7 Reagent in an "add-mix-measure" format results in cell lysis, followed by caspase cleavage of the substrate and generation of a “glow-type” luminescent signal. For preparation of the reagent the Caspase-Glo® 3/7 Buffer and lyophilized Caspase-Glo® 3/7 Substrate were equilibrated to room temperature before use. Then the contents of the Caspase-Glo® 3/7 Buffer bottle was transferred into the amber bottle containing Caspase-Glo® 3/7 Substrate. The contents was mixed by swirling or inverting, until the substrate is thoroughly dissolved to form the Caspase-Glo® 3/7 Reagent.

Caspase-3/7 activity was measured immediately after the detection of CellTiter-Blue® Cell Viability Assay (described above) on the same wells, by adding 100µl of the homogeneous Caspase-Glo® 3/7 assay Reagent (catalog#G8091)(Promega Corporation ,Madison, WI , USA) at the established time after transfection and/or sorafenib treatments, to each well of a 96-well plate containing 100µl of blank, negative control cells or treated cells in culture medium. Because of the sensitivity of this assay, we Covered the plate with a plate lid. contents of wells gently was mixed using a plate shaker at 300–500rpm for 30 seconds, depending upon the cell culture system. The optimal incubation period was determined

empirically between 60, 90 and 120min. the luminescence of each sample was measure in a plate-reading illuminometer (infinite F200 PRO) (Tecan Group Ltd, Seestrasse 1038708 Männedorf ,Switzerland), as directed by the illuminometer manufacturer. We Subtracted the value for the blank reaction which show the background luminescence from experimental values. Negative control reactions were important for determining the basal caspase activity of the cell culture system and vehicles (refers to solvent of drug and transfection solution). Caspase-3/7 activity is expressed as luminescence of treated sample / mock control×100. Data were confirmed in at least two independent experiments.

3.9.4. Annexin V Apoptosis & Dead Cell Assay

Apoptosis, or programmed cell death, is an important regulator of cell growth and proliferation. Induction of apoptosis is characterized by a progressive series of cellular biochemical and morphological changes. One of the hallmarks of apoptosis is the translocation of phosphotidylserine from the inner to the outer leaflet of the plasma membrane and exposure to the outer surface of the cell. This universal phenomenon is independent of species, cell type, and induction system and occurs early in the apoptotic process.

HepB3 cells were selected to test the effect of arresting of miR-221 by sponge and to confirm the effect of chemically modified antimiR-221 alone or in combination with sorafenib on apoptosis, Muse™ Annexin V & Dead Cell Kit (Catalog#MCH100105)(EMD Millipore, Billerica, MA, USA) in Muse® Cell Analyzer: Mini, Affordable Flow Cytometry. This kit allows for the quantitative analysis of live, early and late apoptosis, and cell death on both adherent and suspension cell lines on the Muse™ Cell Analyzer. The software provides concentrations (cells/mL) for live, early apoptotic, late apoptotic, total apoptotic, and dead cells as well as Percentage of live, early apoptotic, late apoptotic, total apoptotic, and dead cells. The Muse™ System makes sophisticated fluorescent-based analysis. Annexin V is a calcium-dependent phospholipid-binding protein with a high affinity for PS, a membrane component normally localized to the internal face of the cell membrane. Early in the apoptotic pathway, molecules of PS are translocated to the outer surface of the cell membrane where Annexin V can readily bind them. The Muse™ Annexin V & Dead Cell Assay utilizes Annexin V to detect PS on the external membrane of apoptotic cells. A dead cell marker is also used as an indicator of cell membrane

structural integrity. It is excluded from live, healthy cells, as well as early apoptotic cells. Four populations of cells can be distinguished in this assay:

• non-apoptotic cells: Annexin V (-) and 7-AAD (-)

• early apoptotic cells: Annexin V (+) and 7-AAD (-)

• late stage apoptotic and dead cells: Annexin V (+) and 7-AAD (+)

• mostly nuclear debris: Annexin V (-) and 7-AAD (+)

For this assay Hep3B cells were plated into 24-well culture plates at density of (1×10^5) and infected with rAAV-miR-221sponge at MOI:100 or treated with miR-221 inhibitor oligos (100nM)and/or 5 and 10μM of sorafenib as well as vehicle-treated and untreated negative controls for 24 and 48h. Each condition was performed in triplicate .Cells were detached with trypsin. fresh serum containing medium was added to each well so final concentration was 1 x 10^5 cells/mL. 100μL of cells in suspension transferred to a new tube and 100μL of the Muse™ Annexin V & Dead Cell Reagent was added to each tube. Samples were stained for 20 minutes at room temperature in the dark. After that assay was run in Muse™ Cell Analyzer according to its manual.

3.10. Statistical Analysis

Significance was determined with the two-tailed Student's t test. A p-value threshold < 0.05 was considered significant. All real time RT-PCR (assayed in triplicate), Western blotting, and transfection experiments were repeated twice, and reproducible results were obtained. Values were presented as the mean ± standard deviation (SD).

CHAPTER 4.

RESULTS

4.1. PART I: Development of Viral vector for Inhibition of miR-221 in HCC Cell Lines.

4.1.1. Development of a Novel Sequestering Tools as microRNA Sponge for Inhibiting the miR-221.

4.1.1.1. Designing and Construction of miR-221Sponge

For this study the sequence of mature miR-221 (hsa-miR-221 MIMAT0000278) at URL: http://atlasgeneticsoncology.org/Genes/MIRN221ID44277chXp11.html, was considered for designing an antimiR-221. A sponge oligonucleotide contained 4 copies of the miR-221 binding sites and 4 nucleotides spacer. Each MBS included a bulged site, as imperfect miRNA "bulged sponges" were reported to be more effective for the sequestration of miRNAs than sponges with perfect antisense sequence(177). The sequence of endogenous miR-221 and designed sponge is depicted in Figure 4.1.

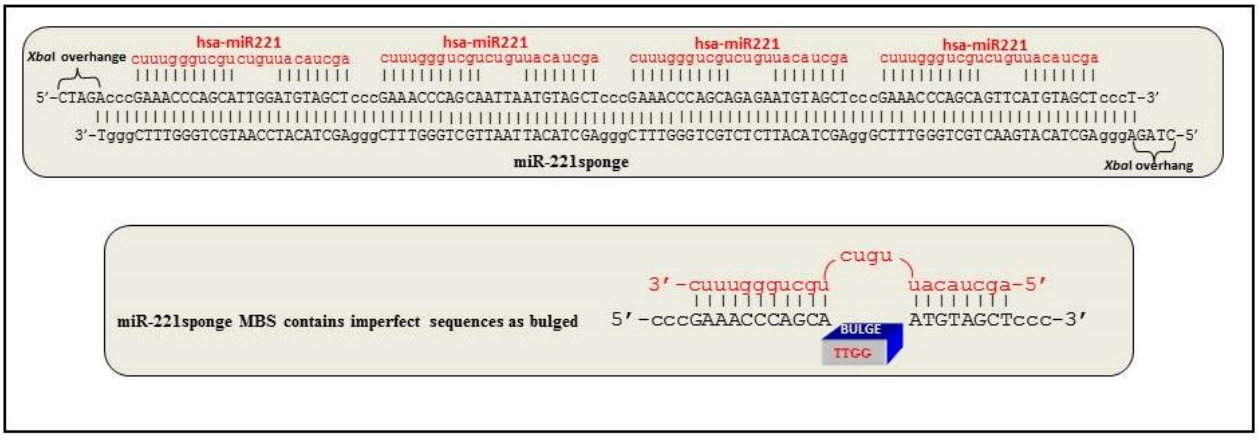

Figure 4.1. Schematic targeting of hsa-miR221 by sponge duplex oligonucleotide. miR-221 sponge designed with 4 copies of miR-221 binding site and 4 nucleotides spacer as imperfect sequences in the positions 12-15 of each MBS.

The designed sponge sequence equipped to overhangs that were compatible with the restriction endonuclease *Xba*I, so it enabled us for directional cloning of repetitive miRNA binding site sequences. The synthetic sponge oligos were assembled to make double-stranded DNA duplexes. The annealed sponge was 113bp long and cloned into pGl3-control using *XbaI* restriction sites for further sub clonning steps.

4.1.2. Adeno-Associate Viral Vectors Expressing miR-221Sponge Along with Reporters GFP/ LUC Constructed for *in vitro* and *in vivo* Studies.

We chose DJ serotype of AAV for this study. It is created by DNA family shuffling technology and allowed highly efficient transduction in comparison with any other wild type serotypes, particularly in hepatocytes(198). pAAV vectors expressing miR-221sponge were constructed for the *in vitro* and *in vivo* studies. For *in vitro* study an AAV vector system to simultaneously express a transgene (miR-221 sponge) and GFP was engineered. Also in the interest of inhibiting miR-221 *in vivo*, GFP cassette of pAAV-IRES-GFP Expression Vector was replaced with Luciferase expressing cassette. By placing reporter genes under the same promoter as the transgene constructs, transgene expression and/or viral integration can be monitored by detecting the reporter signal. Presence of IRES sequence in the backbone of viral vector allowing simultaneous production of reporter gene and transgene from a single transcript and confers a high level of translation. Figure 4.2 showed the final genome packaged as rAAV-miR-221sponge.

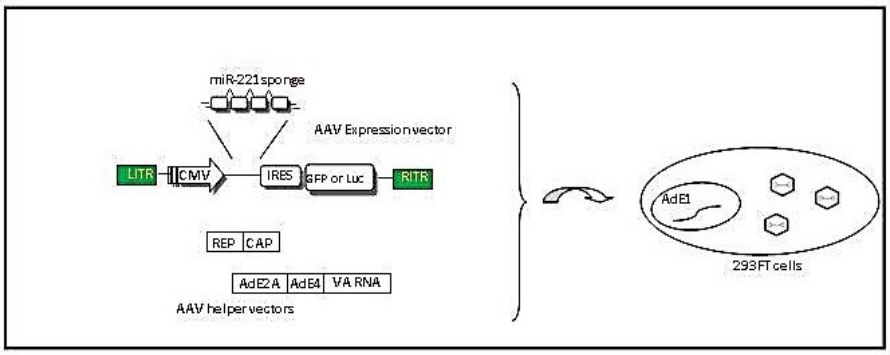

Figure 4.2. Schematic illustration of enclosing miR-221sponge oligo in AAV. miR-221sponge oligo inserted downstream of the IRES-GFP/Luc reporter cassette in the AAV expression vector and rAAV developed by triple transfection of expression and helper vectors into 293FTcells.

4.1.2.1. pAAV-miR-221Sponge-IRES-GFP Construction

Construction of pAAV-miR-221sponge-IRES-GFP plasmid was a straightforward process. 2ug of pAAV-IRES-GFP was excised with *Xba*I fast digest restriction enzyme (Fermetase) according to manufacturer's manual. Digested vector was subjected to the dephosphorylation step using 1µl Calf Intestinal Phosphatase (CIP) followed by incubation at 37°C for 1 hour. Dephosphorylation improved the probability of ligation of inset by preventing the self-ligation of vector. Complete digestion of vector were confirmed by agarose gel electrophoresis compared to undigested one. Digestion of pAAV-miR-221sponge-IRES-GFP lined up vector and produced a 5983bp fragment (Figure 4.3). The desired fragment was recovered from the gel. Then, the miR-221sponge with *Xba*I cut overhanges ligated into cut and purified pAAV-IRES-GFP (see material and methods for details). The re-ligation efficiency of vector was evaluated by including the ligation control. The ligation products were then transformed into DH10β cells according to the chemically transformation methods using KCM buffer and allowed to grow overnight on ampicillin plates to select for cells containing plasmids. After overnight culture incubation, several randomly chosen ampicillin-resistant colonies were picked and dissolved in 100µl water. 1µl of resolved colonies was used in a PCR colony reaction as template and the remains was grown in 3mL of LB broth for isolation of plasmid DNA (sigma mini-prep kit).

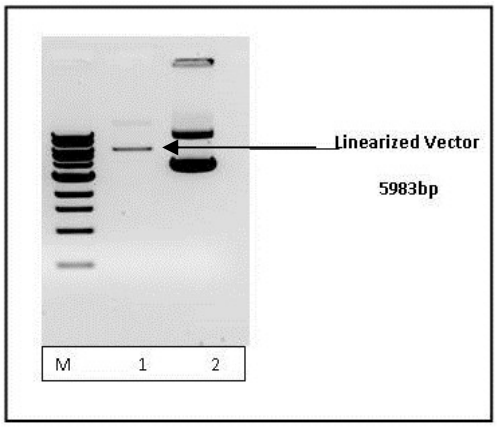

Figure 4.3. Control digest of pAAV-IRES-GFP. Lane1: pAAV-IRES-GFP digested with *Xba*I .Lane1:The lined up vector was visible at 5983bp. Lane2: undigested pAAV-IRES-GFP vector. M: 1kb DNA marker.

Purified plasmid of the test samples were assayed for the presence of the 113bp sponge insert through excising by *Xba*I . Analysis of digested clones were visualized on 1% gel electrophoresis (Figure 4.4A). The correct orientation of the insert was verified by PCR. For colony PCR screening, pAAV-antimiR221-1339F and pAAV-antimiR221-1941R primers was used as a forward and reverse primer respectively. Sequences of primers used for verification of cloning steps are shown in the table 3.1. Primers were designed in Primer3Plus (http://www.bioinformatics.nl/cgi-bin/primer3plus/primer3plus.cgi/). The forward primer was picked up from a overlapping sequence of MCS and the 3' sequence of miR-221sponge as insert. So it could show the orientation of insert inside backbone. The PCR reaction was prepared in 10nM of dNTPs, 1X PCR buffer (Qiagen), 10µM of forward and reverse primers and 0.2µl of Taq polymerase (Qiagen) in a final volume of 12.5µl . PCR was performed in condition of 94°C for 30 second ,54°C for 30 second followed up 72°C for 45 second during 30 cycles. Amplification of a 603bp PCR product was illustrated on agarose gel 1% in TAE 0.5x along with 1kb DNA ladder(Figure 4.4B). The positive clones were designed as pAAV-miR-221sponge-IRES-GFP.

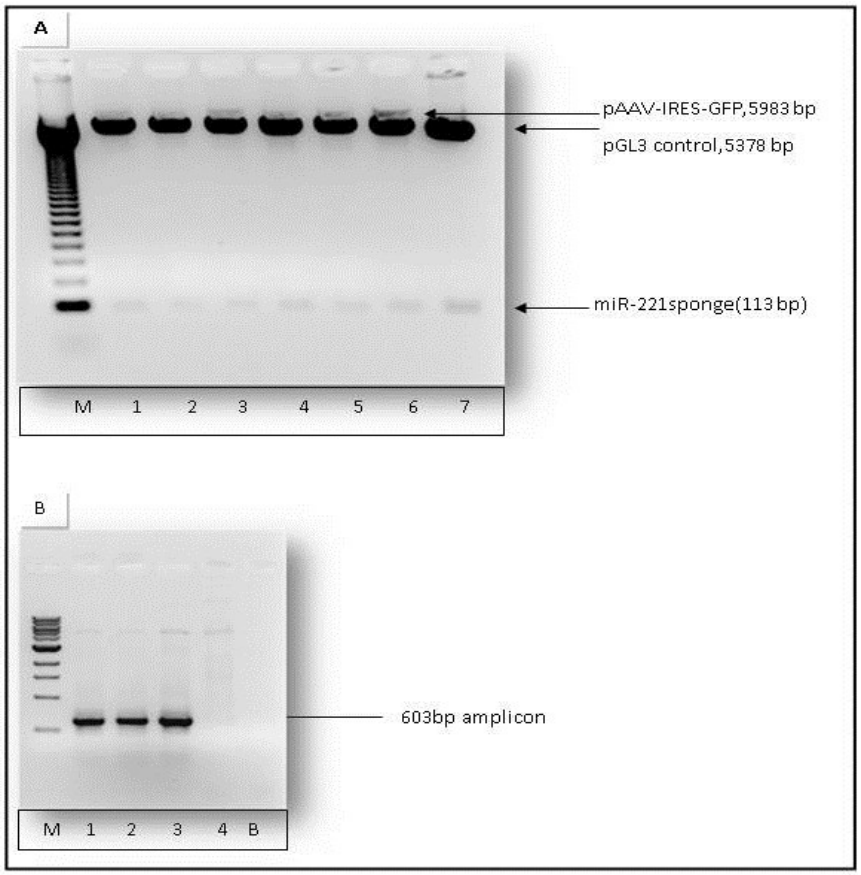

Figure 4.4. Screening of recombinant pAAV-miR-221sponge-IRES-GFP construct. (A): Restriction digestion screening. Lane 1-6: Recombinant clones digested with *Xba*I , lane 7: positive control contains the same insert. lower arrow show the yielding 113bp insert fragment after digestion, M: 123bp DNA marker. **(B): PCR screening.** Lane1-3: clones in sense orientation of inset, PCR product contains a 603bp amplicon. Lane4: clone in antisense orientation. B: Blank sample, M: 1kb DNA marker.

We checked the efficiency of integrity of engineered vector before using it in the packaging step as virus. The 145 nucleotide ITR Sequences in the shuttle vector are capable of forming T-shape secondary structure and are the only cis elements that are required for AAV replication, packaging, integration, and rescue. The gene of interest along with a promoter to drive transcription of the gene usually are inserted between two inverted terminal repeats (ITR) that aid in concatemer formation in the nucleus after the single-stranded vector DNA is converted by host cell DNA polymerase complexes into double-stranded DNA. The integrity of ITRs can be verified by restriction digestion with *Sma*I. More than 80% digested can be considered as functional ITRs. Restriction digestion was done on 400ng of recombinant pAAV expression vectors using *Sma*I (New England , Cell Biolabs) according to manufacturer's instruction. The resulted fragments were visualized on agarose gel 0.8% in TAE buffer 0.5X. (Figure 4.5). The result shows complete digestion of ITR sequences implied that ITR sequences remains intact during cloning steps.

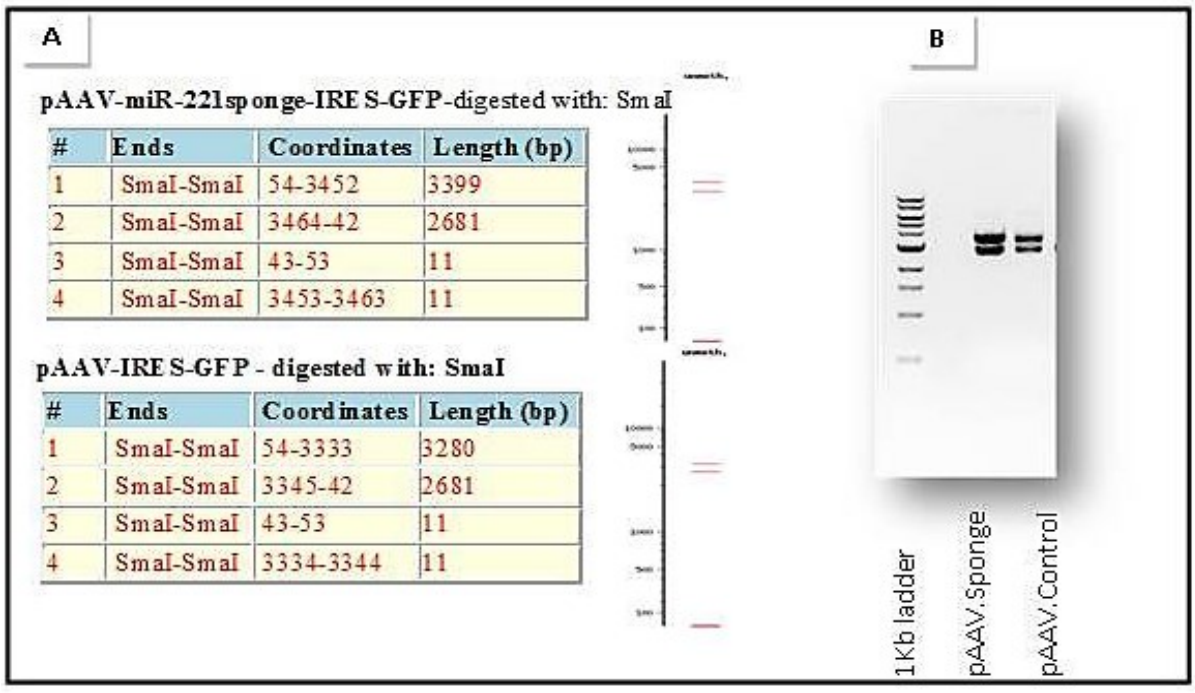

Figure 4.5. Integrity of ITRs was verified by *Sma*I digestion. More than 80% digested can be considered as functional ITRs. The result shows complete digestion of ITR sequences implied that ITR sequences remains intact during cloning steps. **(A):** The expected features of bands after digestion designed in NEBcutter v2.0(http://tools.neb.com/NEBcutter2/). **(B):** pAAV-miR-221sponge and control vector cut with *sma*I.

4.1.2.2. pAAV-miR-221Sponge-IRES-Luc Construction

In the interest of testing Anti-miRNA221 expression *in vivo*, we positioned the miR-221sponge sequences upstream of Luciferase gene as a reporter within the AAV shuttle vector. The IRES-GFP sequence in pAAV- miR-221sponge -IRES-GFP was substituted with the sequence of IRES-Luc from pIRES-Luc vector (Figure 4.6).

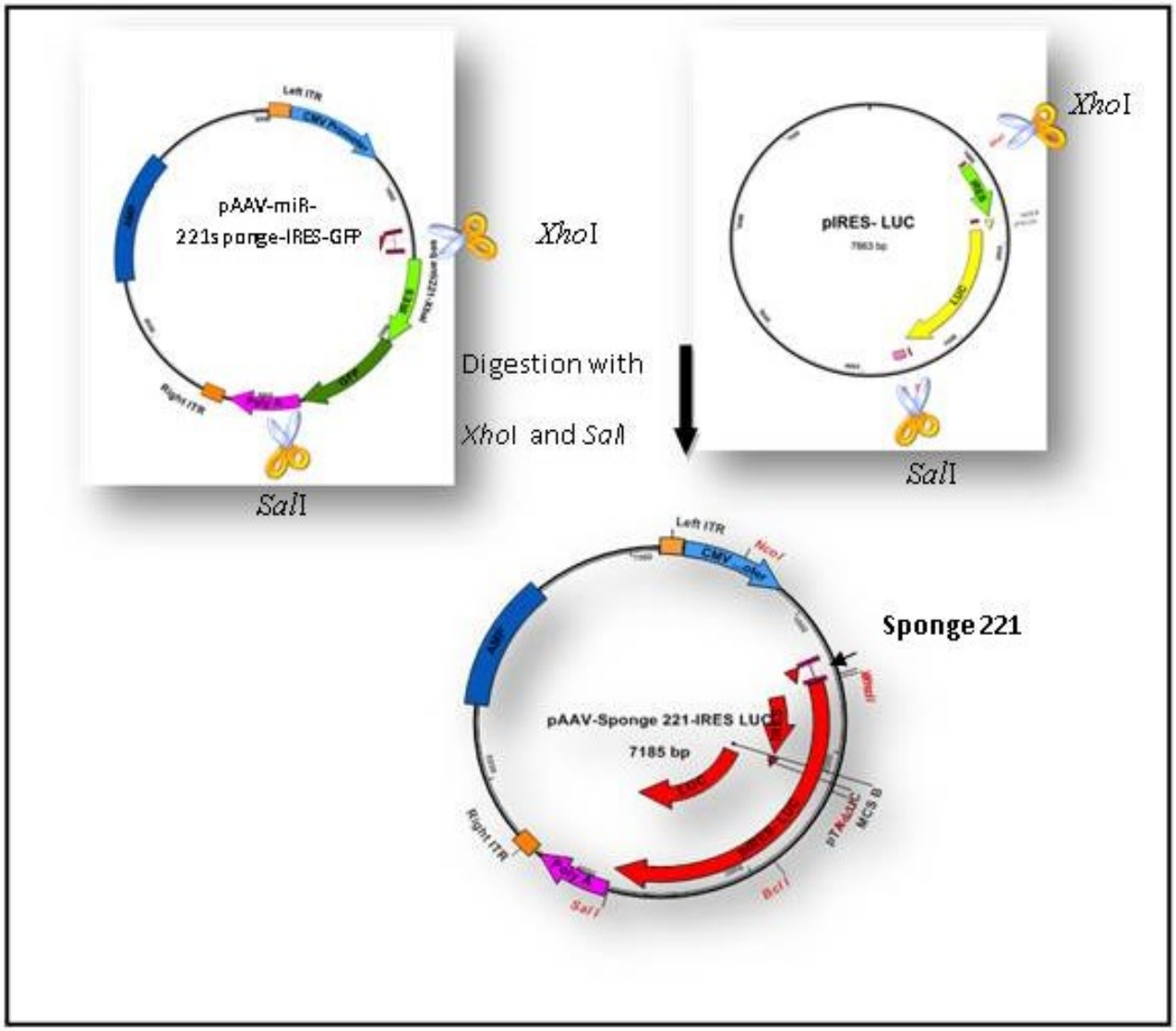

Figure 4.6. Schematic illustration of cloning steps of pAAV-miR-221sponge-IRES-Luc construction

pAAV-miR-221sponge-IRES-GFP and pIRES-Luc were double digested with *Xho*I and *Sal*I restriction enzymes, according to the enzyme manufacturer's instructions. Complete digestion were confirmed by agarose gel electrophoresis(Figure 4.7).

A 4.7kb vector fragment from pAAV- miR-221sponge -IRES-GFP and 2.4kb IRES-luc cassette were recovered from the agarose gel. Luciferase expression cassette was ligated into the purified and dephosphorylated vector fragment using T4 DNA ligase(Roche) based on standard DNA ligation protocols. An aliquot of the ligation mixture was transformed into DH10β competent cells.

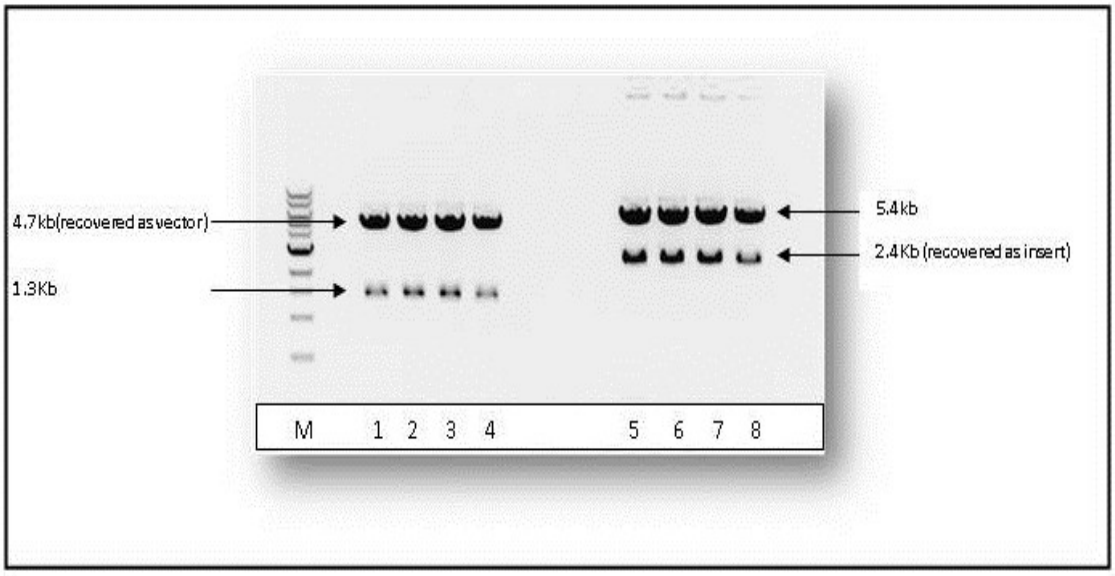

Figure 4.7. Control digest with *Xho*I and *Sal*I. Lane 1-4: Double digestion of pAAV-miR-221sponge-IRES-GFP which produced a 4.7 kb vector fragment containing the AAV- ITRs miR-221sponge and a 1.3 kb fragment containing the IRES-GFP cassette. Lane 5-8: Double digestion of pIRES-Luc which cut into 2.4kb IRES-Luc fragment and 5.4kb backbone fragment. M: 1kb DNA marker.

Identification of correct recombinant clones were done by PCR and restriction digestion analysis. Colony PCR screening was performed with primers lied down in luciferase sequence designated Luc 296F and Luc 764R as forward and reverse primers, respectively. The sequence of primers are summarized in table 3.1. Polymerase chain reaction was done according 94°C for 30", 58°C for 30" and 72°C for 30" , repeated 30 cycles. Figure 4.8A shows the results of PCR screening after electerophoresis on agarose gel 0.8% in TAE 0.5x. The positive recombinant clones from the previous step were screened for the orientation of insert by digestion with *Bam*HI according to the standard protocol for digestion. The results were analyzed by gel electrophoresis alongside digested and undigested (Figure 4.8B). The positive clones with insert in correct orientation were designated as pAAV-miR-221Sponge -IRES-Luc.

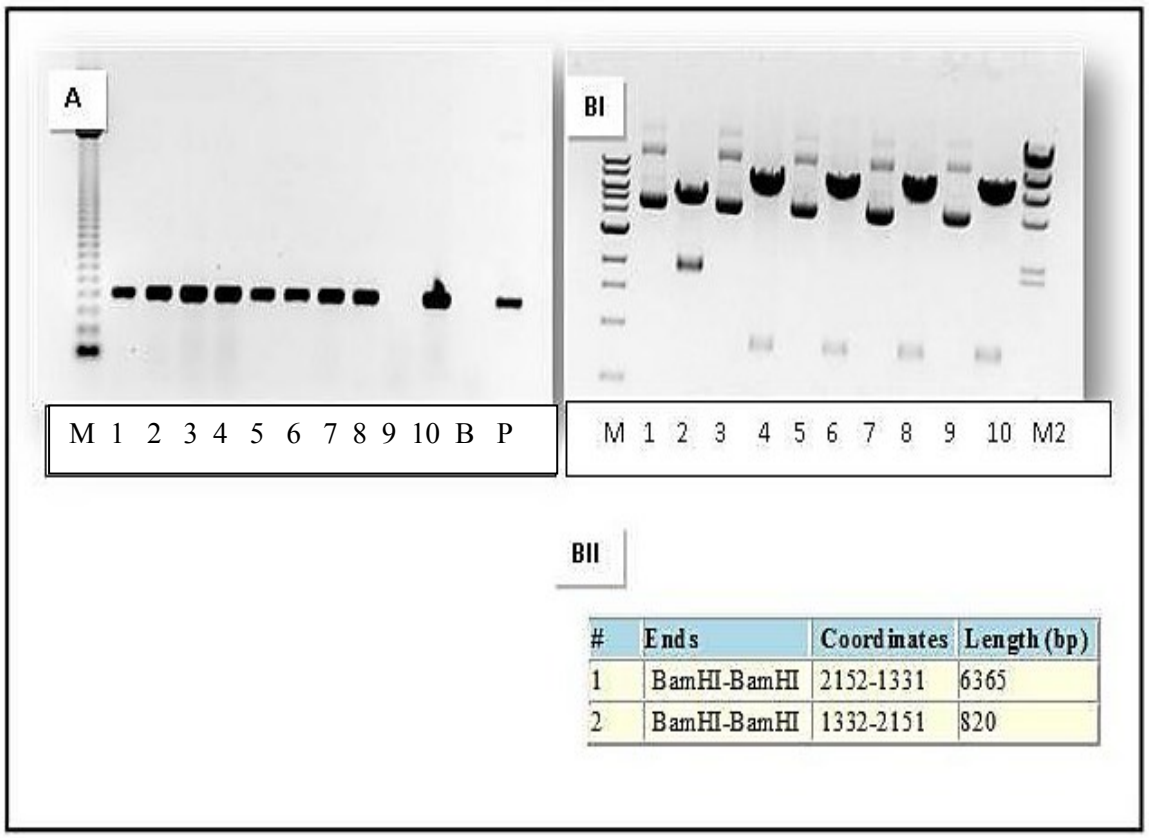

#	Ends	Coordinates	Length (bp)
1	BamHI-BamHI	2152-1331	6365
2	BamHI-BamHI	1332-2151	820

Figure 4.8. Screening of recombinant pAAV-miR-221Sponge-IRES-Luc construct. (A): PCR screening. Lane1-10: PCR results of recombinant clones, positive clones contain a 497bp amplicon. B: Blank sample. P: positive clone ,M: 1kb DNA marker. **(B): Analysis of recombinant clones through restriction digestion BI:** The electrophoresis of cut clones on 0.8% agarose gel. Lane with odd number: undigested recombinant clones, Lane with even number: compatible digested clones., M: 1Kb DNA marker M2: *λhid*III ladder. **BII:** The expected features of pAAV-miR-221Sponge-IRES-Luc orientation of insert, digested with *Bam*HI designed in NEBcutter v2.0(http://tools.neb.com/NEBcutter2/).as shown incorporation of insert in sense orientation into backbone results in two 6.36kb and 0.8kb fragments.

4.1.2.3. Transient Transfection of miR-221Sponge Inhibits miR-221 and Affect Regulation of its Targets.

- **Duel Luciferase Assay Reveals Down-Regulation of miR-221 Following Transient Transfection of miR-221Sponge**

To evaluate the suppressive activity of the sponge construct *in vitro*, we asked whether the sequestration of miR-221 by the sponge products could disrupt the binding of miRNA to target sites in 3'-UTR of a target mRNA and thereby regulate its translation and/or abundance. Thus, we performed a dual luciferase assay using the luciferase reporter pGL3-3'UTRp27, a vector in which the 3'-UTR of CDKN1B/*p27* mRNA, a known target of miR-221, was cloned downstream of the firefly luciferase gene(199). The renilla luciferase reporter vector pRL-TK was used as normalizer. These plasmids were co-transfected along with AAV vector harboring miR-221sponge and the control vector into HEK-293 cells. Transfection efficiency was monitored by GFP reporter expression (Figure 4.9). A scheme of the experiment is depicted in Figure 4.10A. We assumed that binding of the sponge to endogenous miR-221 could rescue the target site in 3'UTR of pGL3-3'UTRp27 vector and lead to an increased level of firefly luciferase activity. Firefly and renilla luciferase expression were measured 24 hours post-transfection and their ratio was used to calculate the relative luciferase activity. The average luminescence for each experimental sample was measured in triplicate. The ratio of control vector without sponge sequence was set at 100%. Results showed that sponge construct were highly effective and revealed an increase of relative Luc expression by more than 2 times. Analysis of non-transfected control (NTC) showed no significant expression levels of lucifease in the absence of treatment. (Figure 4.10B). These results indicated that miR-221sponge could be used to sequester miRNA activity on target genes.

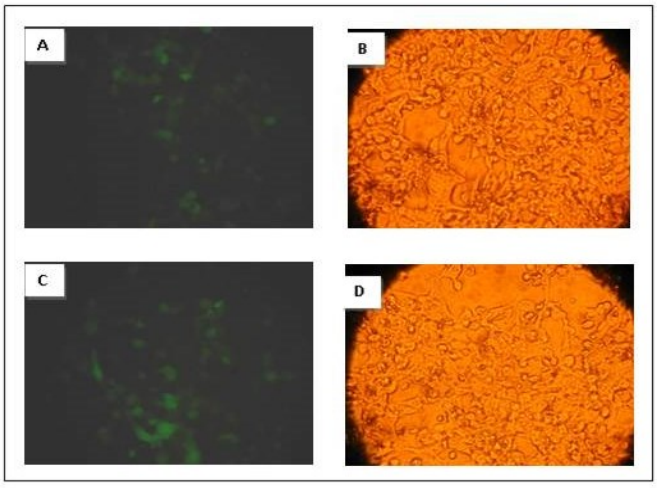

Figure 4.9. Florescent microscopy showed transfection efficiency and GFP expression of pAAV-IRES-GFP expressing constructs in 293 cells (20X). (A) GFP expression of pAAV-miR-221sponge-IRES-GFP (**B):** White Balance feature of cells tranfected by pAAV-miR-221sponge-IRES-GFP **C:** GFP expression of pAAV- IRES-GFP **D:** White Balance feature of cells tranfected by pAAV-IRES-GFP.

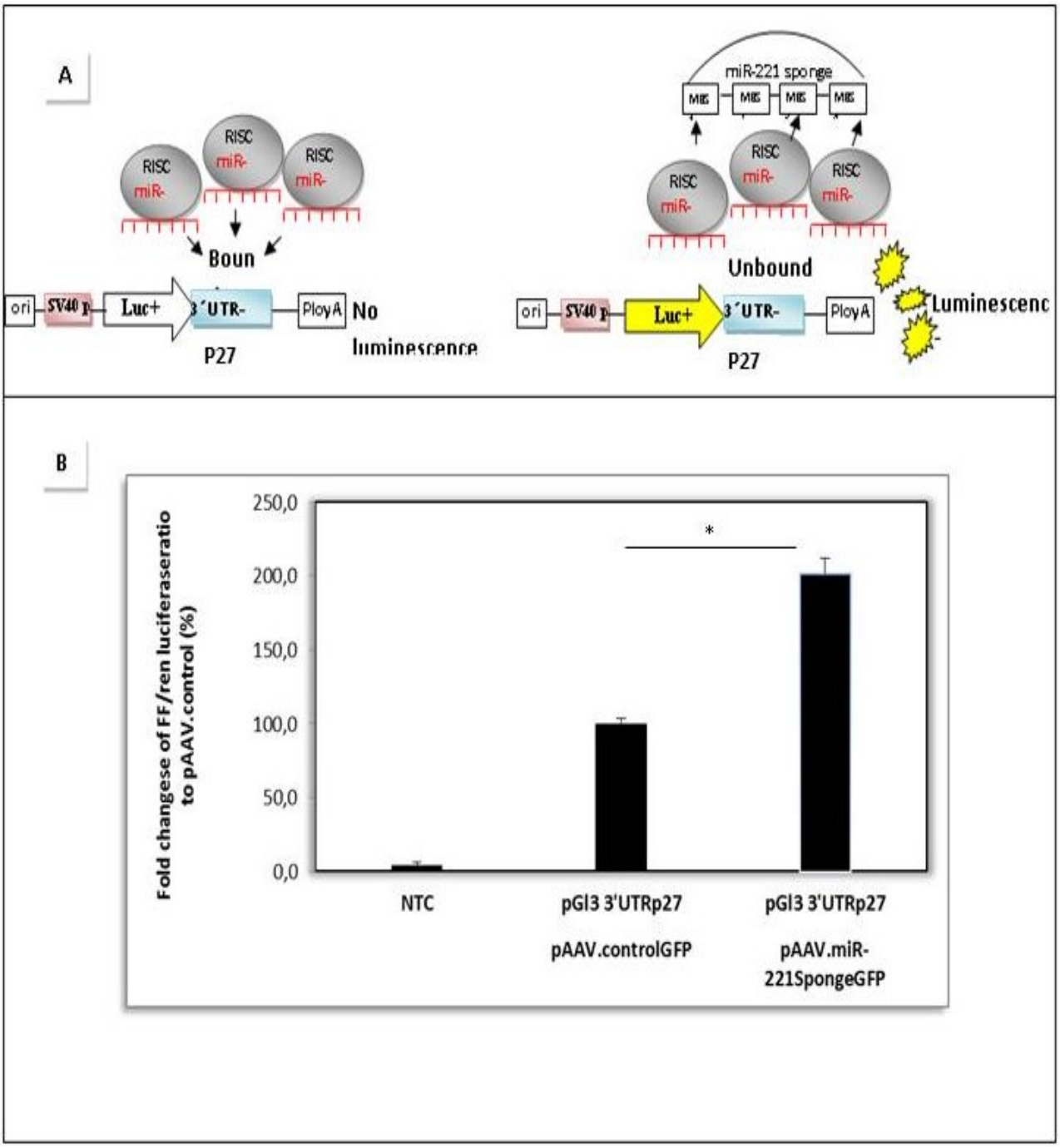

Figure 4.10. Inhibition of endogenous miR-221 by sponge construct *in vitro.* (A): A scheme of luciferase reporter assay that shows function of miR-221sponge. In the lack of sponge inhibitor, miRNA such as miR-221, loaded in RNA induced silencing complexes (RISCs), will bind to their endogenous targets and silence target genes and subsequently luciferase gene. In the presence of sponge transcripts, however, miR-221 will bind to the exogenous binding sites and be unavailable for silencing endogenous targets (3'UTR27), resulted in raising the luciferase expression. **(B):** Duel luciferase reporter assay. The control-GFP construct lack of sponge sequence was used as a control means 100% FF/renilla luc expression in the case of co-transfection with pGl3-3'UTRp27. miR-221sponges construct was able to relieve 3'UTRp27 via blocking by endogenous miR-221,as detected by increased luciferase activity around 200%. n=3, *p=0.001.

- **Western Blot Analysis Validates Inhibitory Activity of miR-221Sponge**

Next we used western blot analysis to determine protein levels of a validated miR-221 target genes upon its inhibition by sponge. We transfected HEK-293cells with 0,4µg pAAV.miR-221sponge and or pAAV.control without miR-221sponge expression cassette. For each transfection triple wells were considered. 48h after transfection cells were trypsinized and subjected for protein extraction as described in material and method. Blotting was performed for CDKN1B/*p27* (BD Transduction Laboratories™, 610242, dilution 1:1500) a known target of miR-221. Beta-actin (Sigma Aldrich,A4700,dilution 1:1000) was used for normalization purposes. We observed 2.6 and 1.73 fold increase in CDKN1B/*p27* protein level in comparison with non-transfected control and pAAV.control transfected cells, respectively (Figure 4.11). These results validated that miR-221sponges could be used to sequester miRNA activity on target genes.

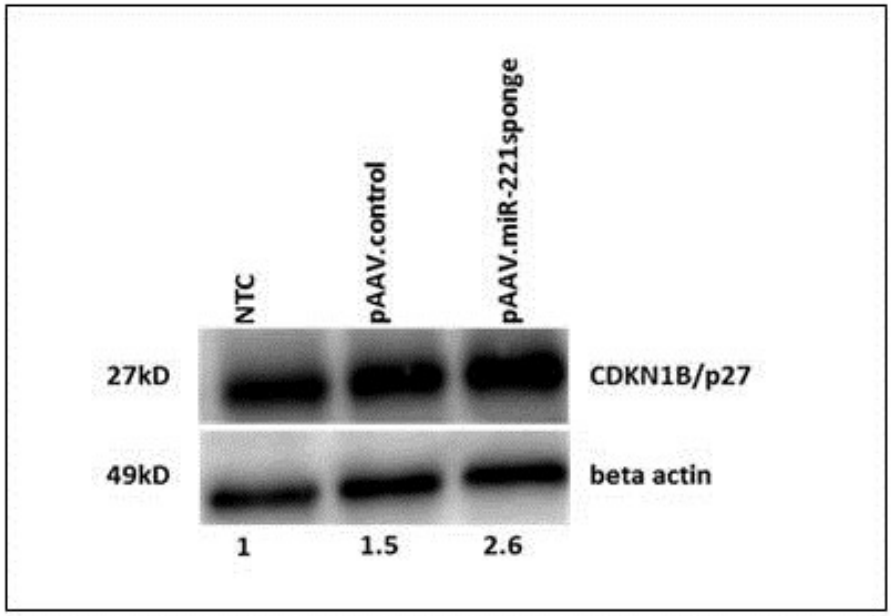

Figure 4.11. Western blot analysis of p27 target protein and beta actin. Transfection of HEK-293 cells by sponge expressing vector (pAAV.miR-221sponge) revealed 2.6 and 1.73 fold increase in CDKN1B/*p27* protein level compared to non-transfected control (NTC) and control construct without sponge (pAAV.control), respectively.

4.1.3. Adeno-Associated Viral Delivery of miR-221Sponge Suppresses the Endogenous Up-Regulated miR-221 in HCC cell lines

rAAV for delivery of miR-221sponge produced through triple transfection of *pAAV Expression Vector:pAAV-J:pHelper*. Transfection efficiencies were visualized under fluorescence microscopy (Figure 4.12A,B). The most obvious sign of viral production was a color change in the medium from red to yellow (compare to negative control). As viral production proceeds, some of the cells were round up and detach from the plate, and saw floating in the medium. In addition the population of cells started to distance each other so some big spaces were seen in cultured cells. Microscope photographs of AAV-producing versus non-AAV-producing cells were shown in Figure 4.12C,D. Generally, three days post-transfection was the optimal time to prepare AAV stocks. The ability of rAAV-miR-221sponge-IRES-eGFP to knock-down endogenous miR-221 was assessed in Hep3B cells. For *in vitro* assay rAAVs were used to transduce cells at MOI:100. Uninfected and rAAV-control infected cells were considered as controls. A TaqMan microRNA assay was employed to quantify miR-221 inhibition. As shown in Figure 4.13A, sponge against miR-221 reduced expression of endogenous miR-221 by 45% and 42% in comparison with uninfected and control virus infected cells respectively. Furthermore, the protein level of CDKN1B/*p27* exhibited a 2.2 fold up-regulation respect to uninfected cells. Also 1.46 fold increase was detected compared to rAAV-control (Figure 4.13B). These data demonstrated that rAAV provides an effective means to deliver a functional miR-221sponge.

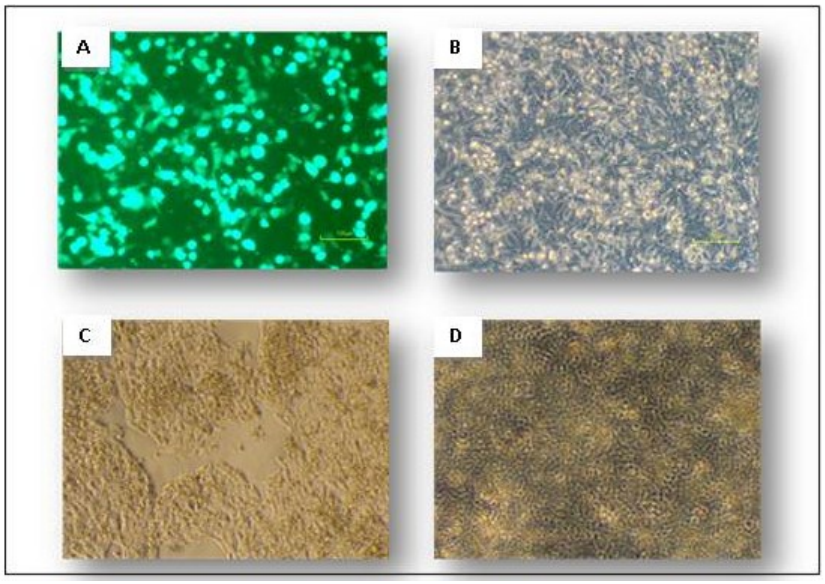

Figure 4.12. Development of rAAV. (A): Fluorescent features that shows triple transfection efficiency of pAAV-GFP Expression vector: pAAV-DJ: pHelper after 24 hours(10X). **(B):** White balance feature (10X). **(C):** Features of transfected cells after 72 hours visualized under light microscope(10X) **(D):** non-transfected control culture (10X

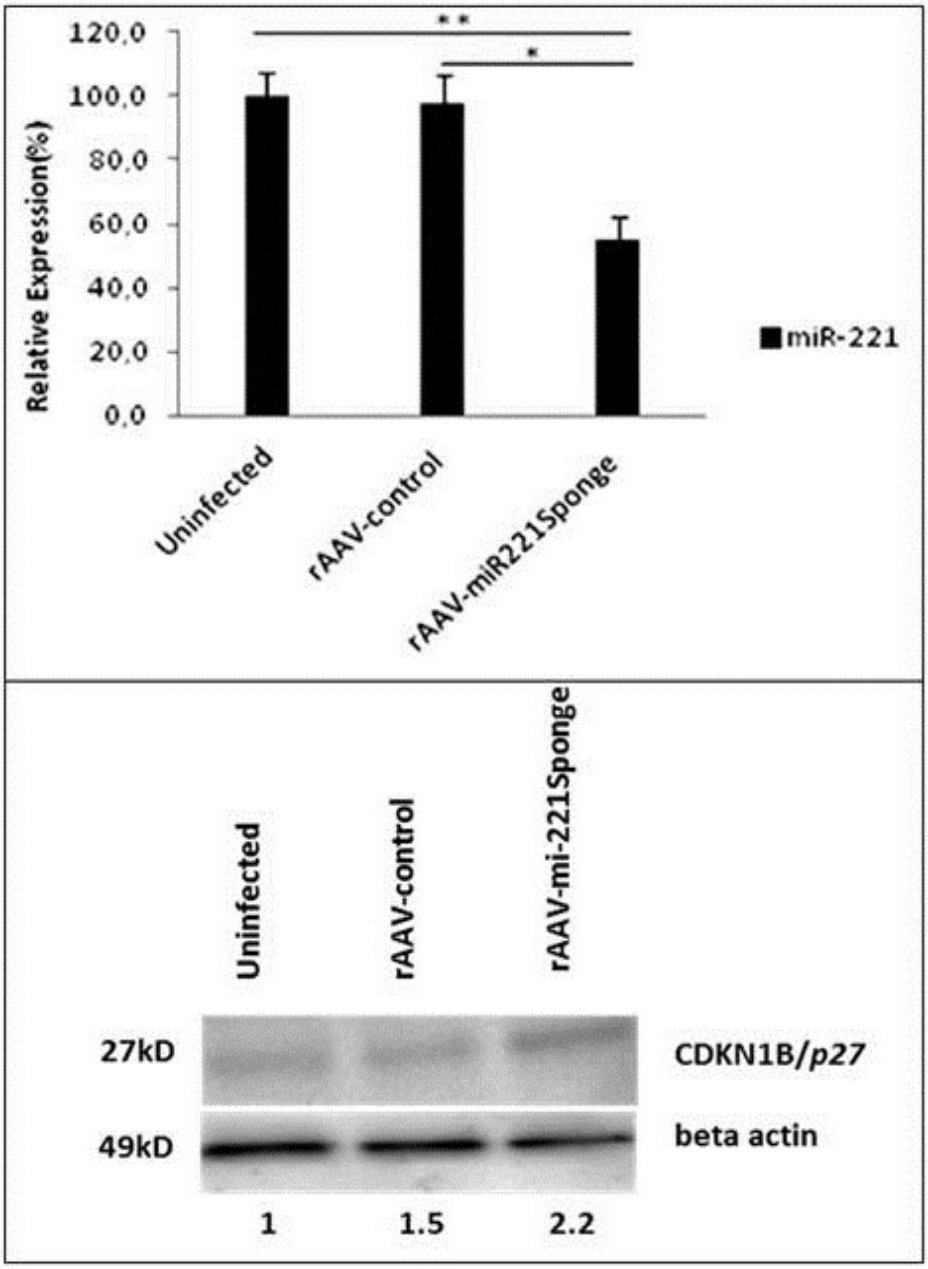

Figure 4.13. Molecular assay of rAAV-sponge221-IRES-GFP. (A): Quantitative RT-PCR detection of miR-221 at 72 hours post infection of Hep3B cells with rAAV-miR-221sponge or rAAV-control, at MOI=100. Data are represented as mean values +/- SD from three replicates. rAAV-miR-221sponge induced a 45% and 42% reduction in miR-221 expression level in comparison with uninfected (**: p-value = 0.01) or rAAV-control infected cells (*: p = 0.02), respectively. **(B):** Western blot analysis of CDKN1B/*p27* protein in cells infected with rAAV-miR-221sponge vector caused a 2.2 and 1.46 fold raise in p27/kip1 protein level in comparison with uninfected and rAAV-control, respectively. Beta actin protein was employed as reference normalize.

4.1.4. miR-199-Dependent Recombinant Adenovirus Express Functional miR-221Sponge *in vitro*.

We hypothesized that the incorporation of miR-221sponge into Ad-199T (196) could provide the capability of inhibiting miR-221 specifically in HCC cells. Details of vectors construction are described in Materials and Methods and depicted in Figure 4.14A. To verify whether engineered adenovirus was able to express a functional miR-221sponge, we infected HepG2 cells with rAd-199T-miR-221sponge and rAd-199T control at MOI=10. Real Time TaqMan assay revealed that sponge decrease the level of miR-221 up to 75.5% and 55% relative to uninfected and control virus infected samples, respectively (Figure 4.14B). To assess if the miR-221sponge expressed by rAd could modulate protein level of miR-221 target, we assayed CDKN1B/*p27* levels by western blot analysis. Following 72 hours of infection, increasing in the p27/Kip1 protein levels by ~8.5 fold was detected compared to uninfected and rAd control infected samples (Figure 4.14C). As designed (196), this adenoviral vector is expected to replicate only in the absence of miR-199, like in HCC cells. To verify that miR-199 could indeed regulate viral replication of rAd-199T-miR-221sponge, the viral vector was used to infect cells of two different cell lines: HepG2, which do not express miR-199; HepG2/199, a derivative of HepG2 cells engineered to constitutively express miR-199a (196). To this purpose, 7.5×10^4 cells of each cell line were seeded and infected with rAd-199T-miR-221sponge or control virus at MOI=10. The cells were harvested at various time points. The results shown in Figure 4.15 established that viral replication of rAd-199T-miR-221sponge was indeed miR-199-dependent.

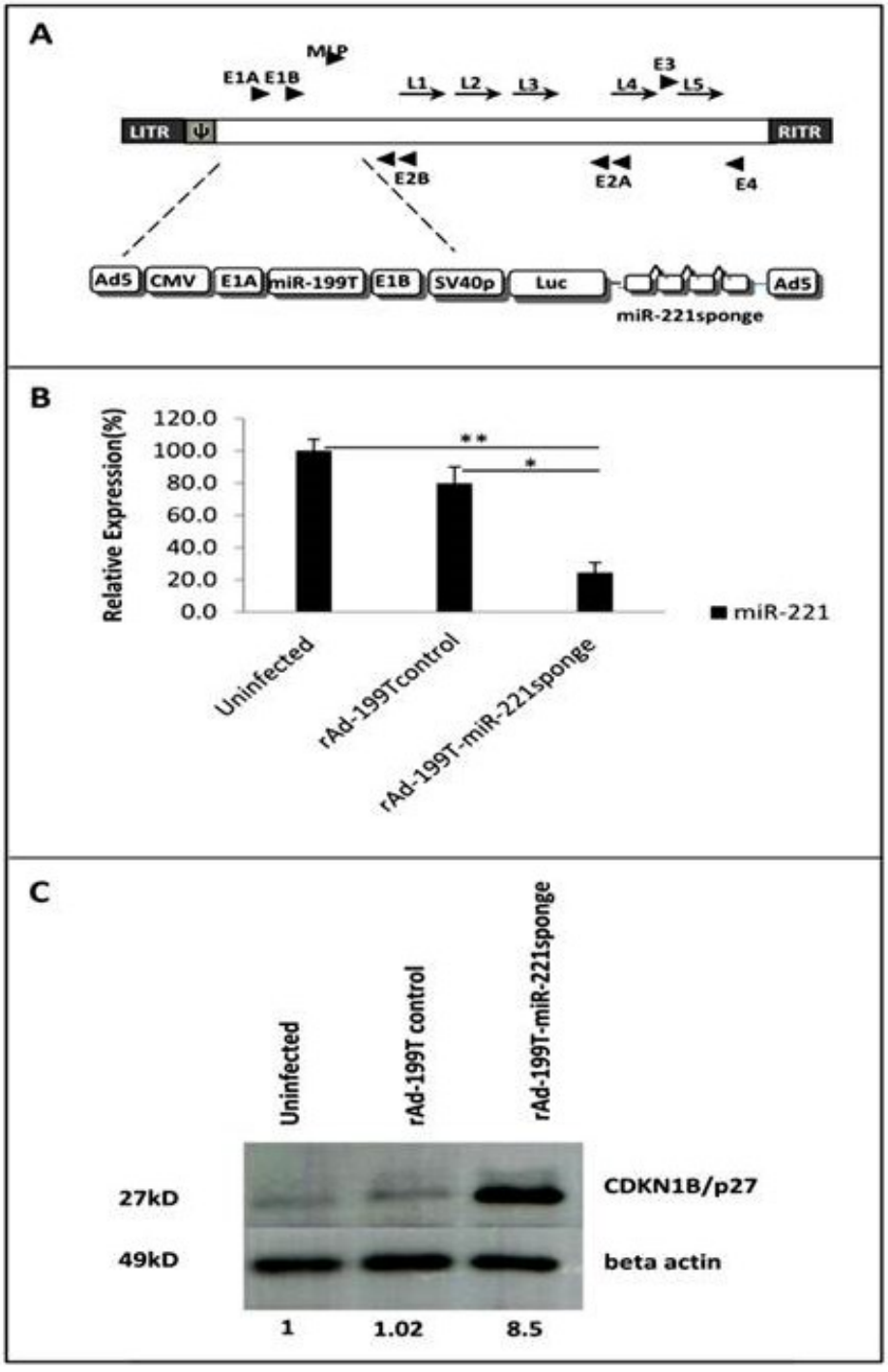

Figure 4.14. Functionality of oncolytic recombinant adenovirus expressed microRNA sponge. **(A)** Scheme of the Ad-199T-miR-221sponge adenoviral vector, showing the location of the critical elements in the context of the adenoviral vector genome: CMV = CMV promoter; E1A = adenoviral E1A gene; miR-199T = target site for miR-199a; E1B = adenoviral E1B gene; SV40p = SV40 early promoter; Luc = firefly luciferase gene; miR-221sponge. **(B)** Quantitative RT-PCR detection of miR-221 at 24 hours following infection of HepG2 cells with rAd-199T-miR-221sponge or rAd-199T-control, at MOI=10. Data are represented as mean values + SD from three replicates. The results showed that miR-221 expression was inhibited 75.5% and 55% compared to uninfected (**: p-value = 0.002) or control virus infected (*: p-value = 0.001) samples, respectively. **(C)** Western blot analysis of CDKN1B/*p27* protein, confirmed an increase in target protein around 8.5 fold in comparison with uninfected or rAd-199T control virus in HepG2 cells. Beta actin protein was employed as reference normalize.

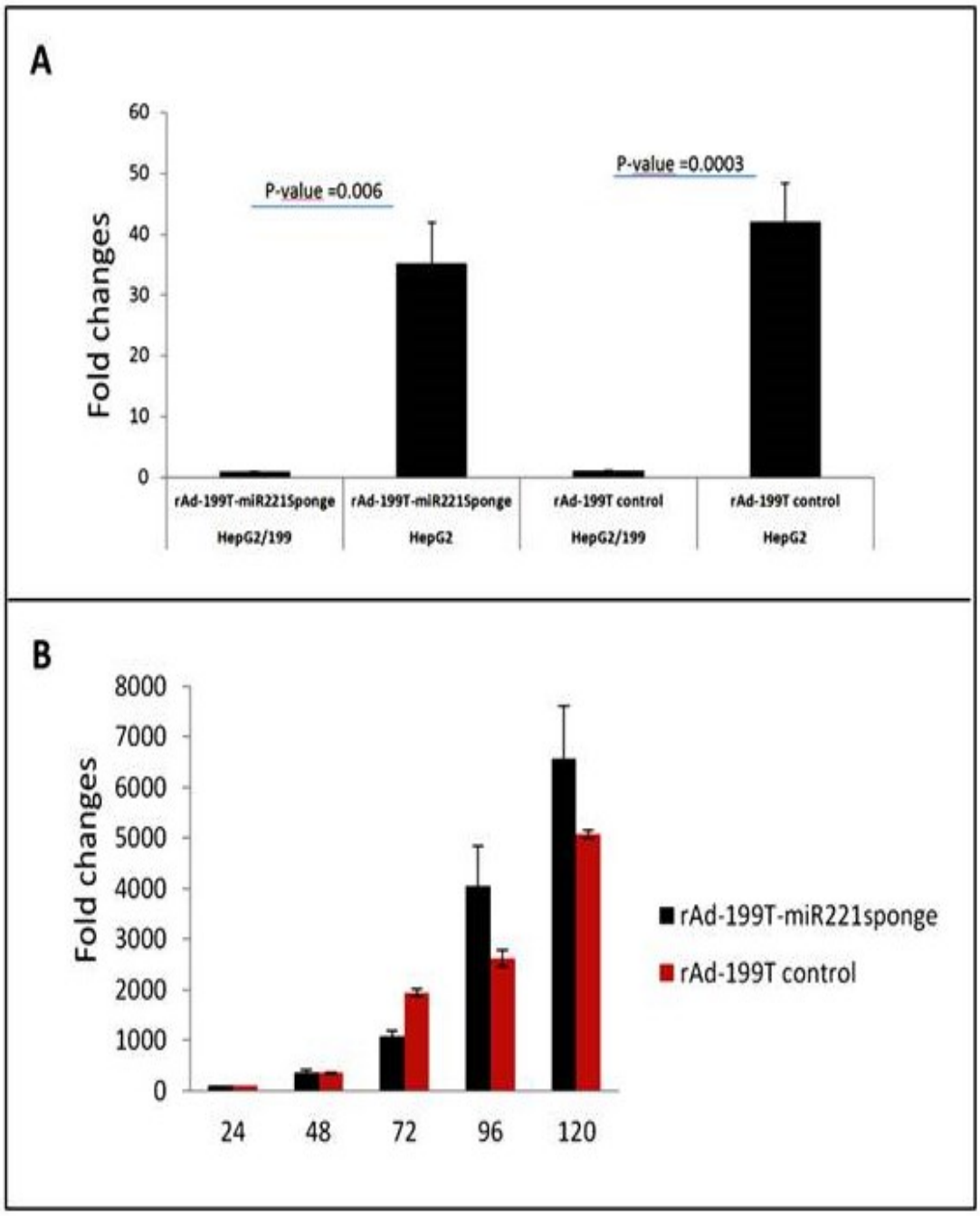

Figure 4.15. Replications of recombinant adenovirus is restricted to HCC cell lines. **(A)** Conditional replication of rAd-199T-miR-221sponge and rAd-199T control in HepG2 and HepG2/199 cells (Callegari, 2013). Results showed the inhibition of virus replication in miR-199-expressing cells, like the HepG2/199 cells, which mimic the situation of miR-199 expression in normal hepatocytes. **(B)** Time course of rAd vectors replication of in HepG2 cells. Data are represented as mean values +SD from three replicates.

4.1.4.1. miR-221Sponge Mediated Viral Delivery Induces Cell Apoptosis and Reduces Viability in HCC Cells

To verify whether miR-221sponge is able to influence apoptosis and cell viability, we transduced hepatocellular carcinoma Hep3B cell line, which are characterized by high level of miR-221 expression with rAd-199T-miR-221sponge at MOI:10 as well as rAAV-miR-221sponge at MOI:100. Comparable control rAd and rAAV infected cells were considered. We investigated the effect of miR-221 inhibition with 7-Amino-actinomycin D (7-AAD)/PE Annexin V staining. The results showed a highly increase in late apoptosis along with reducing the number of viable cells in rAd-199T-miR-221sponge infected cells compared to control virus infection condition. On the other hand an slightly increase in both early and late apoptosis consistent with decrease in number of viable cells were achieved for rAAV-miR-221sponge respect to rAAV-control infected cells. In this case no increase in number of dead cells was detected (Figure 4.16).

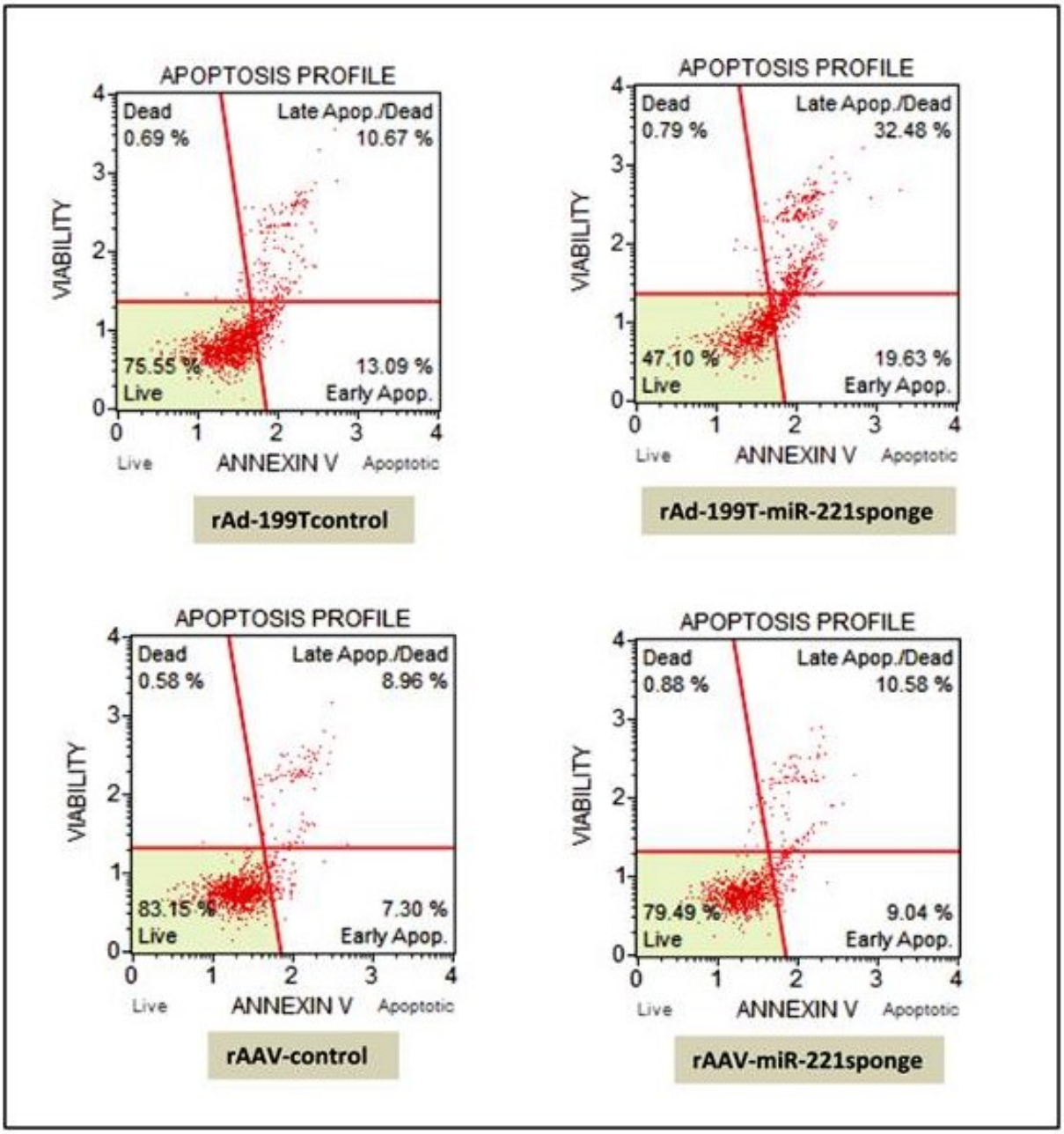

Figure 4.16 Effect of miR-221sponge mediated viral delivery on apoptosis of HCC HepB3 cells by Mini, Affordable flow cytometry. HepB3 cells were infected by rAd-199T-miR-221sponge at MOI = 10 and collected after 24 hrs, or rAAV-miR-221sponge, at MOI = 100 and collected after 72 hrs. Control viruses were employed for comparison. Harvested cells were assayed for Annexin V and death markers to reveal the percentage of cells in early and late apoptotic as well as viable cells. A strong apoptotic effect was produced by rAd-199T-miR-221sponge in comparison with rAd-199T control and a little increase in apoptosis was also induced by rAAV-miR-221sponge in comparison with rAAV control.

4.2. PART II: Development of Adeno-Associated Viral Vector for Restoration of miR-199a in HCC Cell Lines.

4.2.1. Recombinant AAV Plasmids Engineered for Expressing miR-199a and GFP/ LUC Reporters for *in vitro* and *in vivo* Studies.

4.2.1.1. pAAV-miR-199a-IRES-GFP Construction

Construction of pAAV-miR-199a-IRES-GFP was done by substitution of miR-221 sponge sequence in already engineered pAAV-miR-221sponge-IRES-GFP with miR-199a sequences from pIRESneo2miR199(Figure 4.17).

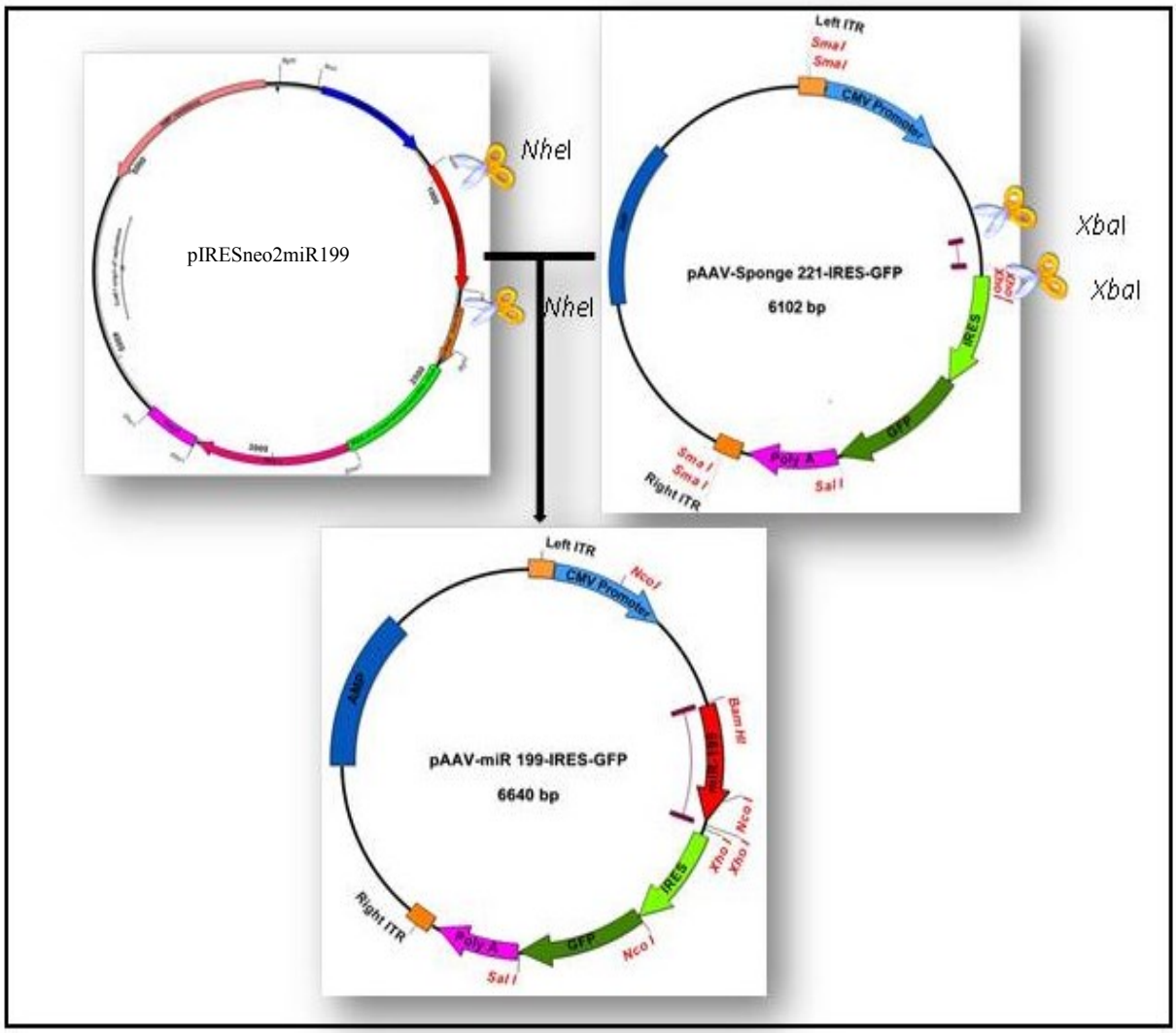

Figure 4.17. Schematic illustration of cloning steps of pAAV-miR-199-IRES-GFP construction

2ug of pAAV-miR-221sponge IRES-GFP and pIRESneo2miR199 were excised with *Xba*I and *Nhe*I restriction enzymes (Fermentase), respectively according to manufacturer's manual. Digested vector dephosphorylated using 1µl Calf Intestinal Phosphatase (CIP) followed by incubation at 37°C for 1 hour. Digested material in parallel with DNA ladder were run on agarose gel and electrophoresis at 80V. for 45 min. Digestion of pAAV-miR-221sponge-IRES-GFP produced a 5989bp fragment as vector. Insert excised from pIRESneo2miR199, with 647bp in length (Figure 4.18).

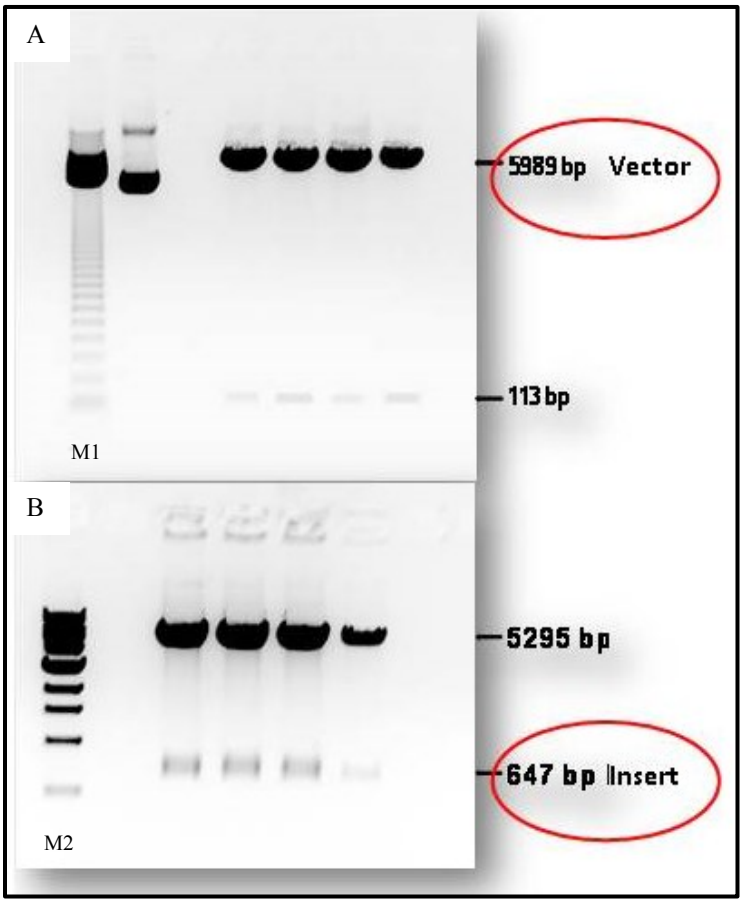

Figure 4.18. **Control digestion of pIRESneomiR199 and pAAV-miR-221sponge-IRES-GFP vectors . A. pAAV-miR221sponge-IRES-GFP cut by *Xba*I** . to provide source of vector in ligation step (5989bp band) M1: 123 DNA marker **B.pIRESneomiR199 digested with *Nhe*I** . 647bp miR199 sequence was used as insert M2: 1kb DNA marker

The desired fragments was recovered from the gel. Then, the miR-199a with *Nhe*I overhangs ligated into the vector; pAAV-IRES-GFP. The chance of re-ligation of vector was evaluated by providing the ligation control samples. The ligated products were then transformed into DH10β cells by the chemically transformation methods using KCM buffer, then allowed colonies to grow overnight on ampicillin plates to select for cells containing plasmids.

After an overnight culture incubation, several randomly chosen ampicillin-resistant colonies were picked and used in a PCR colony screening to detect the presence of the 647bp miR-199a sequence. For colony PCR screening, miR-199NheI FWD and miR-199NheI REV primers was used as a forward and reverse primer respectively. Sequences of primers used for verification of cloning steps are shown in the table 3.1. The PCR reaction was prepared in 10nM of dNTPs, 1X PCR buffer (Qiagen), 10µM of forward and reverse primers and 0.2µl of Taq polymerase (Qiagen) in a final volume of 12.5µl. PCR was performed in condition of 94°C for 30 second ,68°C for 30 second followed up 72°C for 45 second during 30 cycles. Amplification of a 647bp PCR product was illustrated on agarose gel 1% in TAE 0.5x along with 1kb DNA ladder(Figure 4.19A). The positive clones were designed as pAAV-miR-199a-IRES-GFP. Restriction digestion also was done for screening of colonies harboring miR-199a sequence in correct direction. Plasmid DNA was extracted using sigma mini-prep kit according to manuals of sigma company. 300ng of DNA treated with 0.5µl of *Nco*I Restriction enzyme(Fermentase). By this mean, sense clone could be differentiate from antisense clone by the size of bands visualized on the agarose gel(Figure 4.19B).

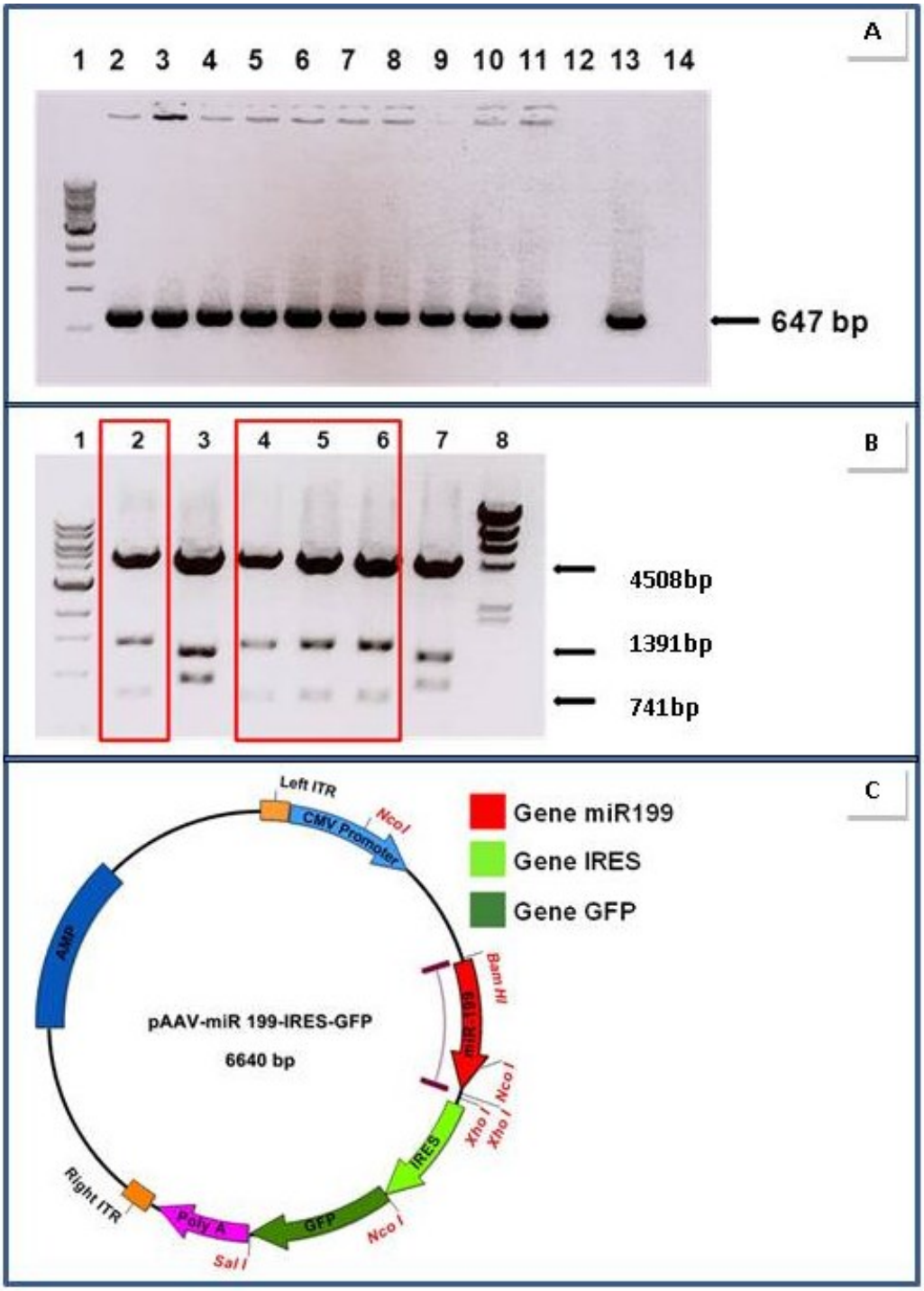

Figure 4.19. Screening of recombinant pAAV-miR199-IRES-GFP construct. (A): PCR screening. Lane1: 1kb DNA marker. Lane 2-11: PCR results of recombinant clones, positive clones contain a 647bp amplicon. 12: Blank sample. 13: positive clone 14: negative clone . **(B): Analysis of recombinant clones through restriction digestion** The electrophoresis of cut clones on 0.8% agarose gel. Lane1: 1kb DNA marker. Lane 2,4,5,6 positive clones harboring insert in sense direction, Lane 3,7 clones harboring insert in antisense direction **C:** The schematic features of pAAV-miR-199-IRES-GFP .

4.2.1.2. pAAV-miR-199a-IRES-Luc Construction

This cloning step was done by substitution of IRES-Luc with IRES-GFP fragment in the pAAV-miR-199a-IRES-GFP from step 4.2.1.1. pIRES-Luc and pAAV-miR-199a-IRES-GFP were double digested with *Xho*I and *Sal*I restriction enzymes, according to the manufacturer's instructions. Complete digestion were confirmed by agarose gel electrophoresis(Figure 4.20A).

A 5282bp vector fragment from pAAV-miR199a-IRES-GFP and 2.4kb IRES-luc cassette were recovered from the agarose gel. Luciferase expression cassette was ligated into the purified and dephosphorylated vector fragment using T4 DNA ligase(Roche) based on standard DNA ligation protocols. The ligated product was transformed into DH10β competent cells. Identification of correct recombinant clones were done by PCR and restriction digestion analysis as well. Colony PCR screening was performed with primers lied down in luciferase sequence designated for Luc 296F and Luc 764R as forward and reverse primers respectively. The sequence of primers are summarized in table 3.1. Polymerase chain reaction was done according 94°C for 30", 58°C for 30" and 72°C for 30" , repeated 30 cycles. Figure 4.20B shows the results of PCR screening after electerophoresis on agarose gel 0.8% in TAE 0.5x. The positive recombinant clones from the PCR step were screened for the orientation of insert by digestion with *Nco*I according to the standard protocol for digestion. The results were analyzed by gel electrophoresis alongside digested and undigested (Figure 4.20C). The positive clones with insert in correct orientation were designated as pAAV-miR-199a -IRES-Luc.

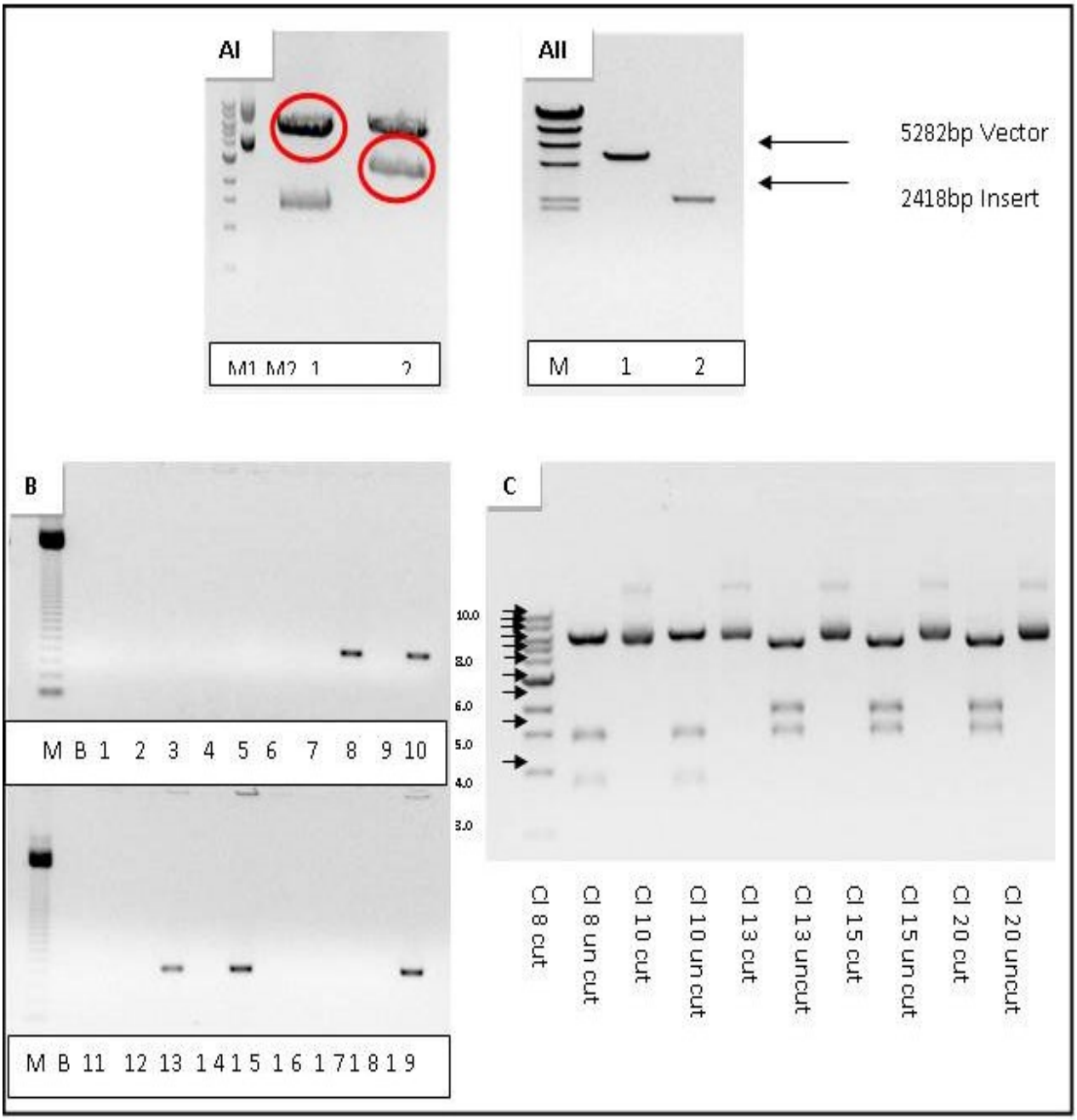

Figure 4.20. Construction of pAAV-miR199-IRES-Luc. AI. Double digestion of pAAV-miR-199-IRES-GFP and pIRES-Luc by *Xho*I and *Sal*I**.** M1: 1kb DNA marker M2: λHindIII molecular weight ladder, Lane 1: Vector, lane 2: Insert**. AII** Quantification of vector and insert for ligation step. M: λHindIII molecular weight ladder, Lane 1: Vector, lane 2: Insert**. B: PCR screening of recombinant pAAV-miR199-IRES-Luc construct.** M1: 123 DNA marker., B: blank, 1-20, clones amplified for Luc sequence with 497bp amplicone. Clones 8,10,13,15 and 20 screened as positive. **C: Restriction digestion Screening** to verified positive clones contains insert at sense direction. The *Nco*I digested and undigested vectors are shown for each clone. M: 1kb DNA marker.Cl8 and Cl10 were detected as positive clone with correct orientation of insert.

4.2.1.3. pAAV-IRES-Luc Construction

To construct luciferase control plasmid, The IRES-GFP sequence in pAAV-IRES-GFP was replaced with the sequence of IRES-Luc from pIRES-Luc. *Xho*I and *Sal*I overhangs were created by double digestion procedure to facilitate ligation of insert into vector. Positive clones were selected by PCR (Figure 4.21A) and restriction digestion using *Nco*I (Figure 4.21B).

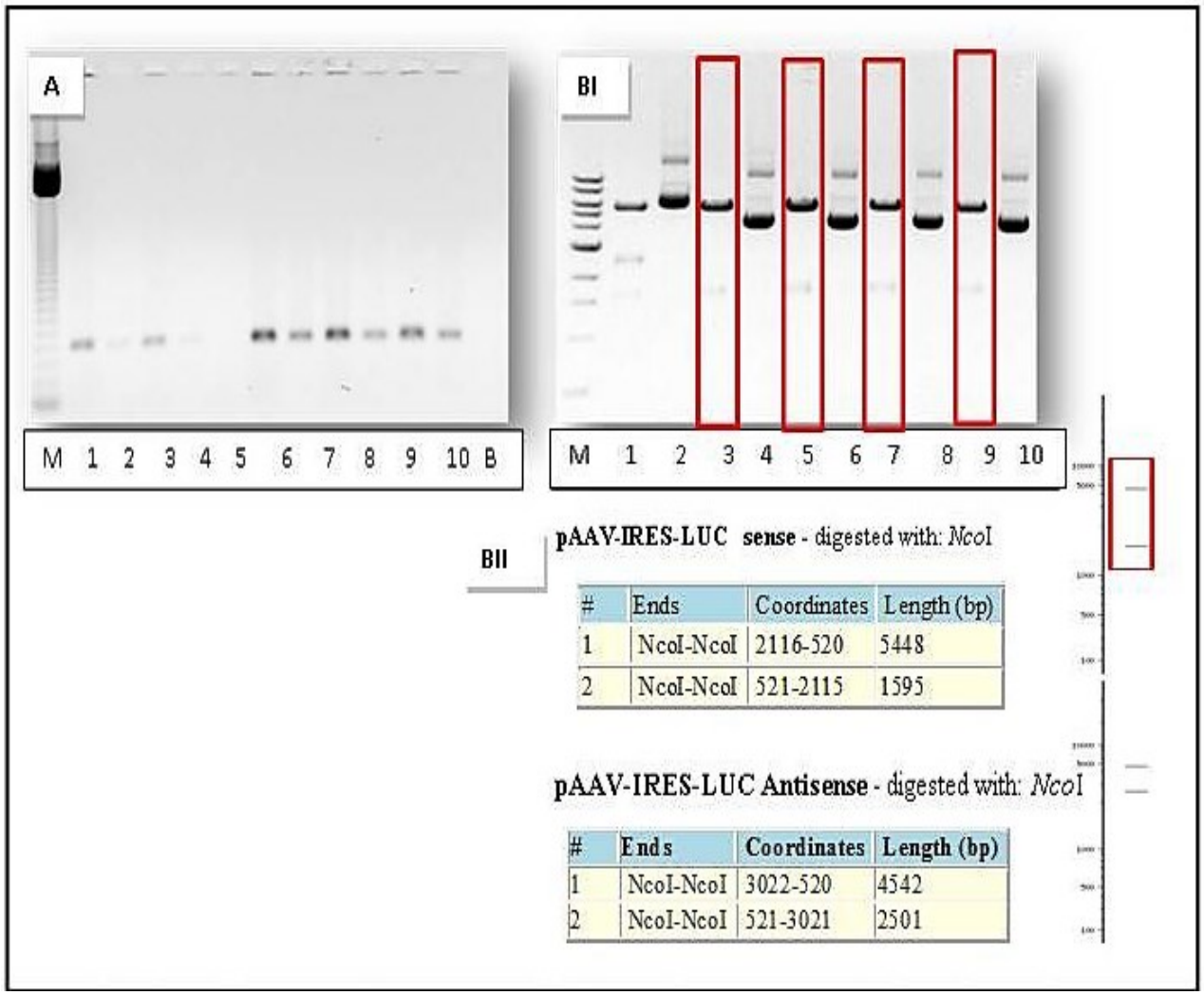

Figure 4.21. Screening of recombinant pAAV-IRES-Luc construct. (A): PCR screening. Lane1-10: results of amplification of recombinant clones with luc_296_F and luc_764_R as forward and reverse primers respectively. positive clones produce a 497bp amplicon. B: Blank sample. M: 123 DNA marker. **(B): Restriction digestion screening BI: The electrophoresis of cut clones on 0.8% agarose gel**. Lane with odd number: Digested recombinant clones, Lane with even number: Compatible undigested clones, M: 1Kb DNA marker. **BII:** The expected features of bands after digestion of created clones with *Nco*I designed in NEBcutter v2.0(http://tools.neb.com/NEBcutter2/).As shown, incorporation of insert in sense and antisense orientation into backbone results in different fragment in length.

Luciferase expression test demonstrated the expression of firefly (FF) luciferase reporter gene in pAAV-miR-199a-IRES-Luc and pAAV-IRES-Luc as well as pre-constructed pAAV-miR-221sponge-IRES-Luc. A Renilla luciferase vector (pRL-TK) was used to normalize experimental variability caused by differences in cell viability or transfection affiency. Firefly and renilla luciferase were measured by employing a Promega Dual-Luciferase® Reporter Assay System according to the supplemental manual (see material and methods for details). The results showed that pAAV vectors contains miR-221sponge or miR-199a and luc cassettes moderately expressed luciferase by 2.9 and 2.4 fold to NTC(non transfected control) respectively(pvalue: 0.0014, 0.05). Also using engineered pAAV-IRES-Luc control vector we could detected highly expression of luc by 17.1 fold to NTC (pvalue: 0.0011) (Figure 4.22).

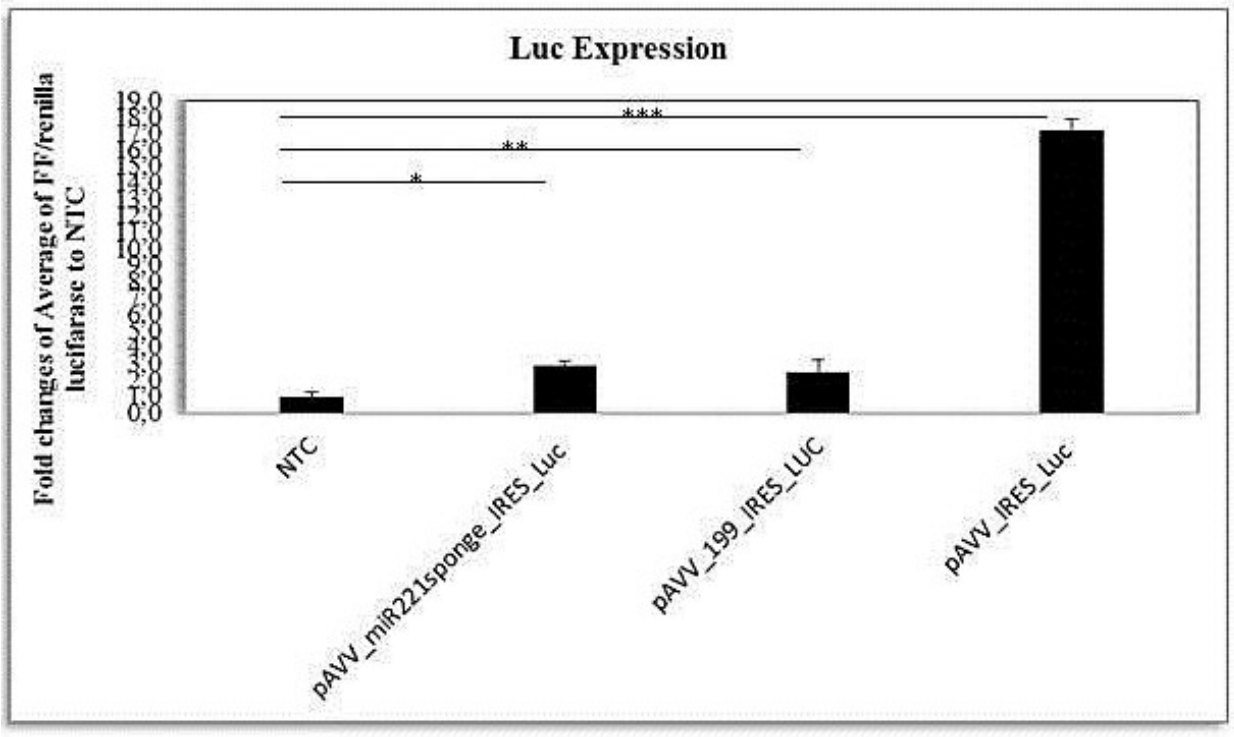

Figure 4.22. Fold changes of average FF/renilla Luminescence of pAAV-miR-199-IRES-Luc , pAAV-IRES-Luc and miR-221sponge-IRES-Luc respect to non-trasfected control (NTC). Each histobar represents the mean values ±SD of triplicate technical observations. Error bars dedicated standard error. The NTC control showed the lowest activity of luciferase. The pAAV-miR-221sponge-IRES-Luc, pAAV-miR-199-IRES-Luc and pAAV-IRES-Luc engineered constructs were able to express luciferase by 2.9 (*p=0.0014), 2.4 (**p=0.052), and 17.1 (0**p=0.0011) to NTC control respectively.

4.2.2. Recombinant Adeno-Associated Virus Developed to regulate the expression of miR-199a.

pAAV vector harboring the coding sequence of miR-199a was packaged into adeno-associated vector by triple transfection methods(see material and methods for details).To verify whether engineered adeno-associate virus was able to express miR-199a, we infected HepG2 cells with rAAV-199 and rAAV-control (rAAV-IRES-GFP) at MOI=500. Infected cells were harvested after 72h post-infection .Total RNA was isolated by using Trizol (see material and methods) and followed for purification using miRneasy kit. Real Time TaqMan assay with specific primer and probe for miR-199a revealed increasing expression level of miR-199a up to 92.1% (pValue=0.001) relative to control virus infected samples. The level of miR-199a expression in AAV-control infected cells was resulted the same level as uninfected HepG2(Figure 4.23).

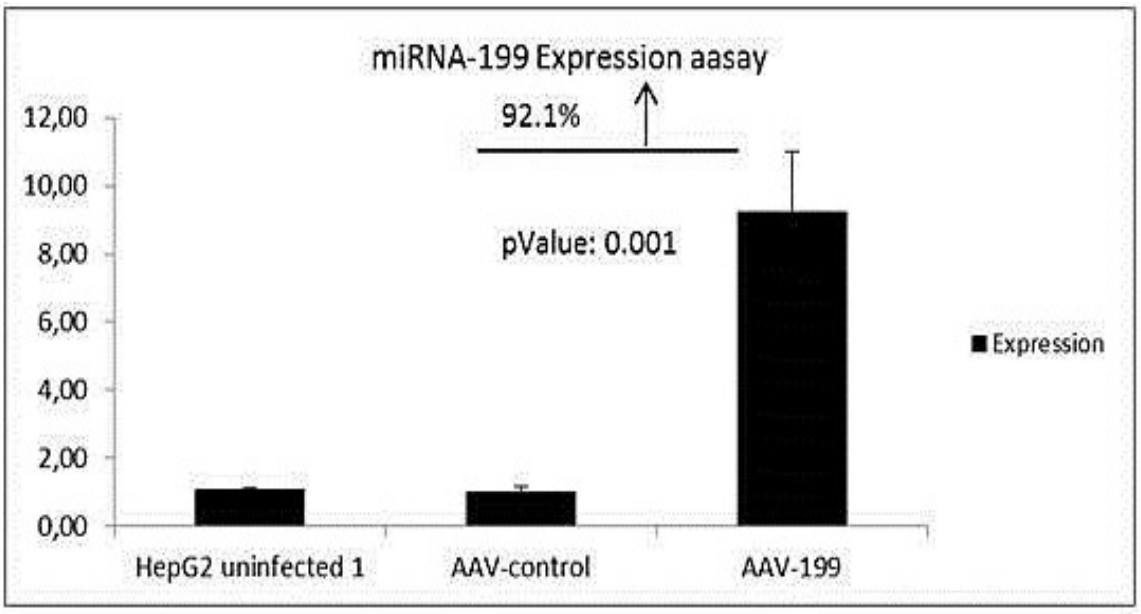

Figure 4.23. Functionality of rAAV expressed microRNA 199. Quantitative RT-PCR 72 hours following infection of HepG2 cells with rAAV-199 or rAAV-control, at MOI:500. Data are represented as mean values + SD from three replicates. The results showed that miR-199 expression was 92.1% higher compared to control virus infected (p-value = 0.0001).

4.2.2.1. miR-199a Expression Promotes Apoptotic Cell Death and Reduces Viability in HCC Cells

The hepG2 cells which characterized as HCC cell line with down-regulated level of miR-199a was transduced with rAAV-199 at MOI: 500. Comparable control rAd and rAAV infected cells were considered. The experiment was done in triplicate. We investigated the effect of miR-199a restoration on viability and apoptosis of HepG2 cells. Apoptosis were done through 7-Amino-actinomycin D (7-AAD)/PE Annexin V staining (Figure 4.24 A). The results showed a decrease in viability by around 51% which accompanied with 64.2% increase in the late apoptosis Phase(Figure 4.24 B). In this case no considerable increase in number of dead cells was detected. This results validated the regulation of miR-199a expression in HCC cell lines with low level of miR-199a could affect on cell proliferation and pull them to programmed death. Besides we checked the different concentration of AAV (from MOI: 10 to 10000) used for infection to optimize the most functional titer of virus. Function of rAAV-199 virus in different titers were compared using viability and apoptosis analysis. We showed the functionality of recombinant virus in cellular level is consistently related to titer of virus infected(Figure 4.24C).

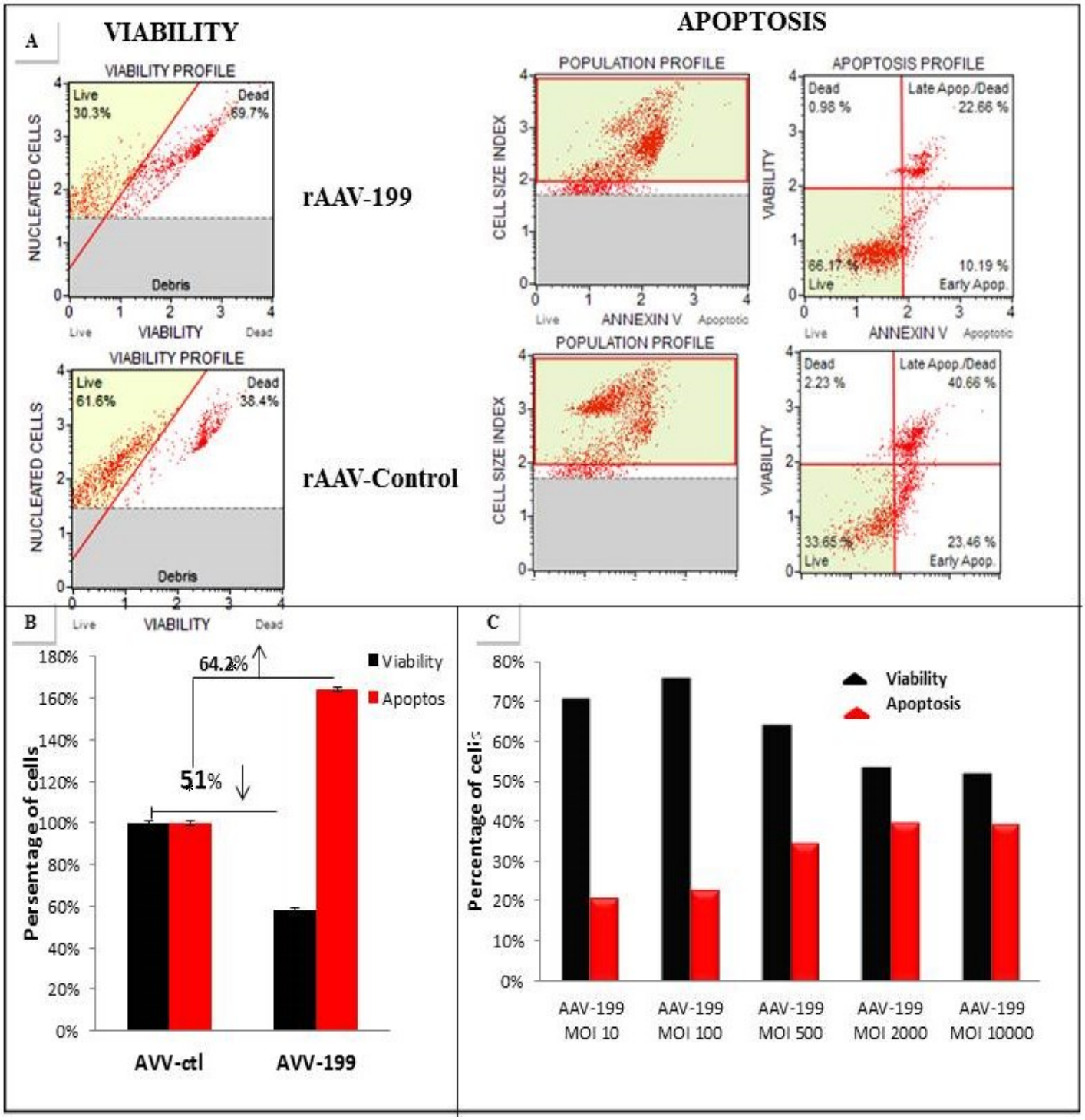

Figure 4.24. Cellular viability and apoptosis assay for HCC cells infected with rAAV-199. **(A)**: HepG2 cells infected with rAAV and control virus at MOI: 500. 72h post infection, Viability and Apoptosis was determined by Mini Affordable flow cytometry**.(B):** Restoration of miR-199 caused the the 51% decrease in viability and 64.2% increase in apoptosis (* pvalue<0.05), in HepG2 cells infected by rAAV-199 compared to control virus. **(C):** Functionality of engineered rAAV-199 is a relationship of titer of virus for infection. By increasing the concentration of virus used for infection a decrease in viability and an increase in apoptosis was observed.

4.3. PART III. Investigation of Combined Anticancer Effects of AntimiR-221/mimics miR-199a and Sorafenib through *in vitro* and *in vivo* Studies.

Lab of professor Negrini recently validated the tumor-promoting effect of miR-221, by showing that *in vivo* delivery of antimiR-221 oligonucleotides leads to a significant reduction of the number and size of tumor nodules(176). In addition, the multi-kinase inhibitor sorafenib has been approved for the therapy of advanced HCC(200). In this study we assessed the combination of anti-miRNA approach, like chemically modified antimiR-221 and sorafenib as a novel therapeutic strategy to potentiate growth inhibitory function of sorafenib in HCC cells. Also, as down-regulation of miR-199a in HCC was frequently reported (124) and important modulator of cell cycle and cell proliferation like mTOR and c-met are in the list of proven target for miR-199a, we decided to test if restoration of miR-199a level, sensitize cells towards drug treatment. We combined miR-199a oligonucleotide treatment with sorafenib and compared with efficacy of miR-199a and sorafenib alone.

4.3.1. Sorafenib Decreases Cell Viability and Promotes Apoptosis in HCC Cell Lines

The viability and apoptotic effect of sorafenib were examined using two different HCC cell lines, HepG2 and Hep3B. Cells were seeded in a 96-well plate and treated with increasing doses of sorafenib from 0.1 to 10μM which is the clinical relevant dose of sorafenib treatment. The effect of sorafenib on cell proliferation was measured by CellTiter-Glo® Luminescence assay and on apoptosis by using Caspase-Glo® 3/7 Assay after 48 hours exposure to drug (Figure 4.25). In both cell line which were tested, sorafenib treatment conducted decrease in viability of cells in a dose-dependent manner (Figure 4.26A). Induction of caspase3/7 apoptosis by sorafenib was further evaluated in the same treated wells. In HepG2 cell line, results showed apoptosis was increased in the presence of 0.01, 0.1 and 1μM of sorafenib respect to non-treated(NTC) and solvent control (CTL). However in higher dose of sorafenib, since the majority of cells go through dead phase, the results were not significant. Induction of apoptosis, in Hep3B cells, appeared to correspond in rising in the drug-dose (Figure 4.26B). All together these data indicated that sorafenib can inhibit proliferation and induced caspase3/7 apoptosis in hepatocellular carcinoma *in vitro*.

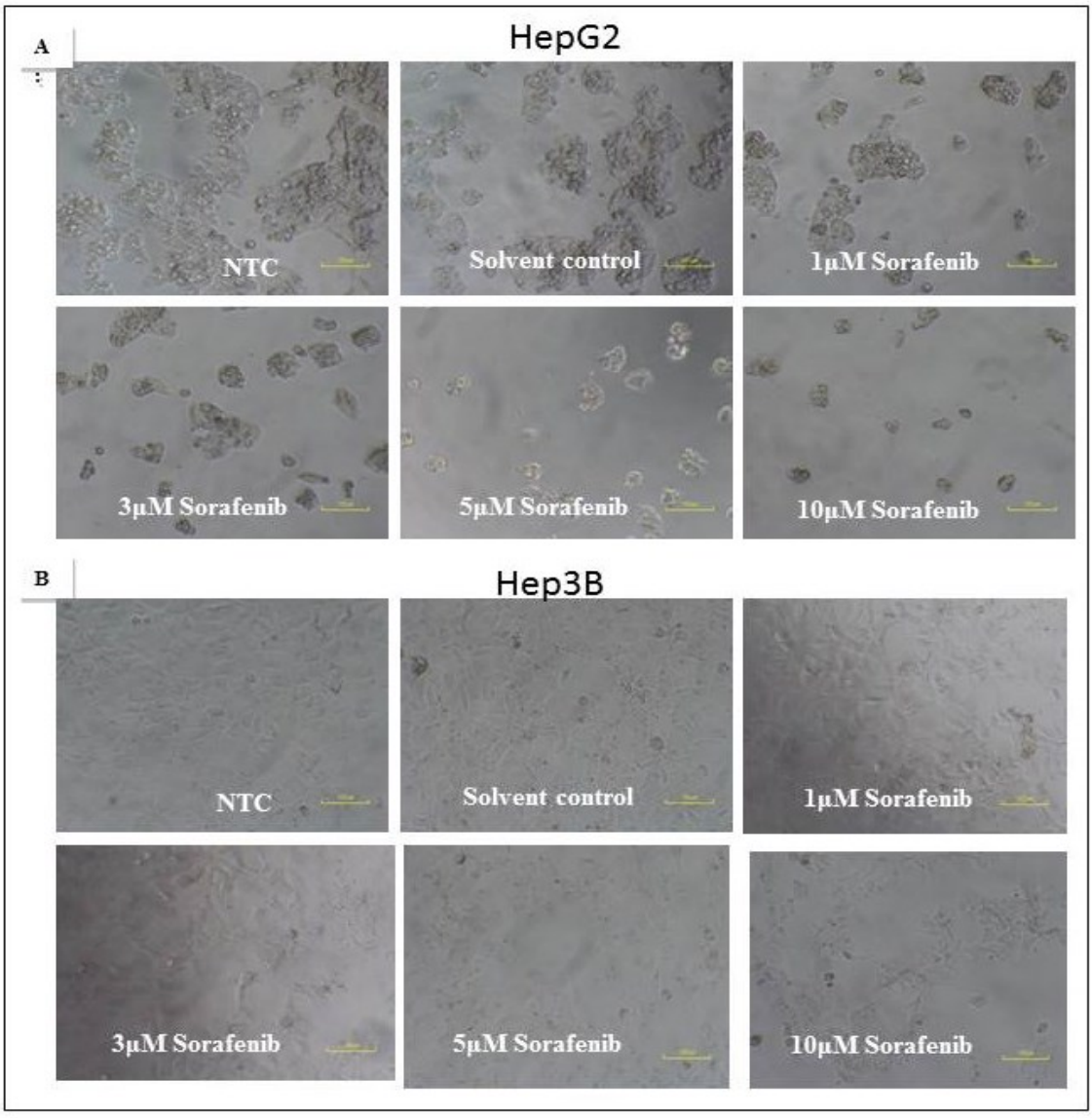

Figure 4.25. Morphological changes induced by different concentration of sorafenib exposure for 48h (A): HepG2 cell line**. (B):** Hep3B cell line

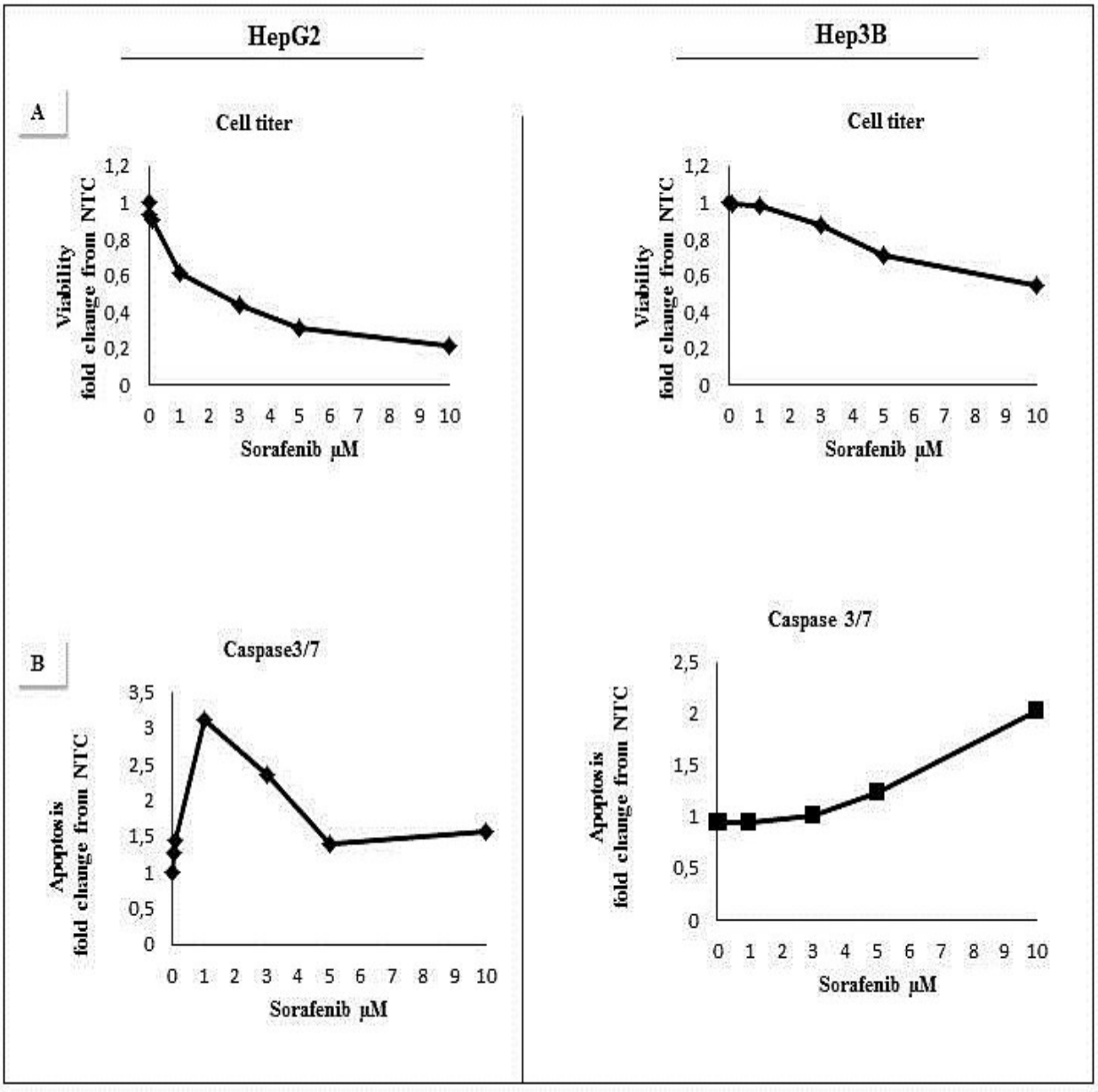

Figure 4.26. Sorafenib decrease viability and induces apoptosis in HCC cells. Sorafenib was added to HepG2and Hep3B cells and cultured for 48 hours in complete culture medium in the presence of 10% FBS. Fold changes of media of each triplicate treatment were analyzed and considered as results. **(A):** inhibition of cell proliferation. **(B):** Induction of apoptosis via caspase3/7 activity analysis.

4.3.2. HCC Cell Lines Show Variable Sensitivity to Sorafenib

We decided to determined IC-50 values of sorafenib in HCC cell lines, at which 50% of the cells were growth-inhibited compared with control. We hypothesized that for detecting the synergistic effects, it is easier to use sub-IC50 concentrations of sorafenib in combination with constant concentration of antimiR-221/mimics miR-199a oligos. Sorafenib dose-dependent inhibition of cell proliferation assessed in HepG2 and Hep3B cell lines. Cells were plated in 96-well plates (10,000 cells per well) and exposed to 0.01, 0.1 ,1 ,3, 5 and 10μM of sorafenib. Cells were tested using CellTiter-Glo® Luminescence Cell Viability Assay kits (Promega Corporation) as assays that require only a few minutes to generate a measurable signal (e.g., ATP quantization or LDH-release assays) provide information representing a snapshot in time and have an advantage over assays that may require several hours of incubation to develop a signal (e.g., MTS or resazurin). The cells were incubated with sorafenib for 24 and 48 hours. Cremophor EL/95% ethanol (50:50) at a concentration equal to that of 5μM drug-treated cells was used for checking the effect of drug-solvent. The results were obtained in two independent experiments, each of which was performed in triplicate. Fold changes of the number of viable cells respect to non-treated cells (NTC) were plotted to varies concentration of sorafenib. As shown in Figure 4.26, sorafenib decreased the number of viable HepG2 cells dose-dependently with an IC50 of around 2μM and more than 10μM for Hep3B cells after 48h drug-exposure. Interestingly, sorafenib exhibited a much stronger inhibitory effect on the survival of HepG2 respect to Hep3B as evidenced by its lower IC50 values.

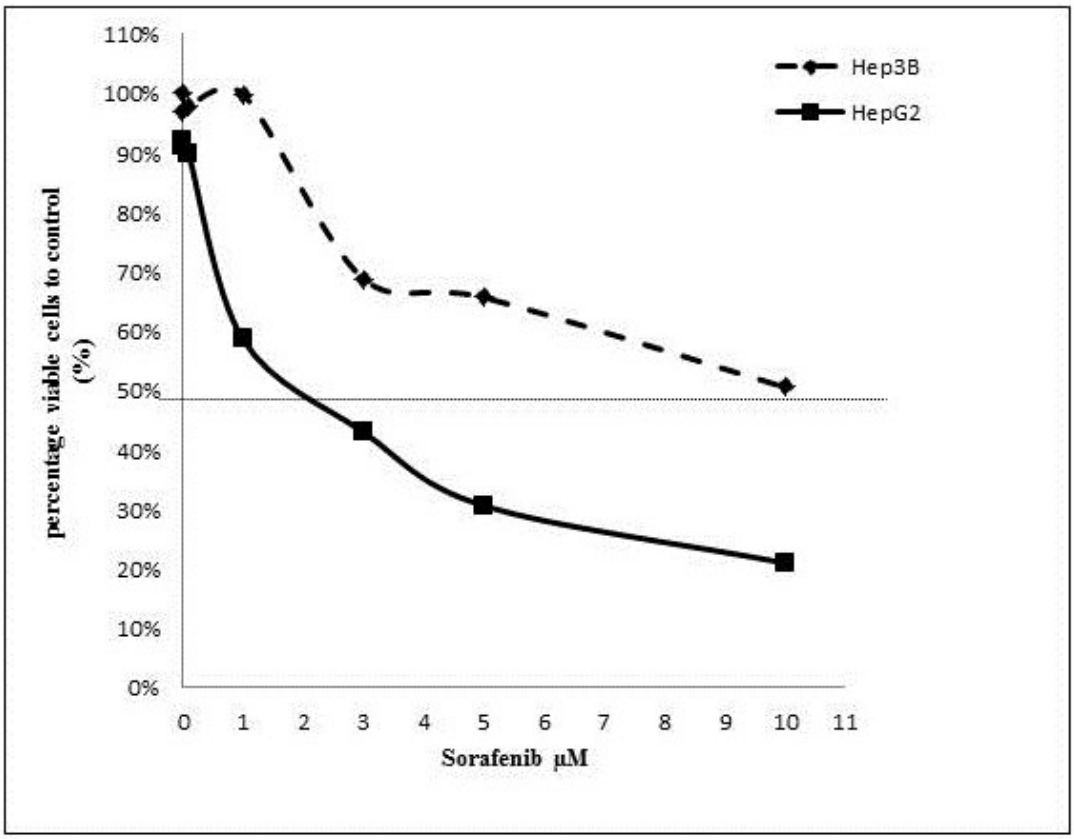

Fig. 4.27. IC50 determination for sorafenib in HepG2 and Hep3B cells. Cells were cultured for 48h in the presence of different concentrations of sorafenib from 0.01µM to 10µM. After which viable cell numbers were determined using cell titer Glo luminescence assay. For HepG2 the IC50 was around 2µM, for Hep3B, IC50 showed higher value shifted towards 10µM.

4.3.3. AntimiR-221/mimics miR-199a Oligos Have Synergistic Effect with Sorafenib in HCC Cell Lines

We further investigated whether down-regulation of an established oncomiR "miR-221" modulate the response of hepatocellular carcinoma cells to a novel drug that is potentially feasible for use in the clinic "sorafenib". Also we tested the efficiency of up-regulation of miR-199a as anti oncomiR in HCC alone or in combination with sorafenib. This possibility was explored through cellular and molecular assay in HCC cell lines, as well by *in vivo* assay for miR-199a.

4.3.3.1. Cell viability in HCC Cell Lines Reduce by Combination Therapy of AntimiR-221 as well as mimics miR-199a and sorafenib

To determine if combining AntimiR-221/miR-199a and/or sorafenib leads to synergistic effect on cell survival *in vitro*, HepG2 or Hep3B cells (10,000 cells per well in 96-well plates) were incubated with 100nM of antimiR-221/premiR-199a-3p oligonucleotides and sub-IC50 concentrations of sorafenib alone or in combinations. Non-transfected (NTC), vehicle (Solvent+lipofectamin2000) or scrambled oligonucleotide controls were considered for establishment and verification of final effects. Cell survival was measured by CellTiter-Blue® fluorescent assay after 24h and 48h of transfection and/or drug exposure for Hep3B and HepG2, respectively. The time points of treatment were optimized in independent experiments between 12, 24 and 48 hours which established by microscopic as well as cell viability and apoptosis analysis (Data not shown). A shorter time of oligo and/or drug exposure that was related to much stronger inhibitory effect of antimiR-221/miR-199a was obtained in Hep3B respect to HepG2, as the most profound effects were achieved at 24h for Hep3B, comparing 48 h for HepG2. Data were obtained in independent experiments, each of which was performed in triplicate. Fold changes of the media fluorescent detected in each treated wells respect to non-treated/transfected wells (NTC) were used to detect the effect of co-treatment of antimiR-221/pre-miR-199a and sorafenib. As shown in Figure 4.28 combining of antisense miR-221 oligos with sorafenib could enhance the antitumor effect of sorafenib through declining the number of viable HCC cells *in vitro* . Figure 4.28 A shows the efficacy of transfection . Viability of HepG2 cells in the presence of antimiR-221 and sorafenib poorly decreased by 5% ,p value= 0.048, n=3 (Figure 4.28B) The cell titer value in untreated Hep3B significantly decreased

more than to 21%,30% and 44% in 5 and 10μM of sorafenib and 100nM antimiR-221 treated cells respect to NTC ($P < 0.005$,n=3), respectively. While in co-treated Hep3B cells (antimiR-221+sorafenib) 36% and 28%($P < 0.005$,n=3), decrease in the number of viable cells was detected respect to 5 μM and 10μM Sorafenib single treatments (Figure 4.28C). Scramble and vehicle controls did not show significantly anti-proliferative effects.

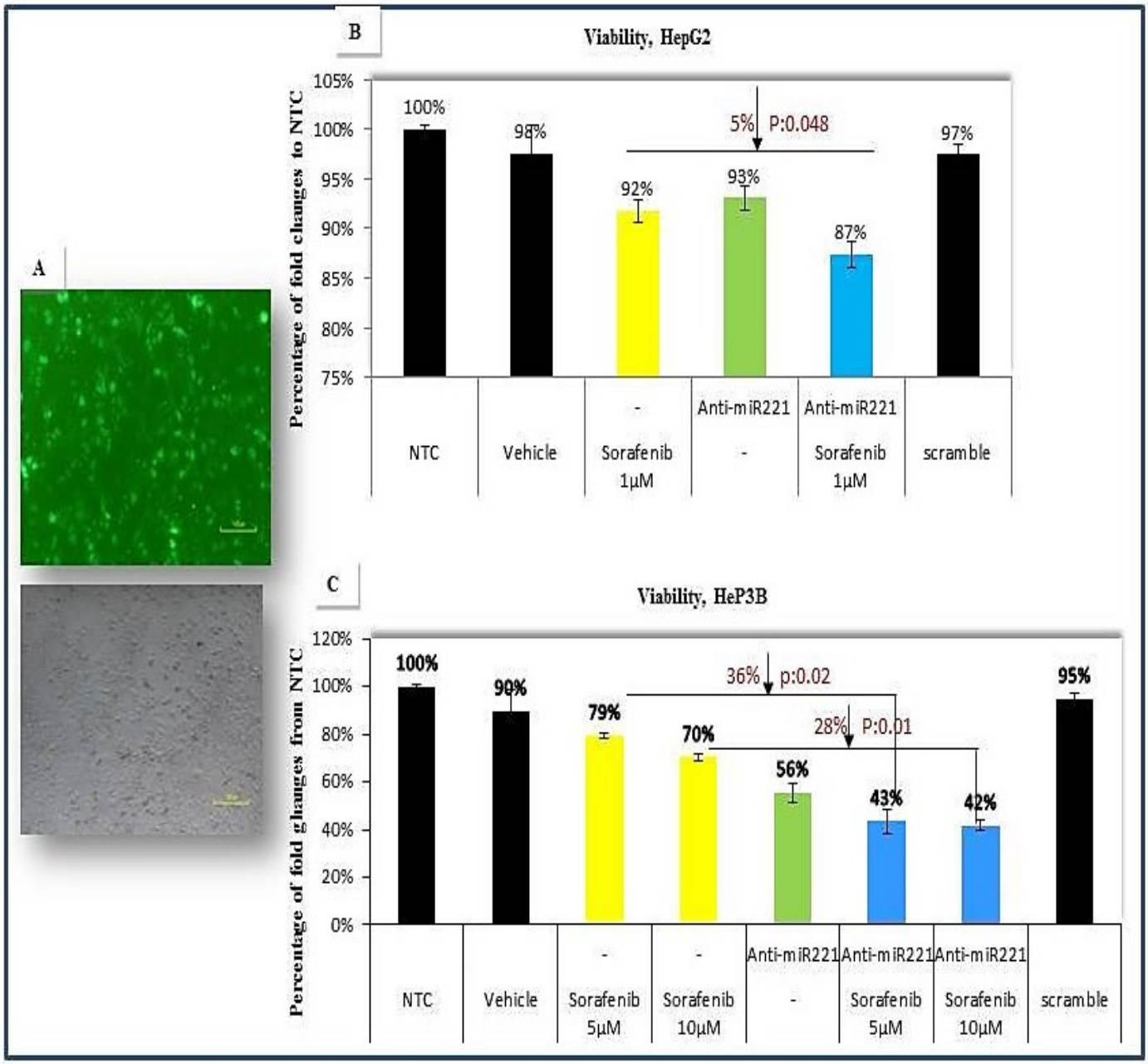

Figure 4.28. AntimiR-221 and/or sorafenib inhibit proliferation of HCC cells.(A) efficiency of transfection revealed under florescent microscope (10x). Results were shown as percentage of fold changes of median luminescence activity to non treated (NTC) control, Pvalue‹0.05 n=3. Vehicle (Solvent of sorafenib+lipofectamine 2000) **(B):** Cell viability assay in HepG2 cell line.**(C):** Cell viability assay in Hep3B cell line.

premiR-199a instead decreased the number of viable cells by 16% regards to un transfected control. This effect were 21% and 30% (P < 0.005,n=3), for sorafenib treatment at concentration of 5 and 10µM(Figure 2.28). Combining premiR-199a and sorafenib treatment showed to be more effective than each treatment alone. We detected 28% (p value=0.042,n=3) and 22%(p value=0.048,n=3) reduce in viability of hep3B cells for premiR-199a combined with 5 and 10µM of sorafenib respect to sorafenib treated alone, respectively(Figure 4.29).

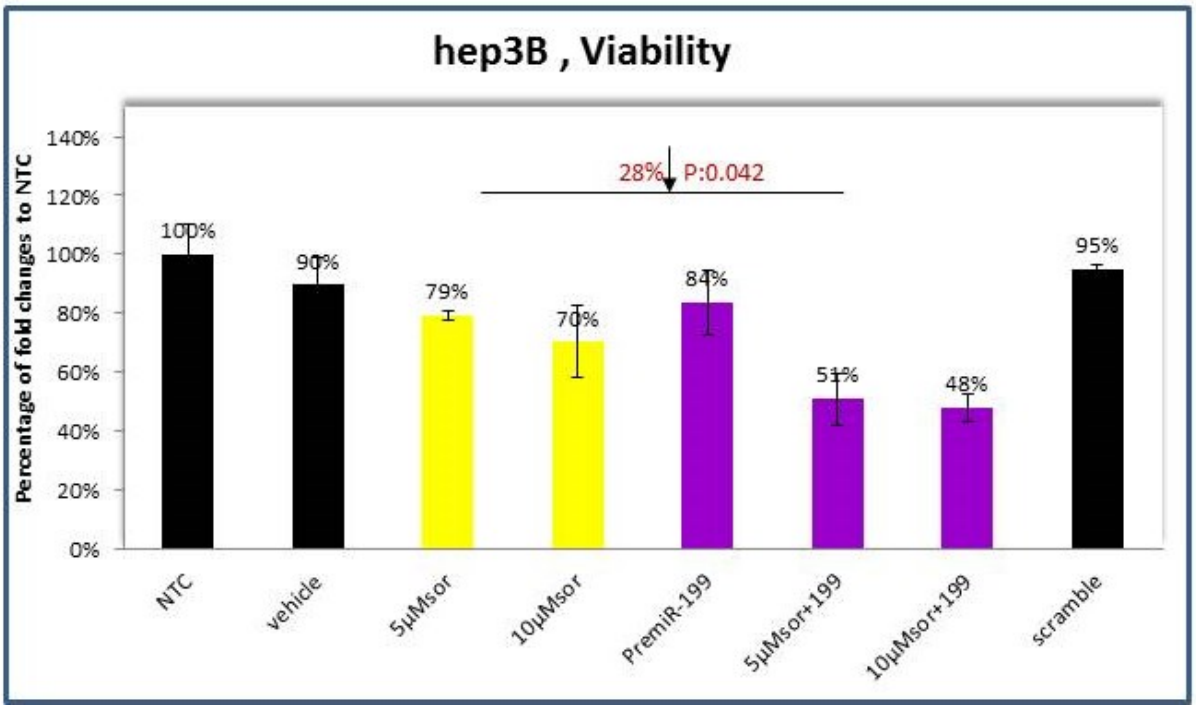

Figure 4.29. PremiR-199 and/or sorafenib inhibit proliferation of HCC cells. Results were shown as percentage of fold changes of median luminescence activity to non treated (NTC) control, Pvalue‹0.05 n=3. Vehicle (Solvent of sorafenib+lipofectamine 2000) **.**

4.3.3.2. Combination Therapy of AntimiR-221/miR-199a Oligos and Sorafenib Increase Caspase-3/7 Apoptosis in HCC Cells.

To assess how combining antimiR-221/premiR-199a oligos and sorafenib, affect cell apoptosis, we examined activation of caspases 3 and 7 in HCC cells. Caspase-3/7 activity was measured immediately after the detection of CellTiter-Blue® Cell Viability Assay (described above) on the same treated wells, by adding Caspase-Glo® 3/7 assay reagent at the established time after transfection and/or sorafenib treatments into HepG2 and hep3B plated cells. The most profound apoptotic effects were achieved at 48h for HepG2 and 24 h for Hep3B. Analysis of apoptosis in HepG2 (Figure 4.30A) revealed that co-treatment of antimiR-221 with 1μM of sorafenib induced a significantly higher increase in luminescence measurement related to activity of caspase 3 and 7 proapoptotic enzyme by more than 72% to sorafenib 1μM and 25% to antimiR-221 oligos single treatments ($P < 0.005$,n=3). The mean caspase 3/7 apoptosis rates respect to untreated control were detected as 20.47% ,66.95% and 92.28% for 1μM of sorafenib and 100nM antimiR-221 and their combination($P < 0.005$,n=3). Scramble and vehicle controls did not show significantly increase in apoptosis. Apoptosis rate for premiR-199a in combination with sorafenib showed increase of 19% and 44% compared to premiR-199a and 1μM sorafenib single treatment, respectively($P < 0.005$,n=3).. In Hep3B(Figure 4.30B), antimiR-221/premiR-199a transfected cells were treated with the combination of different concentration of sorafenib. A moderate dose-dependent caspases-3/7 activation was observed in Hep3B cells exposed to 5μM and 10μM sorafenib alone . However a substantial effect was observed in presence of 100nM of antimiR-221 alone. Analysis of apoptosis attributed to antimiR-221 co-treatment with sorafenib in Hep3B revealed increased induction of apoptosis considering sorafenib single treatments but not to co-treatment with antimiR-221, it was related to extensive effects of antimiR-221 that they not only stopped proliferating, but they actually killed cells during 24-36 h. Using premiR-199a single treatment induce apoptosis 10% more than sorafenib 10μM regards to NTC. However co-treatment of premiR-199a and sorafenib showed higher effect as 119% and 86% increase in apoptosis respect to 5 and 10μM of sorafenib respectively($P < 0.005$,n=3).

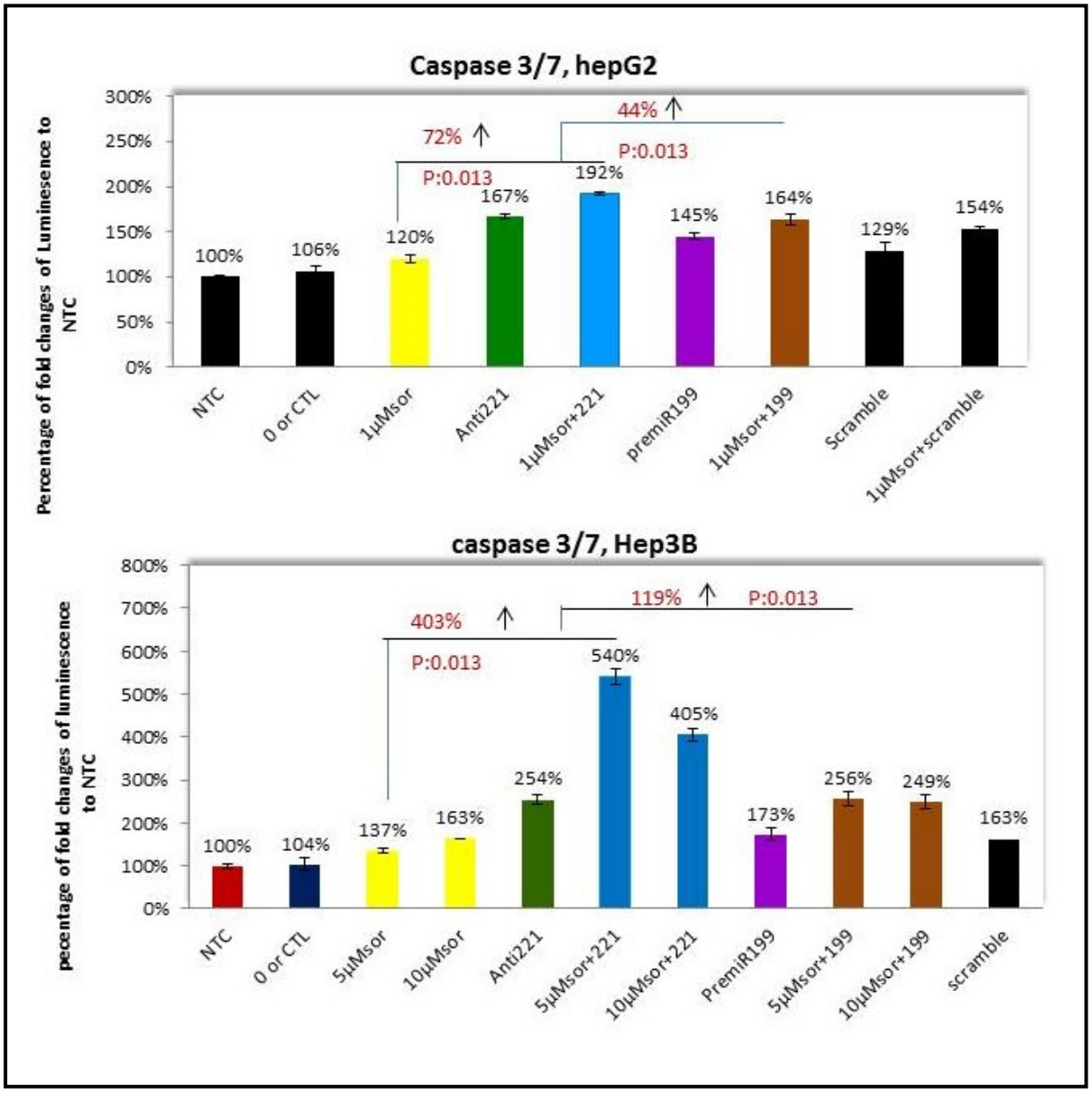

Figure 4.30. Apoptosis induction were detected via caspase3/7 activity following treatment of HepG2 and Hep3B. Results are displayed as percentage of fold changes fluorescence activity respect to non treated control(NTC). The test was done in triplicate and pvalue‹0.05 was considered as significant. Vehicle (Solvent of sorafenib+lipofectamine 2000) **(A):** Caspase 3/7 assay in HepG2 cell line. (B): Caspase 3/7 assay in Hep3B cell line.

4.3.3.3. Annexin V Apoptosis Assay Validates the Synergistic Effect of AntimiR-221 Oligos and Sorafenib.

The Muse™ Annexin V and Dead Cell Assay is based on the detection of phosphatidylserine (PS) on the surface of apoptotic cells, using fluorescently labeled Annexin V in combination with the dead cell marker, 7-AAD (see material and methods for details). Induction of apoptosis by combination of antimiR-221 and sorafenib was further validated by Annexin V and Dead Cell Assay. We exposed HepG2 and Hep3B cells which were seeded in 24 well plate to constant molarities of miR-221(100nM) and different established concentration of sorafenib just below their IC50. After 12,24,48h of drug exposure, we assessed the percentage of apoptotic cells employing Muse™ Annexin V & Dead Cell Kit. In HepG2, effects became apparent from time point 48h, but in Hep3B we saw the apoptotic effect earlier and harvested them at 24h(Figure 4.31).

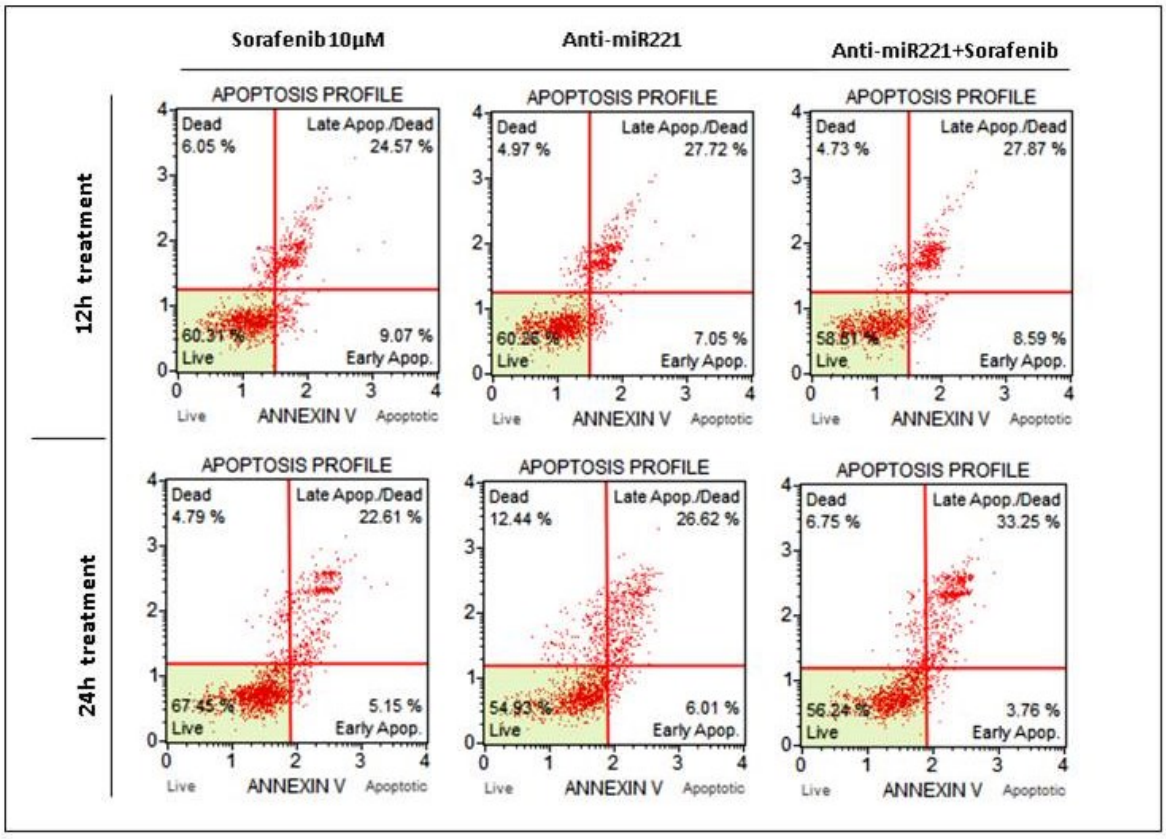

Figure 4.31. Muse Annexin V and Dead Cell analysis .1*10^5 Hep3B cells seeded in 24 well plate. The day after cells were treated with sorafenib in defined concentration and /or AntimiR221 with final concentration at 100nM and incubated for 12, 24 and 48hours. The results of staining 1*10^4 cells/ml with Fluorescent Annexin V and 7-AAD dead marker dyes were visualized in muse mini flowcytometry(see material and methods for details). The final quantitative analysis of live, early and late apoptosis, and cell death for 12 and 24 hours were shown here.

Induction of apoptotic effects of single agent treatments vs. control, as well as combinations vs. single agents reached statistical significance in HepG2 as well as Hep3B cells(Figure 4.32).

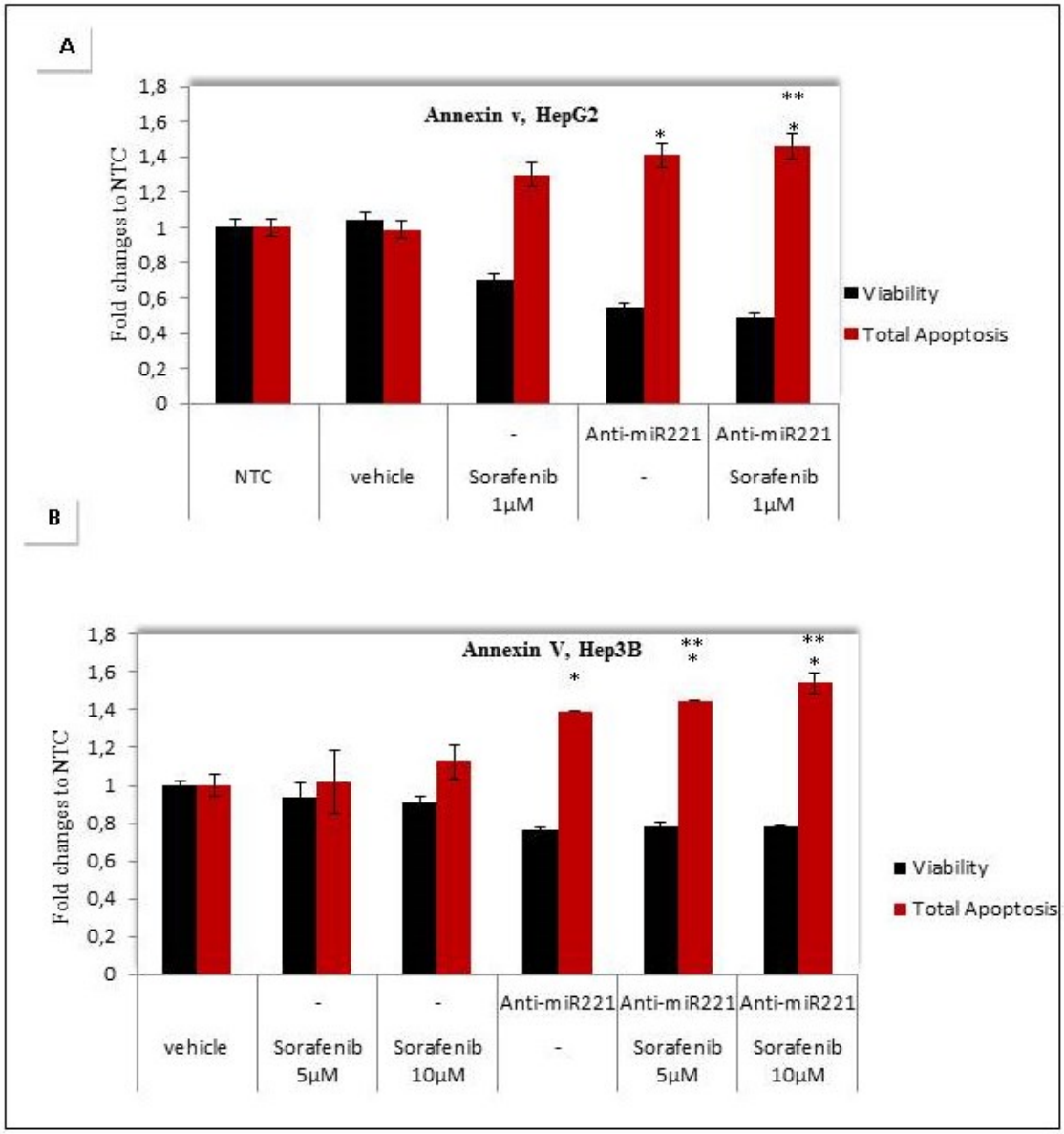

Figure 4.32. Apoptosis induction were detected using fluorescently labeled with Annexin V in combination with the dead cell marker, 7-AAD following treatment of HepG2 for 48h (A) and Hep3B for 24h (B). Results are displayed as fold changes to non treated(NTC) or vehicle control (Solvent+lipofectamine 2000).(*) pvalue ‹0.05 for anti221 transfected alone or in combination with sorafenib respect to control(NTC or CTL) .(**) pvalue ‹0.05 for combination treatment respect to AntimiR-221 trasfected cells alone.

Taq man real time assay was also performed to explain that the cellular anti-proliferative and apoptotic effects of antimiR-221 and/or sorafenib might be ,at least in part, consequence of down-regulating of endogenous miR-221.Using iCycler iQ5 optical system software (BioRad, Hercules, CA, threshold cycle (beginning of the PCR exponential phase) values were analyzed for miR-221 target and amplified U6sn RNA. The levels of miRNAs expression were normalized after subtracting the Ct value of the U6sn RNA internal control from that of miR-221 Ct value for samples In order to compare the levels of miRNA expression between different treated samples . The relative amount of target miR-221 was expressed as a relative ratio versus those of U6sn RNA. Experiments were conducted in triplicate. Probability values of <0.05 were considered significant(Figure 4.33)

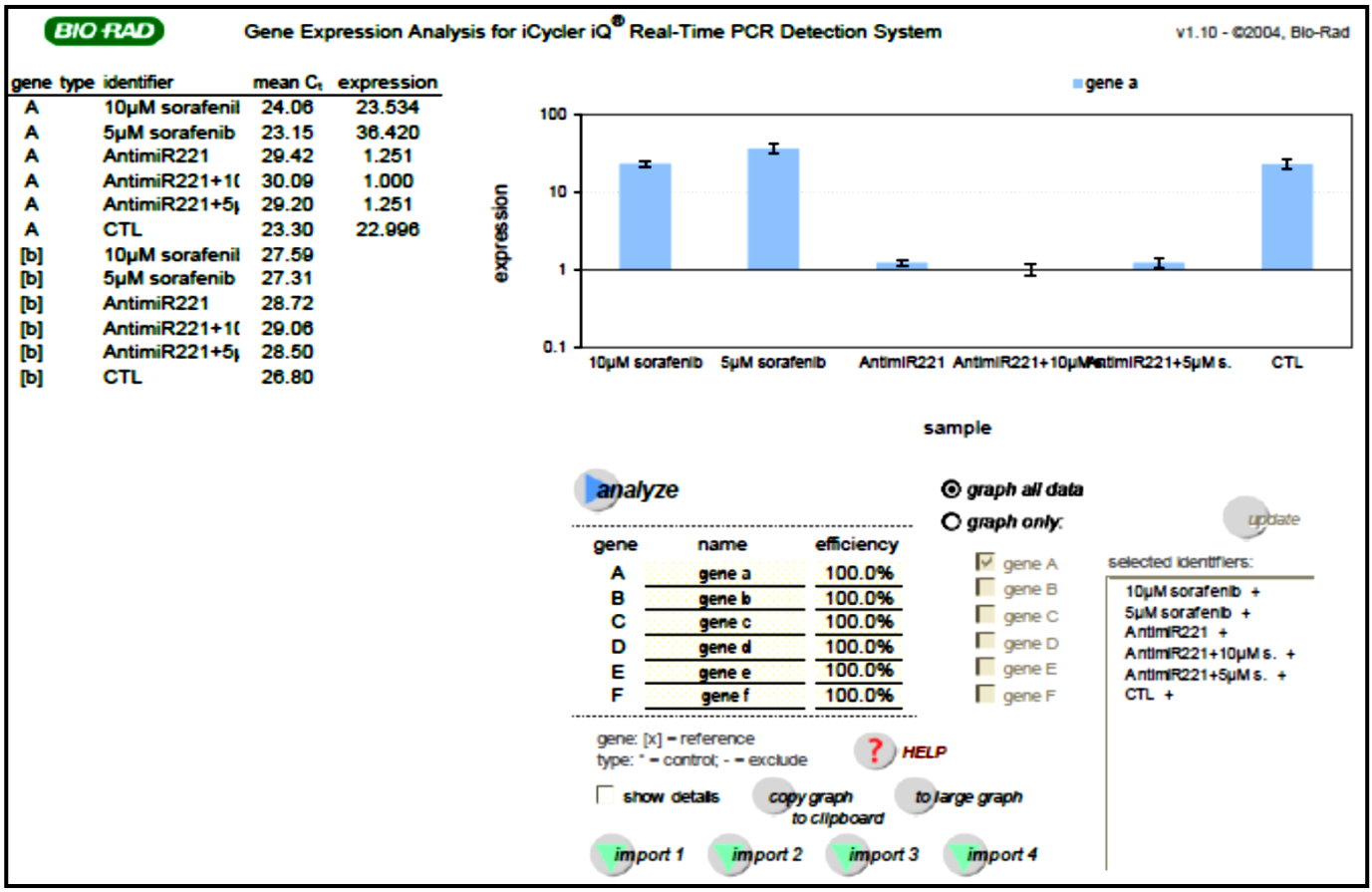

Figure 4.33. Real time TaqMan assay for miR-221. Comprehensive silencing of endogenous miR-221 in samples which tranfected in the presence of antimiR-221oligos were validated as relative to control.

4.3.3.4. AntimiR-221 Induces Cell Cycle Arrest in Hep3B Cells

Next we examined the effect of combination of antimiR-221 and sorafenib by cell cycle analysis. We transfected Hep3B cells with antimiR-221 oligo(100nM). After 48 h cell cycle analyzed with Muse™ Cell Cycle Kit Catalog No. MCH100106 according to instructor's manual. The value of cell populations at different stages of cell cycles are listed within the panels (Figure 4.34). The results showed a 1.4 and 1.2 decrease in S phage of cells treated with antimiR-221 oligo+sorafenib respect to control and cells treated with sorafenib, respectively.

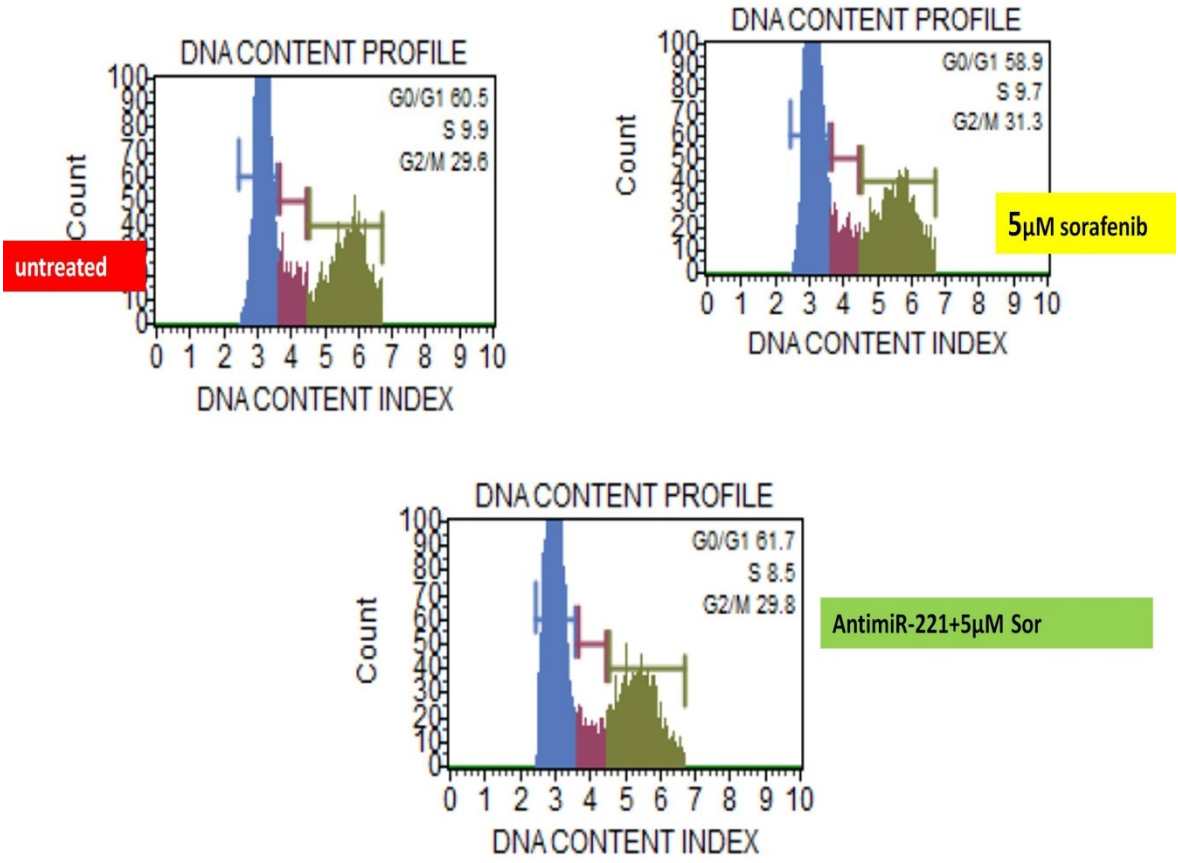

Figure 4.34. cell cycle analysis of AntimiR-221oligoes transfected Hep3B in combination with sorafenib. A decrease in S Phage accompanied with little increase in G1 phase was observed in Cells treated with AntimiR-221oligoes+5µM of Sorafenib compared to Control and sorafenib treated cells.

4.3.4. *In vivo* Anti-tumor Activity of mimics miR-199a Restoration Alone and in Combination with Sorafenib.

We next investigated the effect of miR-199a treatment alone or in combination with sorafenib in miR-221 transgenic (TG221) mouse, which is predisposed to the development of liver cancer. A highly significant(p value=0.006) decrease in number of nodules was detected following 9 injections (3times a week for 3 weeks) of mimics miR-199a oligos regards to control mice(Fig.4.35A) that seems be as effective as clinical dosage of sorafenib. The combination of miR-199a and sorafenib did not show higher effect than single Ones. Furthermore, we measured the diameter of tumor nodules (Fig. 4.35B). The results showed a decrease in size of tumor in groups treated with mimics miR-199a oligos regards to control group although it was not statistically significant, suggesting a need for increasing the number of cases in further experiment. Sorafenib as well as combination therapy did not significantly decrease the size of tumor nodules compared to control.

A

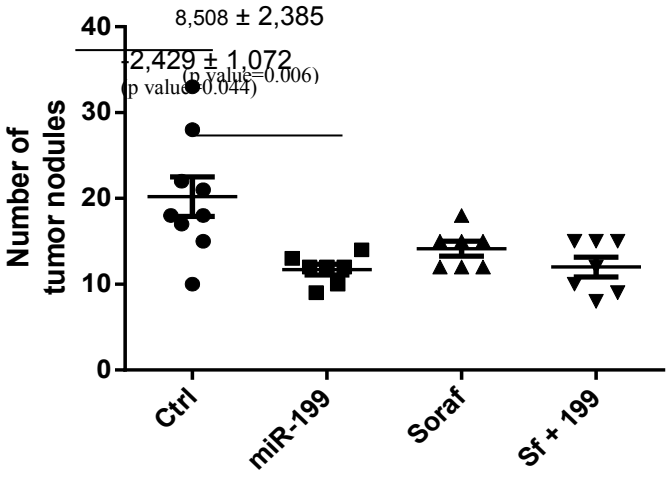

B

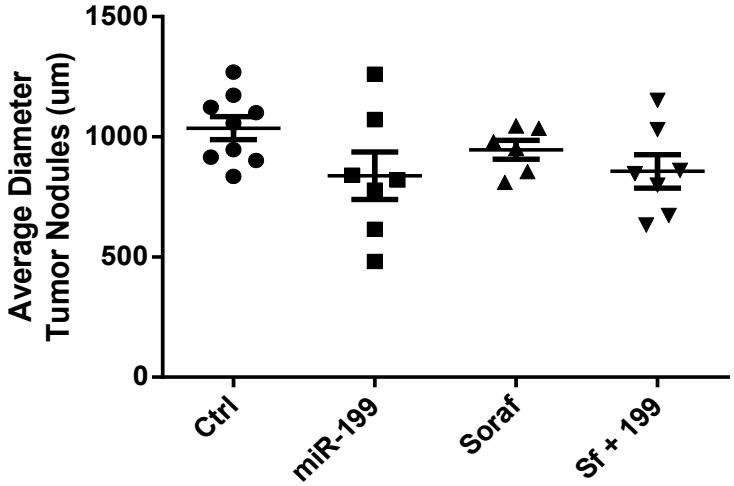

Figure 4.35. in vivo assessment of miR-199a restoration alone or in combination with sorafenib. (A). Number of tumor nodules. 8,508 ± 2,385 (p value=0.006) difference in Mean ± SEM of mimics miR-199a and control groups showed achieving highly decrease in number of tumors in miR-199a based therapy that was accordance with sorafenib and their combination therapy. **(B). Average diameter of tumor nodules(μm).**

4.4. PART IV: Assessment of Novel Cancer-Associated Targets of miR-221

To identify genes controlled by miR-221, we compared gene expression profiling of SNU-398 cells transfected with miR-221 precursor vs. SNU-398 cells transfected with negative control (NC2, Ambion). This cell line was chosen because it expresses low level of miR-221. From the list of genes identified by Sylamer and the list of path-ways significantly affected by miR-221, we focused our attention on genes involved in cell proliferation and apoptosis regulation to individually validate them as miR-221 targets. They included the cell cycle regulators retinoblastoma 1 (RB1) and WEE1, the pro-apoptotic gene Apoptotic Peptidase Activating Factor 1 (APAF1), CCCTC-binding factor (CTCF), a transcriptional repressor and Annexin A1 (ANXA1). In addition, we also investigated Fas Ligand (FASLG), which contains a miR-221 target region in its 3UTR, but was not within the Sylamer-derived- 602 genes list. The genes studied are listed in Table 4.1.

Table 4.1.Genes individually validated as miR-221 targets

Gene	Gene symbol	Sylamer position[a]	3′UTR length (bp)	Number of miR-221 target sequences	Fold-change[b]	Online prediction[c]
Retinoblastoma 1	RB1	1087	1915	2	–1, 2	
Apoptotic Peptidase Activating Factor 1	APAF1	430	2945	2	–1, 3	
Annexin A1	ANXA1	1580	718	2	–1, 16	M
WEE1 homolog (*S. Pombe*)	WEE1	1598	1382	1	–1, 16	
CCCTC-binding factor (zinc finger protein)	CTCF	302	1308	2	–1, 37	D
Fas ligand (TNF superfamily, member 6)	FASLG	N/A	907	1	N/A	

[a] *Position within the first 1800 most down-regulated mRNAs.*

[b] *Calculated on the basis of microarray experiments (3 miR-221 vs. 4 NC2).*

[c] *M, Microcosm; D, Diana microT; T, Targetscan.*

To validate potential miR-221 target genes, we first performed luciferase assays. We cloned a portion of the 3UTRs containing miR-221 target sequences into a psiCheck-2 reporter vector, downstream the luciferase reporter gene. We assayed the luciferase activity in the presence or absence of added miR-221 mimics in three different cell lines: HEK-293 (embryonic kidney derived cells) and two hepatocarcinoma derived cells (SNU-398, HepG2). The reporter vector constructs were transfected into cells together with miR-221 precursor or negative control (NC2). We found that miR-221 induced a significant decrease in luciferase activity of all the vectors containing 3UTRs of genes identified through the Sylamer approach. Instead, no change in luciferase activity could be detected for the psiCheck-FASLG 3UTR vector (Figure 4.36A).

TheabilityofmiR-221toinduceadecreaseinRB1,APAF1, ANXA1, WEE1, and CTCF expression was further demonstrated by measuring the relative amount of their mRNAs in SNU-398 and HepG2 cell lines. We found a significant decrease (p-value< 0.003) of RB1 mRNAs in both cell lines transfected with miR-221 (−64% in SNU-398 and −72% in HepG2); similarly, we found 26 and 42% decrease in APAF1 mRNA level, respectively, in SNU-398 and HepG2 (p-value<0.015); miR-221 caused a decrease of 38% (SNU-398) and 77% (HepG2) of ANXA1 mRNA (p-value<0.018); WEE1 mRNA was 44% (SNU-398) and 61% (HepG2) less expressed in presence of microRNA (p-value<0.013) and CTCF mRNA showed a 38% decrease in miR-221 transfected SNU-398 cells (p-value=0.006), while in HepG2 we found a slight (but not significant) decrease (Figure 4.36B), meaning that specific cell background could modulate microRNA effects on target genes. Finally, protein expression analyses revealed that miR-221 could indeed decrease the levels of RB1, WEE1, APAF1, and ANXA1 proteins in SNU-398 cells; conversely, an oligonucleotide antimiR-221 induced their increase in SNU-398/miR-221 stable clone (Figure 4.36C). We could not test CTCF protein, because available antibodies produced poor quality results.

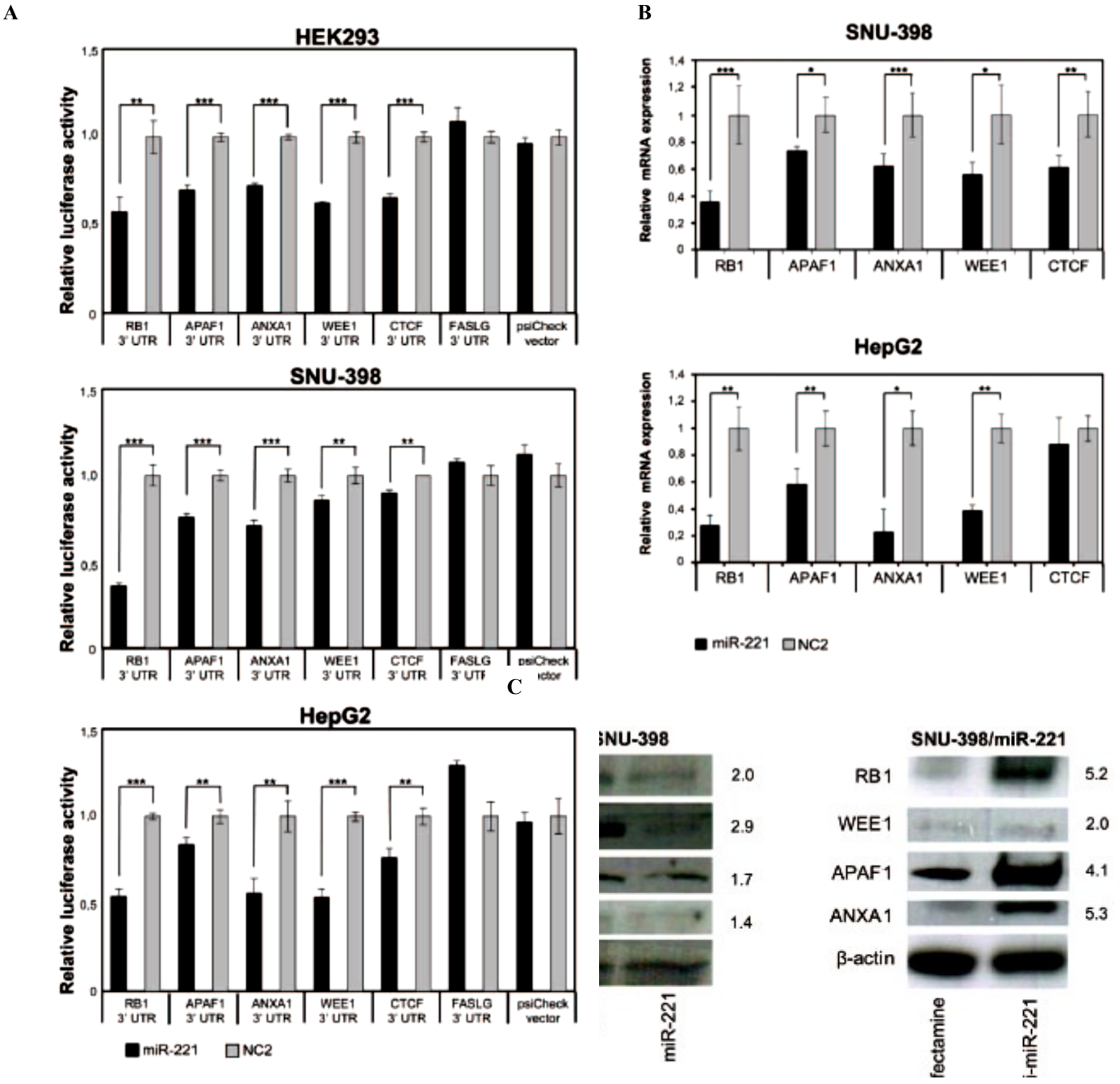

Figure 4.36 Validation of individual miR-221 target genes.
(A). Luciferase assays were performed in Hek293, SNU-398, and HepG2 cells transfected with miR-221 or negative control (NC2), together with psiCheck luciferase vectors containing portions of the 3 UTR of the investigated genes placed downstream the renilla luciferase gene. The renilla luciferase activity was normalized on firefly luciferase activity. Compared to NC2 controls, miR-221 induced a significant decrease in luciferase activity of the vectors containing the RB1, APAF1, ANXA1, WEE1, and CTCF 3 UTR. In contrast, no change in luciferase activity could be detected for the FASLG 3UTR-luciferase vector and the psiCheck control vector.**p-value≤ 0.01;***p-value≤0.001.**(B).** RB1, APAF1, ANXA1, WEE1, and CTCF mRNA expression was measured in SNU-398 and HepG2 cells following transfection with miR-221 or NC2 using Real Time PCR. A significant reduction in mRNA levels was detected for all the investigated genes, with the exception of CTCF mRNA in HepG2 cells.*p-value≤0.05;**p-value≤0.01;***p-value≤0.001.**(C)**Protein expression levels were assessed by Western blot analysis. miR-221 induced a decrease in RB1, APAF1, ANXA1, and WEE1 proteins in SNU398 cells, while transfection of antimiR-221 into SNU-398/miR-221 stable clone induced an increase in target protein levels.Numbers indicate the fold change decrease or increase of proteins expression in miR-221 or antimiR-221 transfected cells vs. the respective controls. Protein expression levels were normalized vs.β-actin expression.

CHAPTER 5.

DISCUSSION

CHAPTER 5 | DISCUSSION

Hepatocellular carcinoma (HCC) is one of the most common solid tumors. More than 626,000 cases of HCC-related deaths are reported yearly worldwide, which ranks it as the third most common of death from cancer(201). It is also one of the deadliest disease, as the annual incidence almost equals the annual mortality, and its incidence is on the rise in developed countries(201). Among all the therapies available for HCC, the surgical resection and liver transplantation are currently best curative options to treat liver cancer. However the high frequency of tumor recurrence and metastasis after curative resection is the major obstacle in the process of HCC treatment. Statistical analysis show that the survival rate of patients who have had a resection is 30% to 40% at 5 years(202). Chemotherapy and radiotherapy, the two conventional therapies applied in the treatment of cancer, also get an unfavorable score because of the resistance of HCC. Moreover, occurrence of HCC often coupled with liver dysfunction, leads to restrict the use of conventional chemotherapeutics, as well as there is more or less non-selective toxicity with significant systemic side effects(6).

Emergence of miRNAs as a new class of gene regulators and their well-known role in cancer progression has opened new avenues for therapeutic discovery. miRNAs potently influence cellular behavior through the regulation of extensive gene expression networks(203). Many experimental and clinical studies revealed that the aberrant expression of miRNAs is associated with initiation, progression and metastasis of cancers(73, 83). Numerous reports have demonstrated that alterations in intracellular miRNAs correlate with liver diseases(14, 199, 204).

Among miRNAs deregulated in HCC, miR-221 and miR-199a are of particular interest(83, 103, 142, 204). As in highly aggressive HCCs, miR-221/-222 was among the most up-regulated of all miRNAs studied(79). miR-221 over-expression inhibits apoptosis of hepatocytes and delays fulminant liver failure(205); It has also been shown that miR-221 accelerates hepatocyte proliferation during liver regeneration(206). miR-221 stimulates the onset of tumors and promotes tumor progression, significantly shortening the median time to death in a mouse liver cancer model(103).

miR-199a is the third most highly expressed miRNA which is consistently decreased in HCC, and its decrement significantly correlates with the malignant potential and poor prognosis of HCC(114, 120). Decreased expression of miR-199a-5p also contributes to increased cell invasion by functional deregulation of DDR1 activity in HCC(207).

Another study in HCC showed that the decrement of miR-199a-3p significantly correlated with poor survival of patients. It could target tumor-promoting PAK4 to suppress HCC growth through inhibiting the PAK4/RAF/MEK/ERK pathway(120).

Therapeutic modulation of a single miRNA may affect many pathways simultaneously to achieve more clinical benefit(185). Hence targeting aberrantly expressed miRNA is logical and attractive. Available evidences indicate that miR-221 as well as miR-199a are potential target for non-conventional treatments against HCC(99).

Over-expression of miR-221 in a transgenic mouse model led to a strong predisposition to the development of liver cancers, whose number and size could be significantly reduced by the delivery of antimiR-221 oligonucleotides(156). For miRNA inhibition, miRNA antisense oligonucleotides and miRNA sponges have been described(155). Antisense oligonucleotides provide a transient inhibition of microRNA. Vector-encoded miRNA sponges are instead expected to inhibit miRNA activity over a longer period of time.

Restoration of miR-199a-3p in Papillary Thyroid Carcinoma cells reduced MET and mTOR protein levels, impaired migration and proliferation and induced lethality through an unusual form of cell death.

This study explored the feasibility of regulation of miR-221 and miR-199a levels as novel therapy in HCC. We firstly showed the practicability of a novel miRNA sequestering methods ”MicroRNA Sponge” for regulating the level of miR-221, noticeably up-regulated in HCC. In addition, we evaluated the restoration of miR-199a mediated adeno-associated viral delivery in HCC. Also we investigated the efficiency of inhibition of miR-221 and restoration of miR-199a using chemically modified antimiR and mimics oligos alone and in combination of FDA approved chemotherapy agent “Sorafenib” in HCC cell lines and mouse model as well.

5.1. Arresting the Oncogenic miR-221 by microRNA Sponge.

MicroRNA sponges offers advantages to inhibit mature miRNA levels. One is the convenience of making dominant negative transgenics over knockouts, and the applicability to a broader range of model organisms and cell lines. In addition, many miRNAs have seed family members encoded at multiple distant loci; due to this functional redundancy, these miRNAs would have to be knocked out individually and the animals bred to generate the complete knockout strain(177). Sponges also offer advantages over chemically modified antisense oligonucleotide inhibitors. First, these antisense inhibitors

appear to be specific for one miRNA as they depend upon extensive sequence complementarily beyond the seed region. Thus, to neutralize a family of miRNAs may require the delivery of a mixture of perfectly complementary oligonucleotides(177). In addition the risk of off-target gene silencing using microRNA Sponge is likely to be lower than synthetic oligonucleotide inhibitor(208). Since physiologic gene expression networks have evolved to accommodate the regulatory effects of endogenous miRNAs , the regulation of hundreds of targets in multiple pathways by miRNAs may reduce at the same time(34).

In our construct, which named “miR-221sponge”, tandem arrayed binding sites for a mature microRNA 221 were inserted near to a reporter gene under the control of the strong promoter. The binding sites were designed to consist of a bulge (i.e., a series of mismatches adjacent to the miRNA seed region (nt 12-15), in order to prevent cleavage by Ago-2 and thus degradation of the sponge(177, 209). Instead, these bulges ideally enforce the stable binding and thus sequestration of the targeted miRNA complexes(15). We showed functionality of designed miR-221sponge through molecular assays following transient transfection of human cell lines. miR-221sponge resulted in significantly reduced miR-221 levels respect to control treatment. These observations supported by an increase in protein level of p27Kip1 ,a cell cycle regulatory factors have been implicated in human HCC. Duel luciferase reporter assay also validated the efficiency of miR-221sponge in inhibition of miR-221. The results described here exhibited sponge designed to inhibit miR-221 as a known oncomiRs are quite promising in modulating the aberration level of miR-221.

So the concept of miRNA sponge was essentially more validated. However sponges are vector driven approaches**.** To provide a safeguard for gene therapy and the feasibility for a clinical application, efforts have been focused predominantly upon constructing liver-targeted vector recently.

Ebert et al. demonstrated the capability of sponges to de-repress endogenous targets in cultured cells, by reporting an up to 2.5-fold increase in a specific miR-20 target (E2F1) following transfection of the miR-20 sponge(185). Considering that maximal effects in Ebert et al.'s hands required transfection of high plasmid copy numbers, it remained unclear whether comparable efficacies can be obtained using viral delivery vectors, especially those based on typical low-copy integrating vectors, such as lentiviruses. The latter issue has been addressed by another group. Gentner et al.(2009) demonstrated an intriguing novel application of lentiviral sponges. They engineered recombinant

lentiviruses to express sponges against miR-223, a highly abundant miRNA in U937 monocytes. When co-transfected with a luciferase reporter regulated by miRNA binding sites in its 3′UTR, sponges effectively (nearly 50%) rescued reporter gene expression. Similarly, they reported successful de-repression of an endogenous miR-233 target. despite the success of Gentner et al.'s work, the general usefulness of lentiviruses to express miRNA sponges remained unclear, especially in an *in vivo* setting. As pointed out by the authors, efficient de-repression of endogenous targets requires high vector copy numbers, which are, however, hard to achieve and maintain with integrating lentiviruses(210). Moreover, raising the number of integrants concurrently increases the risks of adverse insertional mutagenesis. While there is no doubt that lentiviruses hold enormous promise for a large number of gene therapy strategies, other efficient non-integrating viral vectors, such as adenovirus or AAV might ultimately be a better choice for miRNA sponge applications, particularly *in vivo* as reviewed by Grimm et al(2009)(15).

The clinical translatability of such a relatively low efficacy, at the cost of high integration rates and associated risks of insertional mutagenesis in gene transfer by retroviruses, persuade us in providing a proof of concept of sponge transfer using other attractive viral delivery system. We picked up our sponge designed against miR-221 on adeno and adeno-associated virus(AAV).

We proposed that equipping the engineered adeno-associated virus to sponge antisense miR-221 provide a tool for stable inhibition of miRNAs and guide further development of therapeutic strategies. rAAV are suited to mediate miRNA inhibitors because they can safely transduce a wide range of tissues and provide sustained level of gene expression. This system is used to introduce genes into cells for gene therapy studies(34, 198, 211). Compared to retro viral delivery systems, AAV carry substantially diminished risk of insertional mutagenesis since viral genomes persist primarily as episomes(212). Further, the availability of multiple AAV serotypes allows efficient targeting of many tissues of interest(211, 213). Finally, the general safety of AAV has been well documented, with clinical trials(214, 215). This study is the first to our knowledge that shows a miR-221 Sponge delivered by AAV was effective at reducing endogenous miR-221 and altering the level of miR-221 target proteins. In addition miR-221Sponge mediate by rAAV reduced viable tumor cell and increased markers of apoptosis.

In this study also we described a oncolytic rAd-based delivery for conditionally inhibition of endogenous miR-221.

Among Adenovirus vector, we selected an oncolytic adenovirus, with the property of replicating in and killing cancer cells. We selected a Conditionally Replicative Adenoviruses (CRAds), whose replication was controlled by miR-199, which has been recently developed by Callegari, et al;2013 (196). miR-199 is highly expressed in normal liver, while it is strongly down-regulated in essentially 100% of HCCs, making cancer cells, but not normal hepatocytes permissive to viral expression and replication. We proposed that equipping the engineered adenovirus to sponge antisense miR-221 can arrest miR-221 mainly in HCC cells. The Ad-199T-miR-221sponge was indeed able to replicate in HepG2 cells, but not in the HepG2-199 cells that express significant levels of miR-199. In the same experimental setting, we have shown that Ad-199T-miR-221sponge produced a significant reduction of miR-221 levels and a concomitant increase of the CDKN1B/p27 gene, a miR-221 target, in comparison with control virus treatment.

In conclusion Adenovirus, likely because of the high copy number that can achieve was more effective, but rAAV produced significant, albeit lower effects. rAAV effects could however persist for months and viral infections could be repeated in vivo without being inhibited by the immune response.

In summary, while not tested, the viral vectors developed in this work are ready to *in vivo* testing. These viruses can be produced at high titer, they can induce miR-221 inhibition and re-expression of its targets, So they may potentially induce measurable anti-cancer activity.

5.2. Restoration of miR-199a Providing AAV Delivery.

The most widely used cancer model in studying miR-199a is liver cancer. More than 50% of HCC tissues and cells showed significant down-regulation of miR-199a-5p, with increased expression of the pro-invasion molecule DDR1. In addition, miR-199a-3p was shown to be a modulator of cell cycle. It sensitized the cells towards drug treatment through its target mTOR (128). Jia et al (2012) used Lentiviral vectors to study miR-199a functions in HCC cell lines. They found that the involvement of miR-199a in the pathogenesis of HCC was linked to the abnormal regulation of multiple target genes. HIF-1α was identified as a direct target that trough it miR-199a inhibited cell proliferation in both *in vitro* and *in vivo* assays(125). In the present study we tested the practicability of adeno associated virus for delivery and expression of miR-199a sequence. Adeno-

associated virus stably express transgene, thereby can be useful tools to study gene functions and some are now being considered for clinical gene therapy applications(198). We showed that Recombinant adeno-associated viruses generated in this study , express high level miR-199a in HCC cell lines regards to controls. Cancerous features of HCC cell lines like viability and apoptosis affected by restoration of miR-199a through AAV delivery. Indeed AAV mediated inducing down-regulated miRNAs level can be a promising approach for getting through in molecular function of miRs. In addition, cell growth inhibition and apoptosis induction by miR-199a mediated AAV delivery represent great relevance due to its possible therapeutic potential.

5.3. Investigation of Combined Anticancer Effects of AntimiR-221/miR-199 and Sorafenib.

HCC is a multi-factorial disease. Therefore, the expression of a large number of genes, proteins and other molecules from diverse cellular processes and pathways are altered in HCC. Hence, the use of a combination therapy that targets multiple different steps and pathways, rather than a single test or a set of tests, might be an appropriate strategy to combat human HCC(5).

miRNAs that are capable of targeting many mRNAs simultaneously as well as using multikinase inhibitor sorafenib which affect most known molecular pathways associated with hepatocarcinogenesis can fit this bill perfectly.

miRNAs are currently the most widely studied and can simultaneously repress hundreds of genes to directly influence the output of interconnected biological networks. Aberrant miRNA expression patterns have been described in various cancers and alteration in miRNA expression highly correlate with progression and prognosis of human malignant diseases. Although the use of synthetic inhibitor of miR-221 might be a promising approach to HCC therapies, it is assumed that single miRNA replacement or inhibitory therapy for a cancer will not be effective on every patient. Conceivably, a combination approach would have a broader spectrum of susceptible tumors and improved efficacy in patients(157).

On the other hand, the discovery of targeted therapy with multi-tyrosine kinase inhibitors, such as sorafenib has been an important breakthrough for patients with advanced cancer(216). Sorafenib (Nexavar, BAY 43-9006) is a multikinase inhibitor which affect

most known molecular pathways associated with hepatocarcinogenesis include the Ras/Raf/MAP/ERK, the PI3K/Akt/mTOR, the Wnt/β-catenin and the JAK/STAT pathways(201). It is the only FDA approved medication for treatment of this disease that has shown efficacy against a wide variety of tumors in preclinical models(217). In two recent phase III trials in patients with advanced HCC an overall survival benefit of three months compared to placebo was demonstrated(7, 218). Although these results are encouraging, the use of sorafenib is hampered by two phenomena. First of all, up to 80% of patients treated with sorafenib suffer from side effects. The most important grade 3 adverse events include hand-foot syndrome, diarrhea, hypertension and fatigue(219, 220). In the SHARP trial 26% in the sorafenib arm needed dose reductions, 44% had short-term ‘‘drug holidays’’ and 11% had to permanently discontinue the treatment due to drug-related adverse events(7). The second phenomenon is that patients who initially respond to therapy eventually will show progression(216). Combination therapy with cisplatin/interferon/ doxorubicin/5-fluorouracil produced somewhat higher response rates than single agent, however, at the expense of significantly higher toxicity(5).

Positive therapeutic outcomes achieved with sorafenib, as well as evidence that showed the effects of a modified AMO against miR-221 in reducing the number and size of HCC tumors in a miR-221 transgenic mouse model(176) and inhibition of the cell proliferation and cell cycle by restoration of miR-199a in HCC cells(221), lead us hypothesize that the combination of an miR-221 specific inhibitor or mimics miR-199a and sorafenib is a feasible way to improve the drug response.

Herein, we assessed oncogenic effect of combining of antisense miR-221/mimic miR-199a oligos with sorafenib in two hepatocellular carcinoma cell lines, HepG2 and Hep 3B. HepG2 come from 15years old male and hep3b come from 8 years od female. The first do not form tumor in mice, the last yes. Hep3B is p53 null while HepG2 has wild type p53. Hep3B have a higher metabolic rate than HepG2(Source of data: atcc cell line). In the present study, anti-cancer effects were assessed using viability and two different apoptosis assays that explored caspase3/7 or annexin V activity.

We first conducted anti-proliferation and apoptosis analysis of sorafenib on both HCC cell lines. We demonstrated that sorafenib inhibited HCC cell growth and these effects correlate with dose-dependent induction in apoptosis. Our results in agreement with Fernando et al(217) indicated that sorafenib induce apoptosis through p53-dependent and independent pathway, since Hep3B cells show p53 deletion, whereas HepG2 are p53 wild type. However drug susceptibility was obviously different in HepG2 in comparison of

Hep3B cell lines, as HepG2 cell line showed saturation of apoptotic effect at lower dose. So IC50s of sorafenib were calculated in both cell lines. Results revealed that lower dose of sorafenib is needed to diminish the viability by 50% in HepG2 respect to Hep3B cell lines. Combination therapy with oligos (100nM) and sorafenib was conducted in HepG2 and Hep3B cells in sorafenib dose near or lower than IC50 to show the synergic effect more feasible. we applied chemically modified antisense miRNA oligos against miR-221(antimiR-221) and mimics miR-199a. Our data showed that antimiR-221 or miR-199a restoration sensitized HepG2 to sorafenib-induced cell death, indicating that combinational therapy of a miR-221 inhibitor/mimics miR-199a and sorafenib may be a good therapeutic approach to enhance current therapy. More than that, we found that the caspase3/7 activity of HepB3 was significantly increased with miR-221 inhibitor, suggesting that a saturation threshold was reached in these cell .So in spite of the apoptotic features were clearly showed the efficiency of combination therapy, we did not succeed to show the synergistic effect of antimiR-221 and sorafenib in Hep3B through caspase3/7 activity assay. To verify the data of apoptosis, Annexin V/7-AAD staining by flow cytometry were performed. The result of Annexine activity was conversely in line with viability. Successful *In vitro* study in two different HCC cell line, resulted that apoptotic can be induced through p53-dependent and independent pathways.

miR-199a restoration also was tested *in vivo* by applying single administration of miR-199a oligos and sorafenib as well as their combination. The test was done using miR-221 transgenic (TG221) mouse which are predispose to develop HCC. We were successful to show the potency of miR-199 -based restoration therapy in parallel with sorafenib.

In summary, antisense miR-221/mimics miR-199a strengthened the anti-cancer effect of sorafenib. These preliminary results warrant further investigation of combining miRNA therapeutics and traditional anticancer agents for selective, personalized medicine.

5.4. Perspectives

A critical conclusion is that stringent prohibition of miR-221 would be feasible through new technology called sponge as well as antisense microRNA oligos(AMO). Because miR-221 is increased in a number of solid tumors including pancreas(66), non–small cell lung cancer(100), glioblastoma(206), and thyroid cancer(61), optimizing a method to arrest miR-221 and to deliver them efficiently to the target tissues might be a useful approach to

target tumors besides HCC. Also positive anticancer effects of restoration of miR-199a *in vitro* and *in vivo* would open a new hope for developing a novel cancer therapeutic regimen. Indeed to better elucidate the molecular mechanisms of miR-221 and miR-199a and further investigate as a potential biomarker and a promising approach for HCC, additional animal-based experiments are needed.

CHAPTER 6.

REFERENCES

CHAPTER 5 | REFERENCES

1. Karakatsanis A, Papaconstantinou I, Gazouli M, Lyberopoulou A, Polymeneas G, Voros D. Expression of microRNAs, miR-21, miR-31, miR-122, miR-145, miR-146a, miR-200c, miR-221, miR-222, and miR-223 in patients with hepatocellular carcinoma or intrahepatic cholangiocarcinoma and its prognostic significance. *Mol Carcinog*. 2013;**52**(4):297-303.
2. Siegel R, Naishadham D, Jemal A. Cancer statistics, 2013. *CA Cancer J Clin*. 2013;**63**(1):11-30.
3. Society AC. Cancer Facts & Figures 2013. *Atlanta: American Cancer Society*. 2013.
4. Zhang G, Wang Q, Xu R. Therapeutics Based on microRNA: A New Approach for Liver Cancer. *Curr Genomics*. 2010;**11**(5):311-25.
5. Aravalli RN. Development of MicroRNA Therapeutics for Hepatocellular Carcinoma. *Diagnostics*. 2013;**3**:170-91.
6. Tanaka S, Arii S. Molecularly targeted therapy for hepatocellular carcinoma. *Cancer Sci*. 2009;**100**(1):1-8.
7. Llovet JM, Ricci S, Mazzaferro V, Hilgard P, Gane E, Blanc JF*, et al.* Sorafenib in advanced hepatocellular carcinoma. *N Engl J Med*. 2008;**359**(4):378-90.
8. Bruix J, Raoul JL, Sherman M, Mazzaferro V, Bolondi L, Craxi A*, et al.* Efficacy and safety of sorafenib in patients with advanced hepatocellular carcinoma: subanalyses of a phase III trial. *J Hepatol*. 2012;**57**(4):821-9.
9. Ambros V. The functions of animal microRNAs. *Nature*. 2004;**431**(7006):350-5.
10. Griffiths-Jones S, Grocock RJ, van Dongen S, Bateman A, Enright AJ. miRBase: microRNA sequences, targets and gene nomenclature. *Nucleic Acids Res*. 2006;**34**(Database issue):D140-4.
11. Tsuchiya S, Okuno Y, Tsujimoto G. MicroRNA: biogenetic and functional mechanisms and involvements in cell differentiation and cancer. *J Pharmacol Sci*. 2006;**101**(4):267-70.
12. Brown M, Suryawanshi H, Hafner M, Farazi TA, Tuschl T. Mammalian miRNA curation through next-generation sequencing. *Front Genet*. 2013;**4**:145.
13. Kozomara A, Griffiths-Jones S. miRBase: annotating high confidence microRNAs using deep sequencing data. *Nucleic Acids Res*. 2014;**42**(Database issue):D68-73.
14. Szabo G, Bala S. MicroRNAs in liver disease. *Nat Rev Gastroenterol Hepatol*. 2013;**10**(9):542-52.
15. Grimm D. Small silencing RNAs: state-of-the-art. *Adv Drug Deliv Rev*. 2009;**61**(9):672-703.
16. Lee RC, Feinbaum RL, Ambros V. The C. elegans heterochronic gene lin-4 encodes small RNAs with antisense complementarity to lin-14. *Cell*. 1993;**75**(5):843-54.
17. Fire A, Xu S, Montgomery MK, Kostas SA, Driver SE, Mello CC. Potent and specific genetic interference by double-stranded RNA in Caenorhabditis elegans. *Nature*. 1998;**391**(6669):806-11.
18. Ambros V. microRNAs: tiny regulators with great potential. *Cell*. 2001;**107**(7):823-6.
19. Serva A, Claas C, Starkuviene V. A Potential of microRNAs for High-Content Screening. *J Nucleic Acids*. 2011;**2011**:870903.
20. Berezikov E, Guryev V, van de Belt J, Wienholds E, Plasterk RH, Cuppen E. Phylogenetic shadowing and computational identification of human microRNA genes. *Cell*. 2005;**120**(1):21-4.
21. Lewis BP, Burge CB, Bartel DP. Conserved seed pairing, often flanked by adenosines, indicates that thousands of human genes are microRNA targets. *Cell*. 2005;**120**(1):15-20.
22. Brennecke J, Hipfner DR, Stark A, Russell RB, Cohen SM. bantam encodes a developmentally regulated microRNA that controls cell proliferation and regulates the proapoptotic gene hid in Drosophila. *Cell*. 2003;**113**(1):25-36.
23. Hackl M, Brunner S, Fortschegger K, Schreiner C, Micutkova L, Muck C*, et al.* miR-17, miR-19b, miR-20a, and miR-106a are down-regulated in human aging. *Aging Cell*. 2010;**9**(2):291-6.
24. Huang X, Ding L, Bennewith KL, Tong RT, Welford SM, Ang KK*, et al.* Hypoxia-inducible mir-210 regulates normoxic gene expression involved in tumor initiation. *Mol Cell*. 2009;**35**(6):856-67.
25. Johnson CD, Esquela-Kerscher A, Stefani G, Byrom M, Kelnar K, Ovcharenko D*, et al.* The let-7 microRNA represses cell proliferation pathways in human cells. *Cancer Res*. 2007;**67**(16):7713-22.

26. Hu W, Chan CS, Wu R, Zhang C, Sun Y, Song JS*, et al.* Negative regulation of tumor suppressor p53 by microRNA miR-504. *Mol Cell*. 2010;**38**(5):689-99.
27. Nakano H, Miyazawa T, Kinoshita K, Yamada Y, Yoshida T. Functional screening identifies a microRNA, miR-491 that induces apoptosis by targeting Bcl-X(L) in colorectal cancer cells. *Int J Cancer*. 2010;**127**(5):1072-80.
28. Pandey AK, Agarwal P, Kaur K, Datta M. MicroRNAs in diabetes: tiny players in big disease. *Cell Physiol Biochem*. 2009;**23**(4-6):221-32.
29. Croce CM. Causes and consequences of microRNA dysregulation in cancer. *Nat Rev Genet*. 2009;**10**(10):704-14.
30. Jopling CL, Yi M, Lancaster AM, Lemon SM, Sarnow P. Modulation of hepatitis C virus RNA abundance by a liver-specific MicroRNA. *Science*. 2005;**309**(5740):1577-81.
31. Chang S, Wen S, Chen D, Jin P. Small regulatory RNAs in neurodevelopmental disorders. *Hum Mol Genet*. 2009;**18**(R1):R18-26.
32. Xu Y, Li F, Zhang B, Zhang K, Zhang F, Huang X*, et al.* MicroRNAs and target site screening reveals a pre-microRNA-30e variant associated with schizophrenia. *Schizophr Res*. 2010;**119**(1-3):219-27.
33. Takeshita F, Patrawala L, Osaki M, Takahashi RU, Yamamoto Y, Kosaka N*, et al.* Systemic delivery of synthetic microRNA-16 inhibits the growth of metastatic prostate tumors via downregulation of multiple cell-cycle genes. *Mol Ther*. 2010;**18**(1):181-7.
34. Kota J, Chivukula RR, O'Donnell KA, Wentzel EA, Montgomery CL, Hwang HW*, et al.* Therapeutic microRNA delivery suppresses tumorigenesis in a murine liver cancer model. *Cell*. 2009;**137**(6):1005-17.
35. Volinia S, Calin GA, Liu CG, Ambs S, Cimmino A, Petrocca F*, et al.* A microRNA expression signature of human solid tumors defines cancer gene targets. *Proc Natl Acad Sci U S A*. 2006;**103**(7):2257-61.
36. Toffanin S, Hoshida Y, Lachenmayer A, Villanueva A, Cabellos L, Minguez B*, et al.* MicroRNA-based classification of hepatocellular carcinoma and oncogenic role of miR-517a. *Gastroenterology*. 2011;**140**(5):1618-28 e16.
37. Hsu SH, Ghoshal K. MicroRNAs in Liver Health and Disease. *Curr Pathobiol Rep*. 2013;**1**(1):53-62.
38. Lee Y, Ahn C, Han J, Choi H, Kim J, Yim J*, et al.* The nuclear RNase III Drosha initiates microRNA processing. *Nature*. 2003;**425**(6956):415-9.
39. Yi R, Qin Y, Macara IG, Cullen BR. Exportin-5 mediates the nuclear export of pre-microRNAs and short hairpin RNAs. *Genes Dev*. 2003;**17**(24):3011-6.
40. Krol J, Loedige I, Filipowicz W. The widespread regulation of microRNA biogenesis, function and decay. *Nat Rev Genet*. 2010;**11**(9):597-610.
41. Denli AM, Tops BB, Plasterk RH, Ketting RF, Hannon GJ. Processing of primary microRNAs by the Microprocessor complex. *Nature*. 2004;**432**(7014):231-5.
42. Meister G, Landthaler M, Patkaniowska A, Dorsett Y, Teng G, Tuschl T. Human Argonaute2 mediates RNA cleavage targeted by miRNAs and siRNAs. *Mol Cell*. 2004;**15**(2):185-97.
43. Eulalio A, Huntzinger E, Izaurralde E. GW182 interaction with Argonaute is essential for miRNA-mediated translational repression and mRNA decay. *Nat Struct Mol Biol*. 2008;**15**(4):346-53.
44. Tan GS, Garchow BG, Liu X, Metzler D, Kiriakidou M. Clarifying mammalian RISC assembly in vitro. *BMC Mol Biol*. 2011;**12**:19.
45. Dela Cruz F, Matushansky I. MicroRNAs in chromosomal translocation-associated solid tumors: learning from sarcomas. *Discov Med*. 2011;**12**(65):307-17.
46. Farazi TA, Horlings HM, Ten Hoeve JJ, Mihailovic A, Halfwerk H, Morozov P*, et al.* MicroRNA sequence and expression analysis in breast tumors by deep sequencing. *Cancer Res*. 2011;**71**(13):4443-53.

47. Farazi TA, Brown M, Morozov P, Ten Hoeve JJ, Ben-Dov IZ, Hovestadt V*, et al.* Bioinformatic analysis of barcoded cDNA libraries for small RNA profiling by next-generation sequencing. *Methods*. 2012;**58**(2):171-87.
48. Lujambio A, Ropero S, Ballestar E, Fraga MF, Cerrato C, Setien F*, et al.* Genetic unmasking of an epigenetically silenced microRNA in human cancer cells. *Cancer Res*. 2007;**67**(4):1424-9.
49. Yang Z, Wang L. Regulation of microRNA expression and function by nuclear receptor signaling. *Cell Biosci*. 2011;**1**(1):31.
50. Liang D, Shen N. MicroRNA involvement in lupus: the beginning of a new tale. *Curr Opin Rheumatol*. 2012;**24**(5):489-98.
51. Godshalk SE, Bhaduri-McIntosh S, Slack FJ. Epstein-Barr virus-mediated dysregulation of human microRNA expression. *Cell Cycle*. 2008;**7**(22):3595-600.
52. Calin GA, Dumitru CD, Shimizu M, Bichi R, Zupo S, Noch E*, et al.* Frequent deletions and down-regulation of micro- RNA genes miR15 and miR16 at 13q14 in chronic lymphocytic leukemia. *Proc Natl Acad Sci U S A*. 2002;**99**(24):15524-9.
53. Calin GA, Ferracin M, Cimmino A, Di Leva G, Shimizu M, Wojcik SE*, et al.* A MicroRNA signature associated with prognosis and progression in chronic lymphocytic leukemia. *N Engl J Med*. 2005;**353**(17):1793-801.
54. Calin GA, Liu CG, Sevignani C, Ferracin M, Felli N, Dumitru CD*, et al.* MicroRNA profiling reveals distinct signatures in B cell chronic lymphocytic leukemias. *Proc Natl Acad Sci U S A*. 2004;**101**(32):11755-60.
55. Cimmino A, Calin GA, Fabbri M, Iorio MV, Ferracin M, Shimizu M*, et al.* miR-15 and miR-16 induce apoptosis by targeting BCL2. *Proc Natl Acad Sci U S A*. 2005;**102**(39):13944-9.
56. Calin GA, Croce CM. MicroRNA-cancer connection: the beginning of a new tale. *Cancer Res*. 2006;**66**(15):7390-4.
57. Lawrie CH, Soneji S, Marafioti T, Cooper CD, Palazzo S, Paterson JC*, et al.* MicroRNA expression distinguishes between germinal center B cell-like and activated B cell-like subtypes of diffuse large B cell lymphoma. *Int J Cancer*. 2007;**121**(5):1156-61.
58. Ciafre SA, Galardi S, Mangiola A, Ferracin M, Liu CG, Sabatino G*, et al.* Extensive modulation of a set of microRNAs in primary glioblastoma. *Biochem Biophys Res Commun*. 2005;**334**(4):1351-8.
59. He H, Jazdzewski K, Li W, Liyanarachchi S, Nagy R, Volinia S*, et al.* The role of microRNA genes in papillary thyroid carcinoma. *Proc Natl Acad Sci U S A*. 2005;**102**(52):19075-80.
60. Schulte JH, Horn S, Otto T, Samans B, Heukamp LC, Eilers UC*, et al.* MYCN regulates oncogenic MicroRNAs in neuroblastoma. *Int J Cancer*. 2008;**122**(3):699-704.
61. Pallante P, Visone R, Ferracin M, Ferraro A, Berlingieri MT, Troncone G*, et al.* MicroRNA deregulation in human thyroid papillary carcinomas. *Endocr Relat Cancer*. 2006;**13**(2):497-508.
62. Weber F, Teresi RE, Broelsch CE, Frilling A, Eng C. A limited set of human MicroRNA is deregulated in follicular thyroid carcinoma. *J Clin Endocrinol Metab*. 2006;**91**(9):3584-91.
63. Yanaihara N, Caplen N, Bowman E, Seike M, Kumamoto K, Yi M*, et al.* Unique microRNA molecular profiles in lung cancer diagnosis and prognosis. *Cancer Cell*. 2006;**9**(3):189-98.
64. Mattie MD, Benz CC, Bowers J, Sensinger K, Wong L, Scott GK*, et al.* Optimized high-throughput microRNA expression profiling provides novel biomarker assessment of clinical prostate and breast cancer biopsies. *Mol Cancer*. 2006;**5**:24.
65. Iorio MV, Ferracin M, Liu CG, Veronese A, Spizzo R, Sabbioni S*, et al.* MicroRNA gene expression deregulation in human breast cancer. *Cancer Res*. 2005;**65**(16):7065-70.
66. Bloomston M, Frankel WL, Petrocca F, Volinia S, Alder H, Hagan JP*, et al.* MicroRNA expression patterns to differentiate pancreatic adenocarcinoma from normal pancreas and chronic pancreatitis. *JAMA*. 2007;**297**(17):1901-8.
67. Pu XX, Huang GL, Guo HQ, Guo CC, Li H, Ye S*, et al.* Circulating miR-221 directly amplified from plasma is a potential diagnostic and prognostic marker of colorectal cancer and is correlated with p53 expression. *J Gastroenterol Hepatol*. 2010;**25**(10):1674-80.

68. Yang H, Kong W, He L, Zhao JJ, O'Donnell JD, Wang J*, et al.* MicroRNA expression profiling in human ovarian cancer: miR-214 induces cell survival and cisplatin resistance by targeting PTEN. *Cancer Res*. 2008;**68**(2):425-33.
69. Galardi S, Mercatelli N, Farace MG, Ciafre SA. NF-kB and c-Jun induce the expression of the oncogenic miR-221 and miR-222 in prostate carcinoma and glioblastoma cells. *Nucleic Acids Res*. 2011;**39**(9):3892-902.
70. Galardi S, Mercatelli N, Giorda E, Massalini S, Frajese GV, Ciafre SA*, et al.* miR-221 and miR-222 expression affects the proliferation potential of human prostate carcinoma cell lines by targeting p27Kip1. *J Biol Chem*. 2007;**282**(32):23716-24.
71. Gottardo F, Liu CG, Ferracin M, Calin GA, Fassan M, Bassi P*, et al.* Micro-RNA profiling in kidney and bladder cancers. *Urol Oncol*. 2007;**25**(5):387-92.
72. Michael MZ, SM OC, van Holst Pellekaan NG, Young GP, James RJ. Reduced accumulation of specific microRNAs in colorectal neoplasia. *Mol Cancer Res*. 2003;**1**(12):882-91.
73. Lu J, Getz G, Miska EA, Alvarez-Saavedra E, Lamb J, Peck D*, et al.* MicroRNA expression profiles classify human cancers. *Nature*. 2005;**435**(7043):834-8.
74. He L, Thomson JM, Hemann MT, Hernando-Monge E, Mu D, Goodson S*, et al.* A microRNA polycistron as a potential human oncogene. *Nature*. 2005;**435**(7043):828-33.
75. O'Donnell KA, Wentzel EA, Zeller KI, Dang CV, Mendell JT. c-Myc-regulated microRNAs modulate E2F1 expression. *Nature*. 2005;**435**(7043):839-43.
76. Johnson SM, Grosshans H, Shingara J, Byrom M, Jarvis R, Cheng A*, et al.* RAS is regulated by the let-7 microRNA family. *Cell*. 2005;**120**(5):635-47.
77. Lee EJ, Gusev Y, Jiang J, Nuovo GJ, Lerner MR, Frankel WL*, et al.* Expression profiling identifies microRNA signature in pancreatic cancer. *Int J Cancer*. 2007;**120**(5):1046-54.
78. Merritt WM, Lin YG, Han LY, Kamat AA, Spannuth WA, Schmandt R*, et al.* Dicer, Drosha, and outcomes in patients with ovarian cancer. *N Engl J Med*. 2008;**359**(25):2641-50.
79. Park JK, Kogure T, Nuovo GJ, Jiang J, He L, Kim JH*, et al.* miR-221 silencing blocks hepatocellular carcinoma and promotes survival. *Cancer Res*. 2011;**71**(24):7608-16.
80. Boyerinas B, Park SM, Hau A, Murmann AE, Peter ME. The role of let-7 in cell differentiation and cancer. *Endocr Relat Cancer*. 2010;**17**(1):F19-36.
81. Takamizawa J, Konishi H, Yanagisawa K, Tomida S, Osada H, Endoh H*, et al.* Reduced expression of the let-7 microRNAs in human lung cancers in association with shortened postoperative survival. *Cancer Res*. 2004;**64**(11):3753-6.
82. Roderburg C, Trautwein C, Luedde T. MicroRNA-199a/b-3p: a new star in the liver microcosmos. *Hepatology*. 2011;**54**(2):729-31.
83. Negrini M, Ferracin M, Sabbioni S, Croce CM. MicroRNAs in human cancer: from research to therapy. *J Cell Sci*. 2007;**120**(Pt 11):1833-40.
84. Bhardwaj A, Singh S, Singh AP. MicroRNA-based Cancer Therapeutics: Big Hope from Small RNAs. *Mol Cell Pharmacol*. 2010;**2**(5):213-9.
85. Dews M, Homayouni A, Yu D, Murphy D, Sevignani C, Wentzel E*, et al.* Augmentation of tumor angiogenesis by a Myc-activated microRNA cluster. *Nat Genet*. 2006;**38**(9):1060-5.
86. Northcott PA, Fernandez LA, Hagan JP, Ellison DW, Grajkowska W, Gillespie Y*, et al.* The miR-17/92 polycistron is up-regulated in sonic hedgehog-driven medulloblastomas and induced by N-myc in sonic hedgehog-treated cerebellar neural precursors. *Cancer Res*. 2009;**69**(8):3249-55.
87. Si ML, Zhu S, Wu H, Lu Z, Wu F, Mo YY. miR-21-mediated tumor growth. *Oncogene*. 2007;**26**(19):2799-803.
88. Greither T, Grochola LF, Udelnow A, Lautenschlager C, Wurl P, Taubert H. Elevated expression of microRNAs 155, 203, 210 and 222 in pancreatic tumors is associated with poorer survival. *Int J Cancer*. 2010;**126**(1):73-80.
89. Gironella M, Seux M, Xie MJ, Cano C, Tomasini R, Gommeaux J*, et al.* Tumor protein 53-induced nuclear protein 1 expression is repressed by miR-155, and its restoration inhibits pancreatic tumor development. *Proc Natl Acad Sci U S A*. 2007;**104**(41):16170-5.

90. Voorhoeve PM, le Sage C, Schrier M, Gillis AJ, Stoop H, Nagel R*, et al.* A genetic screen implicates miRNA-372 and miRNA-373 as oncogenes in testicular germ cell tumors. *Cell*. 2006;**124**(6):1169-81.
91. Huret JL, Ahmad M, Arsaban M, Bernheim A, Cigna J, Desangles F*, et al.* Atlas of genetics and cytogenetics in oncology and haematology in 2013. *Nucleic Acids Res*. 2013;**41**(Database issue):D920-4.
92. Santhekadur PK, Das SK, Gredler R, Chen D, Srivastava J, Robertson C*, et al.* Multifunction protein staphylococcal nuclease domain containing 1 (SND1) promotes tumor angiogenesis in human hepatocellular carcinoma through novel pathway that involves nuclear factor kappaB and miR-221. *J Biol Chem*. 2012;**287**(17):13952-8.
93. Garofalo M, Quintavalle C, Romano G, Croce CM, Condorelli G. miR221/222 in cancer: their role in tumor progression and response to therapy. *Curr Mol Med*. 2012;**12**(1):27-33.
94. Dentelli P, Traversa M, Rosso A, Togliatto G, Olgasi C, Marchio C*, et al.* miR-221/222 control luminal breast cancer tumor progression by regulating different targets. *Cell Cycle*. 2014;**13**(11):1811-26.
95. le Sage C, Nagel R, Egan DA, Schrier M, Mesman E, Mangiola A*, et al.* Regulation of the p27(Kip1) tumor suppressor by miR-221 and miR-222 promotes cancer cell proliferation. *EMBO J*. 2007;**26**(15):3699-708.
96. Visone R, Russo L, Pallante P, De Martino I, Ferraro A, Leone V*, et al.* MicroRNAs (miR)-221 and miR-222, both overexpressed in human thyroid papillary carcinomas, regulate p27Kip1 protein levels and cell cycle. *Endocr Relat Cancer*. 2007;**14**(3):791-8.
97. Miller TE, Ghoshal K, Ramaswamy B, Roy S, Datta J, Shapiro CL*, et al.* MicroRNA-221/222 confers tamoxifen resistance in breast cancer by targeting p27Kip1. *J Biol Chem*. 2008;**283**(44):29897-903.
98. Fu X, Wang Q, Chen J, Huang X, Chen X, Cao L*, et al.* Clinical significance of miR-221 and its inverse correlation with p27Kip(1) in hepatocellular carcinoma. *Mol Biol Rep*. 2011;**38**(5):3029-35.
99. Fornari F, Gramantieri L, Ferracin M, Veronese A, Sabbioni S, Calin GA*, et al.* MiR-221 controls CDKN1C/p57 and CDKN1B/p27 expression in human hepatocellular carcinoma. *Oncogene*. 2008;**27**(43):5651-61.
100. Garofalo M, Di Leva G, Romano G, Nuovo G, Suh SS, Ngankeu A*, et al.* miR-221&222 regulate TRAIL resistance and enhance tumorigenicity through PTEN and TIMP3 downregulation. *Cancer Cell*. 2009;**16**(6):498-509.
101. Zhang CZ, Zhang JX, Zhang AL, Shi ZD, Han L, Jia ZF*, et al.* MiR-221 and miR-222 target PUMA to induce cell survival in glioblastoma. *Mol Cancer*. 2010;**9**:229.
102. Zhao JJ, Lin J, Yang H, Kong W, He L, Ma X*, et al.* MicroRNA-221/222 negatively regulates estrogen receptor alpha and is associated with tamoxifen resistance in breast cancer. *J Biol Chem*. 2008;**283**(45):31079-86.
103. Pineau P, Volinia S, McJunkin K, Marchio A, Battiston C, Terris B*, et al.* miR-221 overexpression contributes to liver tumorigenesis. *Proc Natl Acad Sci U S A*. 2010;**107**(1):264-9.
104. Terasawa K, Ichimura A, Sato F, Shimizu K, Tsujimoto G. Sustained activation of ERK1/2 by NGF induces microRNA-221 and 222 in PC12 cells. *FEBS J*. 2009;**276**(12):3269-76.
105. Liu X, Yu J, Jiang L, Wang A, Shi F, Ye H*, et al.* MicroRNA-222 regulates cell invasion by targeting matrix metalloproteinase 1 (MMP1) and manganese superoxide dismutase 2 (SOD2) in tongue squamous cell carcinoma cell lines. *Cancer Genomics Proteomics*. 2009;**6**(3):131-9.
106. Felli N, Fontana L, Pelosi E, Botta R, Bonci D, Facchiano F*, et al.* MicroRNAs 221 and 222 inhibit normal erythropoiesis and erythroleukemic cell growth via kit receptor down-modulation. *Proc Natl Acad Sci U S A*. 2005;**102**(50):18081-6.
107. Sarkar S, Dubaybo H, Ali S, Goncalves P, Kollepara SL, Sethi S*, et al.* Down-regulation of miR-221 inhibits proliferation of pancreatic cancer cells through up-regulation of PTEN, p27(kip1), p57(kip2), and PUMA. *Am J Cancer Res*. 2013;**3**(5):465-77.

108. Chun-Zhi Z, Lei H, An-Ling Z, Yan-Chao F, Xiao Y, Guang-Xiu W*, et al.* MicroRNA-221 and microRNA-222 regulate gastric carcinoma cell proliferation and radioresistance by targeting PTEN. *BMC Cancer*. 2010;**10**:367.
109. Medina R, Zaidi SK, Liu CG, Stein JL, van Wijnen AJ, Croce CM*, et al.* MicroRNAs 221 and 222 bypass quiescence and compromise cell survival. *Cancer Res*. 2008;**68**(8):2773-80.
110. Lupini L, Bassi C, Ferracin M, Bartonicek N, D'Abundo L, Zagatti B*, et al.* miR-221 affects multiple cancer pathways by modulating the level of hundreds messenger RNAs. *Front Genet*. 2013;**4**:64.
111. Callegari E, Gramantieri L, Domenicali M, D'Abundo L, Sabbioni S, Negrini M. MicroRNAs in liver cancer: a model for investigating pathogenesis and novel therapeutic approaches. *Cell Death Differ*. 2015;**22**(1):46-57.
112. Yang X, Yang Y, Gan R, Zhao L, Li W, Zhou H*, et al.* Down-regulation of mir-221 and mir-222 restrain prostate cancer cell proliferation and migration that is partly mediated by activation of SIRT1. *PLoS One*. 2014;**9**(6):e98833.
113. Lagos-Quintana M, Rauhut R, Meyer J, Borkhardt A, Tuschl T. New microRNAs from mouse and human. *RNA*. 2003;**9**(2):175-9.
114. Gu S, Chan WY. Flexible and Versatile as a Chameleon-Sophisticated Functions of microRNA-199a. *Int J Mol Sci*. 2012;**13**(7):8449-66.
115. Chen BF, Suen YK, Gu S, Li L, Chan WY. A miR-199a/miR-214 self-regulatory network via PSMD10, TP53 and DNMT1 in testicular germ cell tumor. *Sci Rep*. 2014;**4**:6413.
116. Loebel DA, Tsoi B, Wong N, Tam PP. A conserved noncoding intronic transcript at the mouse Dnm3 locus. *Genomics*. 2005;**85**(6):782-9.
117. Kim S, Lee UJ, Kim MN, Lee EJ, Kim JY, Lee MY*, et al.* MicroRNA miR-199a* regulates the MET proto-oncogene and the downstream extracellular signal-regulated kinase 2 (ERK2). *J Biol Chem*. 2008;**283**(26):18158-66.
118. Cheung HH, Lee TL, Davis AJ, Taft DH, Rennert OM, Chan WY. Genome-wide DNA methylation profiling reveals novel epigenetically regulated genes and non-coding RNAs in human testicular cancer. *Br J Cancer*. 2010;**102**(2):419-27.
119. Mudduluru G, Ceppi P, Kumarswamy R, Scagliotti GV, Papotti M, Allgayer H. Regulation of Axl receptor tyrosine kinase expression by miR-34a and miR-199a/b in solid cancer. *Oncogene*. 2011;**30**(25):2888-99.
120. Hou J, Lin L, Zhou W, Wang Z, Ding G, Dong Q*, et al.* Identification of miRNomes in human liver and hepatocellular carcinoma reveals miR-199a/b-3p as therapeutic target for hepatocellular carcinoma. *Cancer Cell*. 2011;**19**(2):232-43.
121. Lee CG, Kim YW, Kim EH, Meng Z, Huang W, Hwang SJ*, et al.* Farnesoid X receptor protects hepatocytes from injury by repressing miR-199a-3p, which increases levels of LKB1. *Gastroenterology*. 2012;**142**(5):1206-17 e7.
122. Rane S, He M, Sayed D, Yan L, Vatner D, Abdellatif M. An antagonism between the AKT and beta-adrenergic signaling pathways mediated through their reciprocal effects on miR-199a-5p. *Cell Signal*. 2010;**22**(7):1054-62.
123. Haghikia A, Missol-Kolka E, Tsikas D, Venturini L, Brundiers S, Castoldi M*, et al.* Signal transducer and activator of transcription 3-mediated regulation of miR-199a-5p links cardiomyocyte and endothelial cell function in the heart: a key role for ubiquitin-conjugating enzymes. *Eur Heart J*. 2011;**32**(10):1287-97.
124. Jiang J, Gusev Y, Aderca I, Mettler TA, Nagorney DM, Brackett DJ*, et al.* Association of MicroRNA expression in hepatocellular carcinomas with hepatitis infection, cirrhosis, and patient survival. *Clin Cancer Res*. 2008;**14**(2):419-27.
125. Jia XQ, Cheng HQ, Qian X, Bian CX, Shi ZM, Zhang JP*, et al.* Lentivirus-mediated overexpression of microRNA-199a inhibits cell proliferation of human hepatocellular carcinoma. *Cell Biochem Biophys*. 2012;**62**(1):237-44.

126. Henry JC, Park JK, Jiang J, Kim JH, Nagorney DM, Roberts LR*, et al.* miR-199a-3p targets CD44 and reduces proliferation of CD44 positive hepatocellular carcinoma cell lines. *Biochem Biophys Res Commun*. 2010;**403**(1):120-5.
127. Shen Q, Cicinnati VR, Zhang X, Iacob S, Weber F, Sotiropoulos GC*, et al.* Role of microRNA-199a-5p and discoidin domain receptor 1 in human hepatocellular carcinoma invasion. *Mol Cancer*. 2010;**9**:227.
128. Fornari F, Milazzo M, Chieco P, Negrini M, Calin GA, Grazi GL*, et al.* MiR-199a-3p regulates mTOR and c-Met to influence the doxorubicin sensitivity of human hepatocarcinoma cells. *Cancer Res*. 2010;**70**(12):5184-93.
129. Nam EJ, Yoon H, Kim SW, Kim H, Kim YT, Kim JH*, et al.* MicroRNA expression profiles in serous ovarian carcinoma. *Clin Cancer Res*. 2008;**14**(9):2690-5.
130. Duan Z, Choy E, Harmon D, Liu X, Susa M, Mankin H*, et al.* MicroRNA-199a-3p is downregulated in human osteosarcoma and regulates cell proliferation and migration. *Mol Cancer Ther*. 2011;**10**(8):1337-45.
131. Peng W, Chen ZY, Wang L, Wang Z, Li J. MicroRNA-199a-3p is downregulated in gastric carcinomas and modulates cell proliferation. *Genet Mol Res*. 2013;**12**(3):3038-47.
132. Wu D, Huang HJ, He CN, Wang KY. MicroRNA-199a-3p regulates endometrial cancer cell proliferation by targeting mammalian target of rapamycin (mTOR). *Int J Gynecol Cancer*. 2013;**23**(7):1191-7.
133. Chen R, Alvero AB, Silasi DA, Kelly MG, Fest S, Visintin I*, et al.* Regulation of IKKbeta by miR-199a affects NF-kappaB activity in ovarian cancer cells. *Oncogene*. 2008;**27**(34):4712-23.
134. Sun L, Zhu J, Wu M, Sun H, Zhou C, Fu L*, et al.* Inhibition of MiR-199a-5p Reduced Cell Proliferation in Autosomal Dominant Polycystic Kidney Disease through Targeting CDKN1C. *Med Sci Monit*. 2015;**21**:195-200.
135. Reinhart BJ, Slack FJ, Basson M, Pasquinelli AE, Bettinger JC, Rougvie AE*, et al.* The 21-nucleotide let-7 RNA regulates developmental timing in Caenorhabditis elegans. *Nature*. 2000;**403**(6772):901-6.
136. Sekine S, Ogawa R, Ito R, Hiraoka N, McManus MT, Kanai Y*, et al.* Disruption of Dicer1 induces dysregulated fetal gene expression and promotes hepatocarcinogenesis. *Gastroenterology*. 2009;**136**(7):2304-15 e1-4.
137. Hsu SH, Wang B, Kota J, Yu J, Costinean S, Kutay H*, et al.* Essential metabolic, anti-inflammatory, and anti-tumorigenic functions of miR-122 in liver. *J Clin Invest*. 2012;**122**(8):2871-83.
138. Murakami Y, Yasuda T, Saigo K, Urashima T, Toyoda H, Okanoue T*, et al.* Comprehensive analysis of microRNA expression patterns in hepatocellular carcinoma and non-tumorous tissues. *Oncogene*. 2006;**25**(17):2537-45.
139. Lindow M, Kauppinen S. Discovering the first microRNA-targeted drug. *J Cell Biol*. 2012;**199**(3):407-12.
140. Jopling C. Liver-specific microRNA-122: Biogenesis and function. *RNA Biol*. 2012;**9**(2):137-42.
141. Burchard J, Zhang C, Liu AM, Poon RT, Lee NP, Wong KF*, et al.* microRNA-122 as a regulator of mitochondrial metabolic gene network in hepatocellular carcinoma. *Mol Syst Biol*. 2010;**6**:402.
142. Gramantieri L, Ferracin M, Fornari F, Veronese A, Sabbioni S, Liu CG*, et al.* Cyclin G1 is a target of miR-122a, a microRNA frequently down-regulated in human hepatocellular carcinoma. *Cancer Res*. 2007;**67**(13):6092-9.
143. Yang J, Zhou F, Xu T, Deng H, Ge YY, Zhang C*, et al.* Analysis of sequence variations in 59 microRNAs in hepatocellular carcinomas. *Mutat Res*. 2008;**638**(1-2):205-9.
144. Connolly E, Melegari M, Landgraf P, Tchaikovskaya T, Tennant BC, Slagle BL*, et al.* Elevated expression of the miR-17-92 polycistron and miR-21 in hepadnavirus-associated hepatocellular carcinoma contributes to the malignant phenotype. *Am J Pathol*. 2008;**173**(3):856-64.

145. Meng F, Henson R, Wehbe-Janek H, Ghoshal K, Jacob ST, Patel T. MicroRNA-21 regulates expression of the PTEN tumor suppressor gene in human hepatocellular cancer. *Gastroenterology*. 2007;**133**(2):647-58.
146. Wang Y, Lee AT, Ma JZ, Wang J, Ren J, Yang Y*, et al.* Profiling microRNA expression in hepatocellular carcinoma reveals microRNA-224 up-regulation and apoptosis inhibitor-5 as a microRNA-224-specific target. *J Biol Chem*. 2008;**283**(19):13205-15.
147. Gramantieri L, Fornari F, Ferracin M, Veronese A, Sabbioni S, Calin GA*, et al.* MicroRNA-221 targets Bmf in hepatocellular carcinoma and correlates with tumor multifocality. *Clin Cancer Res*. 2009;**15**(16):5073-81.
148. Kutay H, Bai S, Datta J, Motiwala T, Pogribny I, Frankel W*, et al.* Downregulation of miR-122 in the rodent and human hepatocellular carcinomas. *J Cell Biochem*. 2006;**99**(3):671-8.
149. Fan CG, Wang CM, Tian C, Wang Y, Li L, Sun WS*, et al.* miR-122 inhibits viral replication and cell proliferation in hepatitis B virus-related hepatocellular carcinoma and targets NDRG3. *Oncol Rep*. 2011;**26**(5):1281-6.
150. Tsai WC, Hsu PW, Lai TC, Chau GY, Lin CW, Chen CM*, et al.* MicroRNA-122, a tumor suppressor microRNA that regulates intrahepatic metastasis of hepatocellular carcinoma. *Hepatology*. 2009;**49**(5):1571-82.
151. Li N, Fu H, Tie Y, Hu Z, Kong W, Wu Y*, et al.* miR-34a inhibits migration and invasion by down-regulation of c-Met expression in human hepatocellular carcinoma cells. *Cancer Lett*. 2009;**275**(1):44-53.
152. Wong QW, Lung RW, Law PT, Lai PB, Chan KY, To KF*, et al.* MicroRNA-223 is commonly repressed in hepatocellular carcinoma and potentiates expression of Stathmin1. *Gastroenterology*. 2008;**135**(1):257-69.
153. Su H, Yang JR, Xu T, Huang J, Xu L, Yuan Y*, et al.* MicroRNA-101, down-regulated in hepatocellular carcinoma, promotes apoptosis and suppresses tumorigenicity. *Cancer Res*. 2009;**69**(3):1135-42.
154. Fornari F, Milazzo M, Galassi M, Callegari E, Veronese A, Miyaaki H*, et al.* p53/MDM2 Feed-back Loop Sustains miR-221 Expression and Dictates the Response to Anticancer Treatments in Hepatocellular Carcinoma. *Mol Cancer Res*. 2013.
155. Yuan Q, Loya K, Rani B, Mobus S, Balakrishnan A, Lamle J*, et al.* MicroRNA-221 overexpression accelerates hepatocyte proliferation during liver regeneration. *Hepatology*. 2013;**57**(1):299-310.
156. Sharma AD, Narain N, Handel EM, Iken M, Singhal N, Cathomen T*, et al.* MicroRNA-221 regulates FAS-induced fulminant liver failure. *Hepatology*. 2011;**53**(5):1651-61.
157. Rong M, Chen G, Dang Y. Increased miR-221 expression in hepatocellular carcinoma tissues and its role in enhancing cell growth and inhibiting apoptosis in vitro. *BMC Cancer*. 2013;**13**:21.
158. Yoon SO, Chun SM, Han EH, Choi J, Jang SJ, Koh SA*, et al.* Deregulated expression of microRNA-221 with the potential for prognostic biomarkers in surgically resected hepatocellular carcinoma. *Hum Pathol*. 2011;**42**(10):1391-400.
159. Jia CY, Li HH, Zhu XC, Dong YW, Fu D, Zhao QL*, et al.* MiR-223 suppresses cell proliferation by targeting IGF-1R. *PLoS One*. 2011;**6**(11):e27008.
160. Ichimi T, Enokida H, Okuno Y, Kunimoto R, Chiyomaru T, Kawamoto K*, et al.* Identification of novel microRNA targets based on microRNA signatures in bladder cancer. *Int J Cancer*. 2009;**125**(2):345-52.
161. Migliore C, Petrelli A, Ghiso E, Corso S, Capparuccia L, Eramo A*, et al.* MicroRNAs impair MET-mediated invasive growth. *Cancer Res*. 2008;**68**(24):10128-36.
162. Park HS, Kim KR, Lee HJ, Choi HN, Kim DK, Kim BT*, et al.* Overexpression of discoidin domain receptor 1 increases the migration and invasion of hepatocellular carcinoma cells in association with matrix metalloproteinase. *Oncol Rep*. 2007;**18**(6):1435-41.
163. Vogel WF, Aszodi A, Alves F, Pawson T. Discoidin domain receptor 1 tyrosine kinase has an essential role in mammary gland development. *Mol Cell Biol*. 2001;**21**(8):2906-17.

164. Li J, French B, Wu Y, Vanketesh R, Montgomery R, Bardag-Gorce F*, et al.* Liver hypoxia and lack of recovery after reperfusion at high blood alcohol levels in the intragastric feeding model of alcohol liver disease. *Exp Mol Pathol*. 2004;**77**(3):184-92.
165. Yeligar S, Tsukamoto H, Kalra VK. Ethanol-induced expression of ET-1 and ET-BR in liver sinusoidal endothelial cells and human endothelial cells involves hypoxia-inducible factor-1alpha and microrNA-199. *J Immunol*. 2009;**183**(8):5232-43.
166. Dolganiuc A, Petrasek J, Kodys K, Catalano D, Mandrekar P, Velayudham A*, et al.* MicroRNA expression profile in Lieber-DeCarli diet-induced alcoholic and methionine choline deficient diet-induced nonalcoholic steatohepatitis models in mice. *Alcohol Clin Exp Res*. 2009;**33**(10):1704-10.
167. Ogawa T, Enomoto M, Fujii H, Sekiya Y, Yoshizato K, Ikeda K*, et al.* MicroRNA-221/222 upregulation indicates the activation of stellate cells and the progression of liver fibrosis. *Gut*. 2012;**61**(11):1600-9.
168. Honda M, Rijnbrand R, Abell G, Kim D, Lemon SM. Natural variation in translational activities of the 5' nontranslated RNAs of hepatitis C virus genotypes 1a and 1b: evidence for a long-range RNA-RNA interaction outside of the internal ribosomal entry site. *J Virol*. 1999;**73**(6):4941-51.
169. Murakami Y, Aly HH, Tajima A, Inoue I, Shimotohno K. Regulation of the hepatitis C virus genome replication by miR-199a. *J Hepatol*. 2009;**50**(3):453-60.
170. Zhang GL, Li YX, Zheng SQ, Liu M, Li X, Tang H. Suppression of hepatitis B virus replication by microRNA-199a-3p and microRNA-210. *Antiviral Res*. 2010;**88**(2):169-75.
171. Bader AG, Brown D, Winkler M. The promise of microRNA replacement therapy. *Cancer Res*. 2010;**70**(18):7027-30.
172. Jeong SH, Wu HG, Park WY. LIN28B confers radio-resistance through the posttranscriptional control of KRAS. *Exp Mol Med*. 2009;**41**(12):912-8.
173. Reichel M, Li J, Millar AA. Silencing the silencer: strategies to inhibit microRNA activity. *Biotechnol Lett*. 2011;**33**(7):1285-92.
174. Weiler J, Hunziker J, Hall J. AntimiRNA oligonucleotides (AMOs): ammunition to target miRNAs implicated in human disease? *Gene Ther*. 2006;**13**(6):496-502.
175. Krutzfeldt J, Rajewsky N, Braich R, Rajeev KG, Tuschl T, Manoharan M*, et al.* Silencing of microRNAs in vivo with 'antagomirs'. *Nature*. 2005;**438**(7068):685-9.
176. Callegari E, Elamin BK, Giannone F, Milazzo M, Altavilla G, Fornari F*, et al.* Liver tumorigenicity promoted by microRNA-221 in a mouse transgenic model. *Hepatology*. 2012;**56**(3):1025-33.
177. Ebert MS, Sharp PA. MicroRNA sponges: progress and possibilities. *RNA*. 2010;**16**(11):2043-50.
178. Yan LX, Wu QN, Zhang Y, Li YY, Liao DZ, Hou JH*, et al.* Knockdown of miR-21 in human breast cancer cell lines inhibits proliferation, in vitro migration and in vivo tumor growth. *Breast Cancer Res*. 2011;**13**(1):R2.
179. Medina PP, Slack FJ. Inhibiting microRNA function in vivo. *Nat Methods*. 2009;**6**(1):37-8.
180. Elmen J, Lindow M, Schutz S, Lawrence M, Petri A, Obad S*, et al.* LNA-mediated microRNA silencing in non-human primates. *Nature*. 2008;**452**(7189):896-9.
181. Lanford RE, Hildebrandt-Eriksen ES, Petri A, Persson R, Lindow M, Munk ME*, et al.* Therapeutic silencing of microRNA-122 in primates with chronic hepatitis C virus infection. *Science*. 2010;**327**(5962):198-201.
182. Gumireddy K, Young DD, Xiong X, Hogenesch JB, Huang Q, Deiters A. Small-molecule inhibitors of microrna miR-21 function. *Angew Chem Int Ed Engl*. 2008;**47**(39):7482-4.
183. Xiao J, Yang B, Lin H, Lu Y, Luo X, Wang Z. Novel approaches for gene-specific interference via manipulating actions of microRNAs: examination on the pacemaker channel genes HCN2 and HCN4. *J Cell Physiol*. 2007;**212**(2):285-92.
184. Choi WY, Giraldez AJ, Schier AF. Target protectors reveal dampening and balancing of Nodal agonist and antagonist by miR-430. *Science*. 2007;**318**(5848):271-4.

185. Ebert MS, Neilson JR, Sharp PA. MicroRNA sponges: competitive inhibitors of small RNAs in mammalian cells. *Nat Methods*. 2007;**4**(9):721-6.
186. Mukherji S, Ebert MS, Zheng GX, Tsang JS, Sharp PA, van Oudenaarden A. MicroRNAs can generate thresholds in target gene expression. *Nat Genet*. 2011;**43**(9):854-9.
187. Lewis BP, Shih IH, Jones-Rhoades MW, Bartel DP, Burge CB. Prediction of mammalian microRNA targets. *Cell*. 2003;**115**(7):787-98.
188. Gao X, Kim KS, Liu D. Nonviral gene delivery: what we know and what is next. *AAPS J*. 2007;**9**(1):E92-104.
189. Sobrevals L, Enguita M, Rodriguez C, Gonzalez-Rojas J, Alzaguren P, Razquin N*, et al.* AAV vectors transduce hepatocytes in vivo as efficiently in cirrhotic as in healthy rat livers. *Gene Ther*. 2012;**19**(4):411-7.
190. Bauzon M, Hermiston TW. Exploiting diversity: genetic approaches to creating highly potent and efficacious oncolytic viruses. *Curr Opin Mol Ther*. 2008;**10**(4):350-5.
191. Bauzon M, Hermiston TW. Oncolytic viruses: the power of directed evolution. *Adv Virol*. 2012;**2012**:586389.
192. The end of the beginning: oncolytic virotherapy achieves clinical proof-of-concept. *Mol Ther*. 2006;**13**(2):237-8.
193. Pesonen S, Diaconu I, Cerullo V, Escutenaire S, Raki M, Kangasniemi L*, et al.* Integrin targeted oncolytic adenoviruses Ad5-D24-RGD and Ad5-RGD-D24-GMCSF for treatment of patients with advanced chemotherapy refractory solid tumors. *Int J Cancer*. 2012;**130**(8):1937-47.
194. Toth K, Wold WS. Increasing the efficacy of oncolytic adenovirus vectors. *Viruses*. 2010;**2**(9):1844-66.
195. Chung CT, Miller RH. A rapid and convenient method for the preparation and storage of competent bacterial cells. *Nucleic Acids Res*. 1988;**16**(8):3580.
196. Callegari E, Elamin BK, D'Abundo L, Falzoni S, Donvito G, Moshiri F*, et al.* Anti-tumor activity of a miR-199-dependent oncolytic adenovirus. *PLoS One*. 2013;**8**(9):e73964.
197. Rao X, Di Leva G, Li M, Fang F, Devlin C, Hartman-Frey C*, et al.* MicroRNA-221/222 confers breast cancer fulvestrant resistance by regulating multiple signaling pathways. *Oncogene*. 2011;**30**(9):1082-97.
198. Grimm D, Lee JS, Wang L, Desai T, Akache B, Storm TA*, et al.* In vitro and in vivo gene therapy vector evolution via multispecies interbreeding and retargeting of adeno-associated viruses. *J Virol*. 2008;**82**(12):5887-911.
199. Gramantieri L, Fornari F, Callegari E, Sabbioni S, Lanza G, Croce CM*, et al.* MicroRNA involvement in hepatocellular carcinoma. *J Cell Mol Med*. 2008;**12**(6A):2189-204.
200. Coriat R, Nicco C, Chereau C, Mir O, Alexandre J, Ropert S*, et al.* Sorafenib-induced hepatocellular carcinoma cell death depends on reactive oxygen species production in vitro and in vivo. *Mol Cancer Ther*. 2012;**11**(10):2284-93.
201. Beljanski V, Lewis CS, Smith CD. Antitumor activity of sphingosine kinase 2 inhibitor ABC294640 and sorafenib in hepatocellular carcinoma xenografts. *Cancer Biol Ther*. 2011;**11**(5):524-34.
202. Blum HE. Hepatocellular carcinoma: therapy and prevention. *World J Gastroenterol*. 2005;**11**(47):7391-400.
203. Selbach M, Schwanhausser B, Thierfelder N, Fang Z, Khanin R, Rajewsky N. Widespread changes in protein synthesis induced by microRNAs. *Nature*. 2008;**455**(7209):58-63.
204. Callegari E, Elamin BK, Sabbioni S, Gramantieri L, Negrini M. Role of microRNAs in hepatocellular carcinoma: a clinical perspective. *Onco Targets Ther*. 2013;**6**:1167-78.
205. Liu K, Li G, Fan C, Diao Y, Wu B, Li J. Increased Expression of MicroRNA-221 in gastric cancer and its clinical significance. *J Int Med Res*. 2012;**40**(2):467-74.
206. Quintavalle C, Garofalo M, Zanca C, Romano G, Iaboni M, del Basso De Caro M*, et al.* miR-221/222 overexpression in human glioblastoma increases invasiveness by targeting the protein phosphate PTPmu. *Oncogene*. 2012;**31**(7):858-68.

207. Hu Y, Liu J, Jiang B, Chen J, Fu Z, Bai F*, et al.* MiR-199a-5p loss up-regulated DDR1 aggravated colorectal cancer by activating epithelial-to-mesenchymal transition related signaling. *Dig Dis Sci*. 2014;**59**(9):2163-72.
208. Stenvang J, Petri A, Lindow M, Obad S, Kauppinen S. Inhibition of microRNA function by antimiR oligonucleotides. *Silence*. 2012;**3**(1):1.
209. Kluiver J, Gibcus JH, Hettinga C, Adema A, Richter MK, Halsema N*, et al.* Rapid generation of microRNA sponges for microRNA inhibition. *PLoS One*. 2012;**7**(1):e29275.
210. Gentner B, Schira G, Giustacchini A, Amendola M, Brown BD, Ponzoni M*, et al.* Stable knockdown of microRNA in vivo by lentiviral vectors. *Nat Methods*. 2009;**6**(1):63-6.
211. McCarty DM. Self-complementary AAV vectors; advances and applications. *Mol Ther*. 2008;**16**(10):1648-56.
212. Schnepp BC, Clark KR, Klemanski DL, Pacak CA, Johnson PR. Genetic fate of recombinant adeno-associated virus vector genomes in muscle. *J Virol*. 2003;**77**(6):3495-504.
213. Gao GP, Lu F, Sanmiguel JC, Tran PT, Abbas Z, Lynd KS*, et al.* Rep/Cap gene amplification and high-yield production of AAV in an A549 cell line expressing Rep/Cap. *Mol Ther*. 2002;**5**(5 Pt 1):644-9.
214. Park K, Kim WJ, Cho YH, Lee YI, Lee H, Jeong S*, et al.* Cancer gene therapy using adeno-associated virus vectors. *Front Biosci*. 2008;**13**:2653-9.
215. Carter BJ. Adeno-associated virus vectors in clinical trials. *Hum Gene Ther*. 2005;**16**(5):541-50.
216. van Malenstein H, Dekervel J, Verslype C, Van Cutsem E, Windmolders P, Nevens F*, et al.* Long-term exposure to sorafenib of liver cancer cells induces resistance with epithelial-to-mesenchymal transition, increased invasion and risk of rebound growth. *Cancer Lett*. 2013;**329**(1):74-83.
217. Fernando J, Sancho P, Fernandez-Rodriguez CM, Lledo JL, Caja L, Campbell JS*, et al.* Sorafenib sensitizes hepatocellular carcinoma cells to physiological apoptotic stimuli. *J Cell Physiol*. 2012;**227**(4):1319-25.
218. Cheng AL, Kang YK, Chen Z, Tsao CJ, Qin S, Kim JS*, et al.* Efficacy and safety of sorafenib in patients in the Asia-Pacific region with advanced hepatocellular carcinoma: a phase III randomised, double-blind, placebo-controlled trial. *Lancet Oncol*. 2009;**10**(1):25-34.
219. Abou-Alfa GK, Schwartz L, Ricci S, Amadori D, Santoro A, Figer A*, et al.* Phase II study of sorafenib in patients with advanced hepatocellular carcinoma. *J Clin Oncol*. 2006;**24**(26):4293-300.
220. Strumberg D, Clark JW, Awada A, Moore MJ, Richly H, Hendlisz A*, et al.* Safety, pharmacokinetics, and preliminary antitumor activity of sorafenib: a review of four phase I trials in patients with advanced refractory solid tumors. *Oncologist*. 2007;**12**(4):426-37.
221. Song J, Gao L, Yang G, Tang S, Xie H, Wang Y*, et al.* MiR-199a regulates cell proliferation and survival by targeting FZD7. *PLoS One*. 2014;**9**(10):e110074.